ENG 258-(EQC 1993/157)

Elongation of Reinforced Concrete Beam-Column Units with and without Slab - 2 volumes (one updated in Sepbember 1995)

A McBride, Dept of Civil & Resource Engineering, University of Auckland

ENG 258

ENG 258B

UniServices

Auckland UniServices Limited

Our Ref:4742

EQC Project 157

ELONGATION OF REINFORCED CONCRETE BEAM-COLUMNS WITH AND WITHOUT SLAB

AUCKLAND UNISERVICES LIMITED

a wholly owned company of

THE UNIVERSITY OF AUCKLAND

ENG 258B

UniServices

Auckland UniServices Limited

Our Ref:4742

EQC Project 157

ELONGATION OF REINFORCED CONCRETE BEAM-COLUMNS

WITH AND WITHOUT SLAB

AUCKLAND UNISERVICES LIMITED

a wholly owned company of

THE UNIVERSITY OF AUCKLAND

Prepared for:

Earthquake Commission
PO Box 311
Wellington

Consultant:

Mr AP McBride
ME Student
Department of Civil and
Resource Engineering
University of Auckland

Date: September 1995

updated version

ABSTRACT

The elongation of reinforced concrete beams is investigated. Previous research where elongation has been observed is summarised. Two three-bay, single-storey beam-column units were designed according to the requirements of 3101 (1982). A scale factor of one-third was used for the units. The two units were identical except that the first unit contained a cast insitu slab. Each unit was tested under displacement controlled, inelastic cyclic conditions so that the effect of the slab on the behaviour of the beam-column unit could be determined. These tests showed that the presence of the slab had no significant effect on the elongation of the unit. Secondary effects arising from elongation were observed and accounted for. In addition the first unit was also used to illustrate the effective width of the slab contribution to the flexural strength of the beam. It was found that the requirements of 3101 (1982) were likely to underestimate this contribution to strength.

ACKNOWLEDGMENTS

The research in this Thesis was carried out in the Department of Civil and Resource Engineering, University of Auckland. I would to sincerely thank my supervisors, Professor Richard Fenwick and Doctor Barry Davidson for their guidance and help during this work.

I would like to acknowledge the staff of the Test Hall, Hank Mooy and Phil Thomas whose co-operation, friendship and patience made my work that much more enjoyable. Thanks must also go to Doctor Richard Hunt for his eagerness to help and invaluable advice. The assistance of Ken Gotts is also gratefully acknowledged.

To Kim Douglas, Karen Clow, John Mathews, and of course the ever jovial Darren Bell, and to all the other postgraduates of the school, thank you for your friendship which enabled me to survive. To my many friends, thank you for your support.

To my parents, to whom this thesis is dedicated, and to my three sisters for their love, understanding, and tolerance of the late nights I extend my heat felt thanks.

The financial assistance provided by the Earthquake and War Damages Commission is gratefully acknowledged.

CONTENTS

CHAPTER 1

INTRODUCTION

1.1 BACKGROUND

Current codes of practice require reinforced concrete structures to be designed so that they behave in a ductile manner in the event of a major earthquake. The New Zealand Code of Practice for the Design of Concrete Structures [NZS 3101 (1982)] in general requires that, during seismic attack, energy dissipation in reinforced concrete multi-storey frame structures occurs by the formation of a beam sway mechanism, where the plastic hinges are located predominately in the beams and column hinging is limited to just above the column bases [see Fig. 1.1 a)]. The formation of a column sway mechanism is not permitted, except in one or two storey structures, as the ductility demands in the plastic hinges are unacceptably high [see Fig. 1.1b)]. Thus the Concrete Code recommends that in the case of multi-storey structures a "strong column - weak beam" design philosophy be used to achieve the required level of ductility during a major earthquake.

The yielding of the longitudinal reinforcement in a plastic hinge causes elongation of this region to occur. It is not restricted to beams but can occur in any type of reinforced concrete member that undergoes inelastic or plastic hinge rotation. Exceptions to this are when members are subjected to high axial loads when a member is connected to other much stiffer members such as beams connected to much stiffer columns. This can enhance the strength of these members and alter the behaviour of the overall structure. Elongation of longitudinal beams containing cast insitu slabs can cause membrane forces to occur within slabs also enhancing the strength of these beams.

The existence of elongation in reinforced concrete members has been observed in laboratory tests in many different research projects yet its effect on design has been largely overlooked. Elongation was found to have a significant influence on the behaviour of a seven storey reinforced concrete frame wall structure which was tested to destruction [Wight (1984)]. Elongation in the plastic hinge at the base of the wall caused high axial compression forces to be induced in the wall and axial tension forces in the surrounding frame columns.

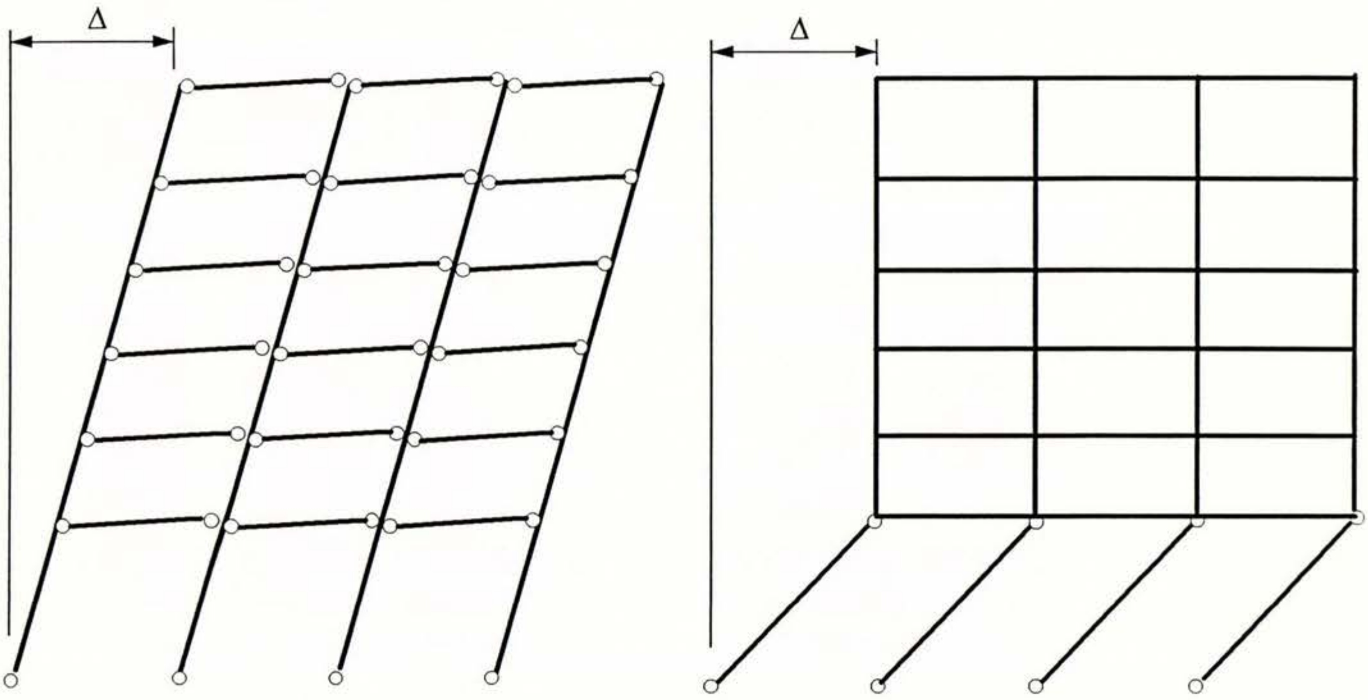

a) Beam Sway Mechanism b) Column Sway Mechanism

Fig. 1.1 - Sway Mechanisms in Multi-storey Moment Resisting Frames

1.2 TYPES OF PLASTIC HINGE ZONES

Two forms of plastic hinge may occur. The first is a gravity dominated or uni-directional plastic hinge, while the second is a seismic dominated or reversing plastic hinge. Both hinge types behave differently and are discussed separately with reference to plastic hinging of beams in a ductile moment resisting frame [Fig. 1.1 a)] rather than in the columns.

1.2.1 Uni-Directional Plastic Hinge Zones

The formation of uni-directional plastic hinges occurs as a result of significant gravity forces being sustained simultaneously with seismic actions in a beam. As shown in Fig. 1.2 a), as the structure sways to the right a negative moment plastic hinge forms in the beam adjacent to the right hand column and a positive moment hinge forms in the beam to the left of mid-span. On load reversal,

[Fig. 1.2 b)] the opposite occurs so that a negative moment hinge forms adjacent to the left hand column while a positive moment hinge forms to the right of mid-span. With each inelastic load reversal, additional rotations accumulate in each of the plastic hinges generating a deflected shape as shown in Fig. 1.2 c). High elongations are induced in such systems due to the accumulation of the inelastic rotations in the plastic hinge zones of the beam.

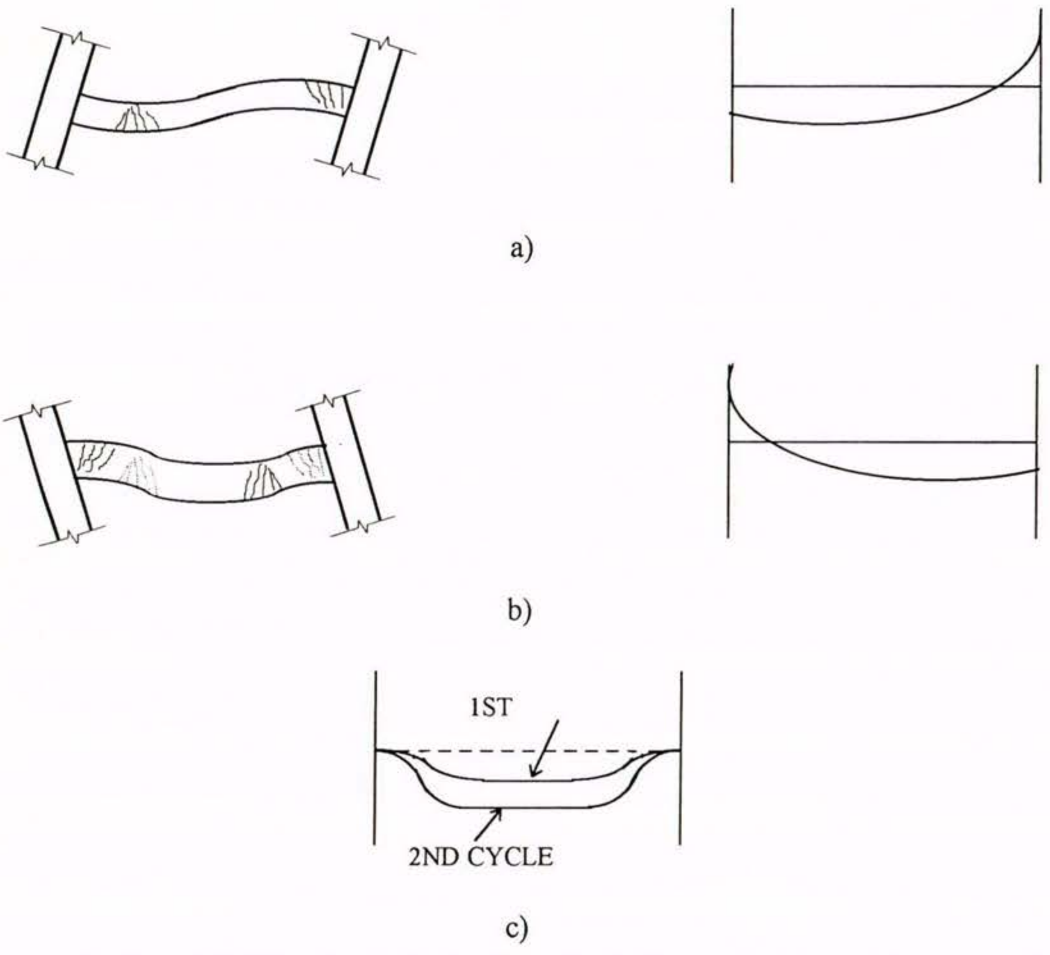

Fig. 1.2 - Mechanism of Unidirectional Plastic Hinges in the Beam of a Frame: a) Right Hand Sway; b) Left Hand Sway; and c) Deflected Shape

1.2.2 Reversing Plastic Hinge Zones

In reversing plastic hinges seismically induced moments dictate the behaviour of the system. As the structure sways to the right, as shown in Fig. 1.3 a), both hinges form adjacent to the column faces and on load reversal, [Fig. 1.3 b)] these hinges form in the same location as in the first direction. Additional cycles do not result in a significant change in the deflected shape of the beam as occurs in beams with uni-directional plastic hinges.

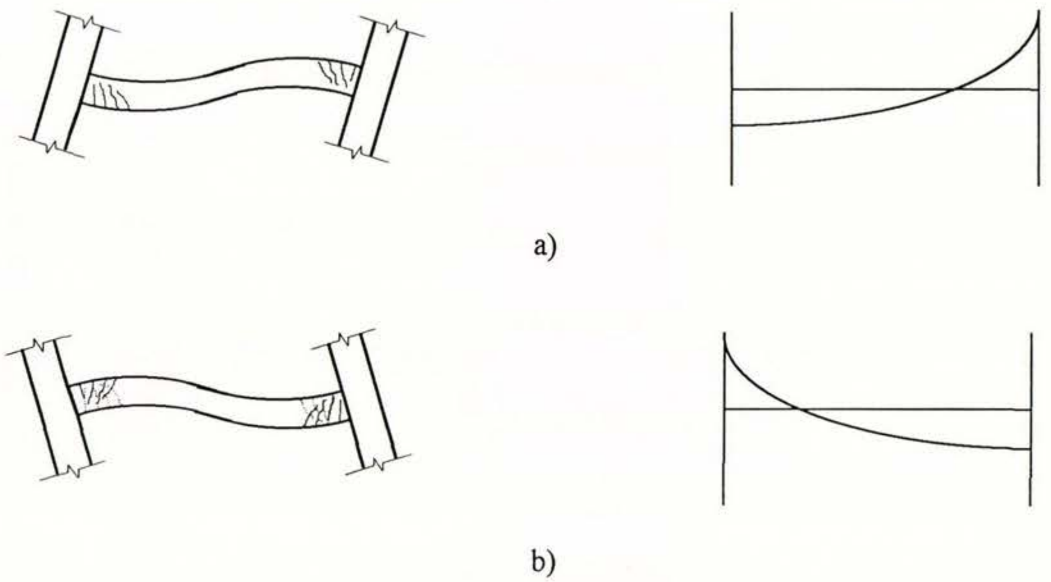

Fig. 1.3 - Mechanism of Reversing Plastic Hinges in the Beam of a Frame: a) Right Hand Sway; b) Left Hand Sway; and c) Moment Conditions

1.3 AIMS OF RESEARCH

The principle aim of this research was to study the effect cast insitu slabs have on the elongation that occurs in beams of multi-storey frames subjected to severe earthquakes. Two tests were made, at approximately 1/3 scale, one on a unit with a cast insitu floor slab and one without. The units were designed in accordance with the New Zealand Code of Practice for the Design of Concrete Structures [NZS 3101 (1982)] and potential plastic hinge zones were specially designed to occur adjacent to the column faces to produce reversing plastic hinges.

Previous work in the United States, Japan and New Zealand on the contribution of slab reinforcement to the flexural strength of beams is summarised. Results observed from measurements on the slab of unit 1 with regard to the contribution to flexural strength is also presented.

1.4 SCOPE

Chapter 2 of this report summarises the observations of elongation reported in the literature. It reviews the theoretical and experimental background from which the test programme was based, including a description of why elongation occurs in reinforced concrete plastic hinges. Chapter 3 describes the test programme on the two three-bay single storey units. It gives details of the loading frames, material properties, construction details, instrumentation and the sequence followed for testing of the units. Chapter 4 presents the tests results of the beam-column-slab unit while Chapter 5 reports on the results of testing of the beam-column unit. Chapter 6 compares the results of the two tests with emphasis on the elongation of both units. Chapter 7 presents the main conclusions and comments on suggestions for further research.

CHAPTER 2

LITERATURE REVIEW

2.1 INTRODUCTION

Observations of beam elongation in various research projects is summarised. This includes a review of differing longitudinal steel quantities. The effects of slabs on the elongation in reversing plastic hinge zones is examined. Experimental results of elongation of uni-directional plastic hinges is compared with the theoretical evaluation of the cause of elongation presented. The reasons why elongation occurs in reinforced concrete beams is presented for both uni-directional and reversing plastic hinges.

2.2 ELONGATION IN PLASTIC HINGE ZONES

In plastic hinges elongation occurs due to the yielding of longitudinal flexural tensile reinforcement. Elongation in reversing plastic hinges also occurs due to the failure of flexural cracks to close in the compression zone of the plastic hinge. This report primarily deals with the elongation in reversing plastic hinge zones and so only a brief description of the way uni-directional plastic hinge zones elongate is given.

2.2.1 Uni-directional Plastic Hinge Zones

In uni-directional plastic hinges elongation occurs mainly as a result of the rotations that the hinges sustain. Figure 2.1 shows the elongation sustained by a beam containing uni-directional plastic hinge zones after repeated cyclic loading. Two tests at Auckland University on uni-directional plastic hinges [Megget and Fenwick (1989), Fenwick and Megget (1993)] showed that strains in the compression zone reinforcement were small and could be neglected. On this basis it was proposed that the elongation at the mid-depth of a beam with uni-directional plastic hinges, δl, is given by Eqn. 2. 1;

$$\delta l = \frac{\Sigma\theta(d - d')}{2} \tag{2.1}$$

where $\Sigma\theta$ is the sum of rotations of the plastic hinges in a bay and (d-d') is the distance between the tension and compression steel centroids.

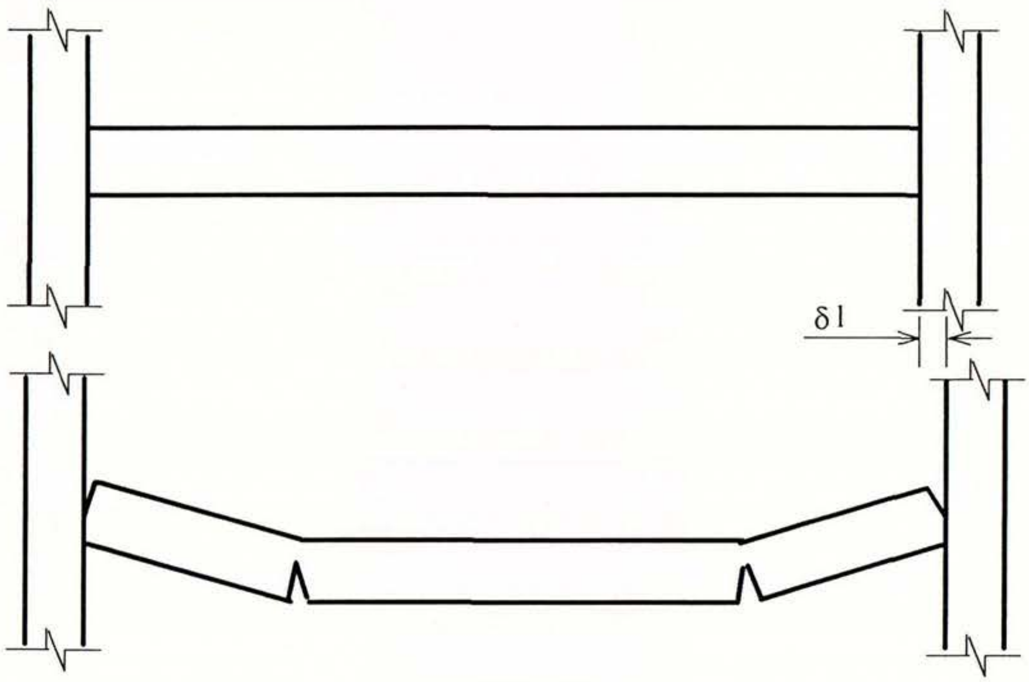

Fig. 2.1 - Elongation in the Beam of a Frame During Uni-directional Plastic Hinging

A model of the uni-directional plastic hinge has been developed in the School of Engineering at the University of Auckland and is being incorporated into the dynamic analysis program DRAIN-2DX. This will enable time history analyses to be made on frame structures which develop uni-directional plastic hinges [Douglas et al (1993)]. The proposed hinge zone substructure model is illustrated in Fig. 2.2. It can be seen from this model that for an inelastic clockwise rotation of the right hand end of the model relative to the left hand end to occur, the steel truss element at the top (or tension side) of the element will yield and increase in length. Because of the bottom concrete truss element's large stiffness in compression it can not significantly reduce in length.

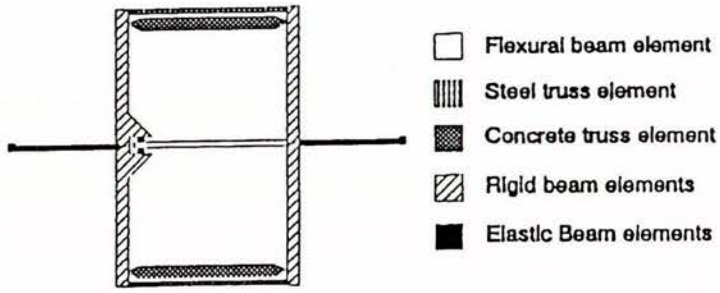

Fig. 2.2 - Proposed Model of Plastic Hinge Zone [after Douglas et al (1993)]

2.2.2 Reversing Plastic Hinge Zones

In reversing plastic hinges the first inelastic half-cycle of deformation causes the tensile reinforcement adjacent to the column faces to yield. After load reversal this tensile reinforcement does not fully yield back in compression. With additional inelastic cycles the compression reinforcement continues to increase in length with the cracks on the compression zone remaining open. Fenwick (1990) suggested that elongation in reversing plastic hinge, zones, δl, is given by;

$$\delta l = \frac{\theta(d - d')}{2} + e \qquad \textbf{(2.2)}$$

where θ is the current rotation of the plastic hinge and "e" is the elongation of the compression zone reinforcement as shown in Fig. 2.3. This figure shows the permanent extension of the compression zone idealised as occurring in one crack. In reality this is not the case. This portion of elongation will be the sum of the deformations in all the cracks in the plastic hinge. This will include micro-cracks initiated from the deformations along the longitudinal reinforcement.

It was suggested that there are two principle reasons why the longitudinal reinforcement in the compression zone does not yield in compression to allow the concrete cracks to close in reversing plastic hinges. These are;

(i) contact stress effects of aggregate particles which become dislocated in concrete tensile cracks, and

(ii) the mechanism of shear resistance.

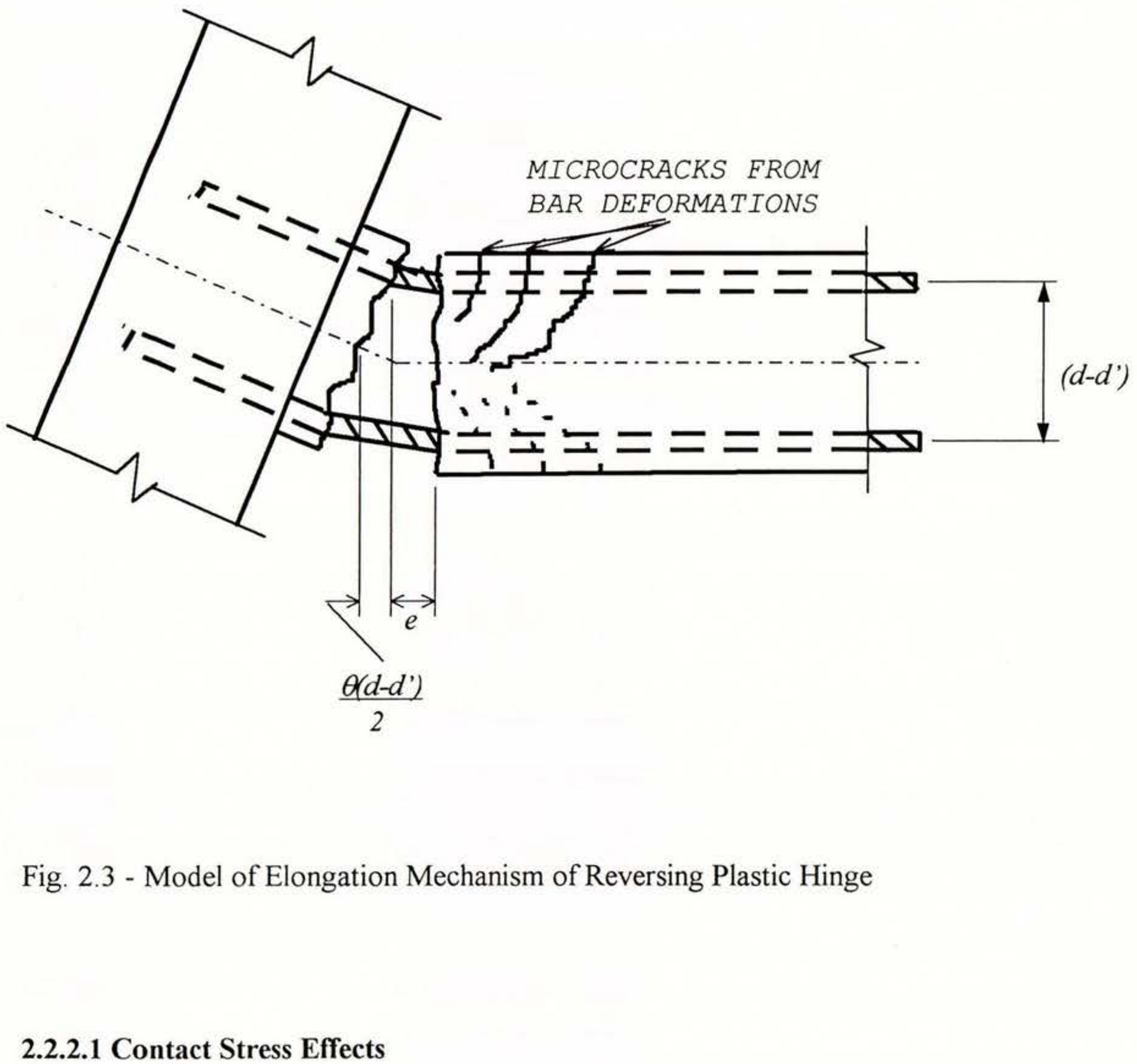

Fig. 2.3 - Model of Elongation Mechanism of Reversing Plastic Hinge

2.2.2.1 Contact Stress Effects

The contact stress effects arise when the concrete in tension cracks and the tensile longitudinal steel yields and dislodges aggregate particles into the cracks. When loading reverses and the longitudinal steel goes into compression, these aggregate particles sustain local contact compression pressure, restricting the closure of the cracks [Tjokrodimuljo (1985)].

2.2.2.2 Mechanism of Shear Resistance in Plastic Hinge Zones

The shear resistance of a cracked section of concrete within a beam undergoing cyclic loading is provided by a truss-like mechanism as shown in Fig. 2.4 [Fenwick (1990)]. In this mechanism, diagonal compression forces occur in the concrete and tensile forces are sustained in the vertical stirrups. From the equilibrium requirements shown in Fig. 2.4, it can be seen that the flexural tension force is always larger than the flexural compression force in the reinforcement. As a consequence, the inelastic rotations in the plastic hinge occur predominately as a result of the tension reinforcement yielding rather than the yielding of the compression reinforcement. This action contributes to the elongation of the plastic hinge.

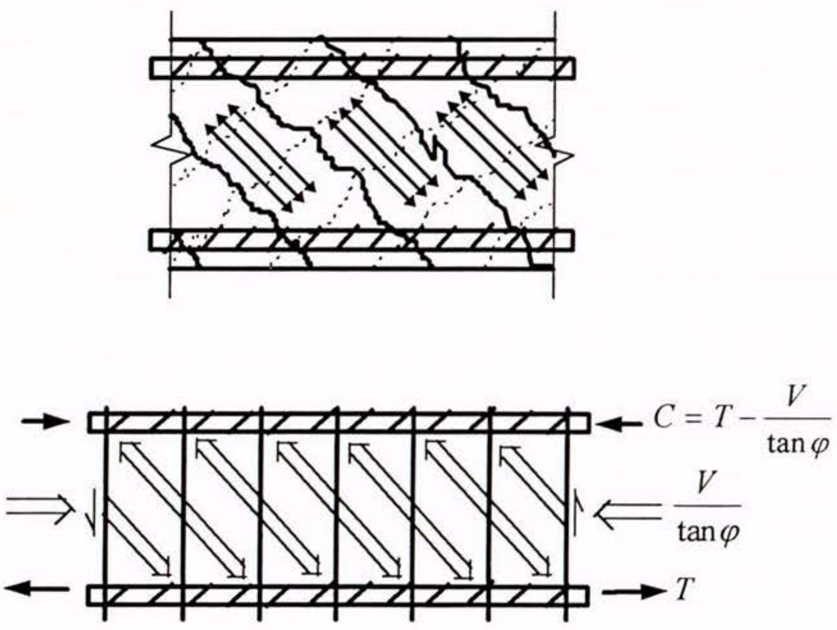

Fig. 2.4 - Mechanism of Shear Resistance in Plastic Hinge

2.3 PREVIOUS REPORTING OF BEAM ELONGATION

Elongation of reinforced concrete members has been observed in a number of research projects in New Zealand, Japan and the United States. This section summarises these observations.

2.3.1 School of Engineering; University of Auckland

Elongation has been reported by Fenwick and Fong (1979), Fenwick et al (1981) and Fenwick and Nguyen (1982) in test programmes performed on cantilever beams forming reversing plastic hinges. With unequal areas of longitudinal reinforcement in the top and bottom sides of the beam, the ultimate moment capacity and hence the magnitude of the flexural forces differs for the two directions of loading. When the smaller area of steel is yielding in tension the magnitude of the flexural compression force is insufficient to cause the steel in the compression side of the beam to yield in compression. As a result any cracks that may have been induced in previous load excursions in which this steel had yielded in tension, remain open, adding to the elongation. With a reversal in load direction the higher compression forces that are sustained in the compression side of the beam, which now contains a smaller area of steel, will tend to close any pre-existing cracks and reduce the elongation [Fenwick and Megget (1993)]. A test with on a beam with a composite slab showed that the slab had very little influence on the magnitude of the elongation which developed under inelastic cyclic loading [Fenwick (1990)].

One test unit reported by Megget and Fenwick (1989) was tested so that a plastic hinge formed on one side of the beam only, thus modelling the behaviour in a uni-directional plastic hinge. In addition a reinforced concrete portal frame was tested under cyclic lateral loading while sustaining high gravity loads so that uni-directional plastic hinges formed in the beam [Megget and Fenwick (1989)]. Elongations reported for both tests were found to be just as significant as elongations observed in reversing plastic hinges. These results correlated well with Eqn. 2.1 as shown in Fig. 2.5.

2.3.2 School of Engineering; University of Canterbury

Beekhius (1971) and Binney (1972) reported significant elongations of up to 4.5% of the member depths in tests performed on shear wall coupling beams. Differing arrangements of reinforcement were used in these test programs. More recently, Cheung (1991) recorded elongations between 2.5% and 4% of the member depths per plastic hinge in tests performed on beam-column-slab units and Restrepo-Posada (1992) has measured elongations between 2.1% and 2.8% in a number of tests performed on various types of pre-cast concrete beam-column units. In all these cases a reversing plastic hinge system was induced.

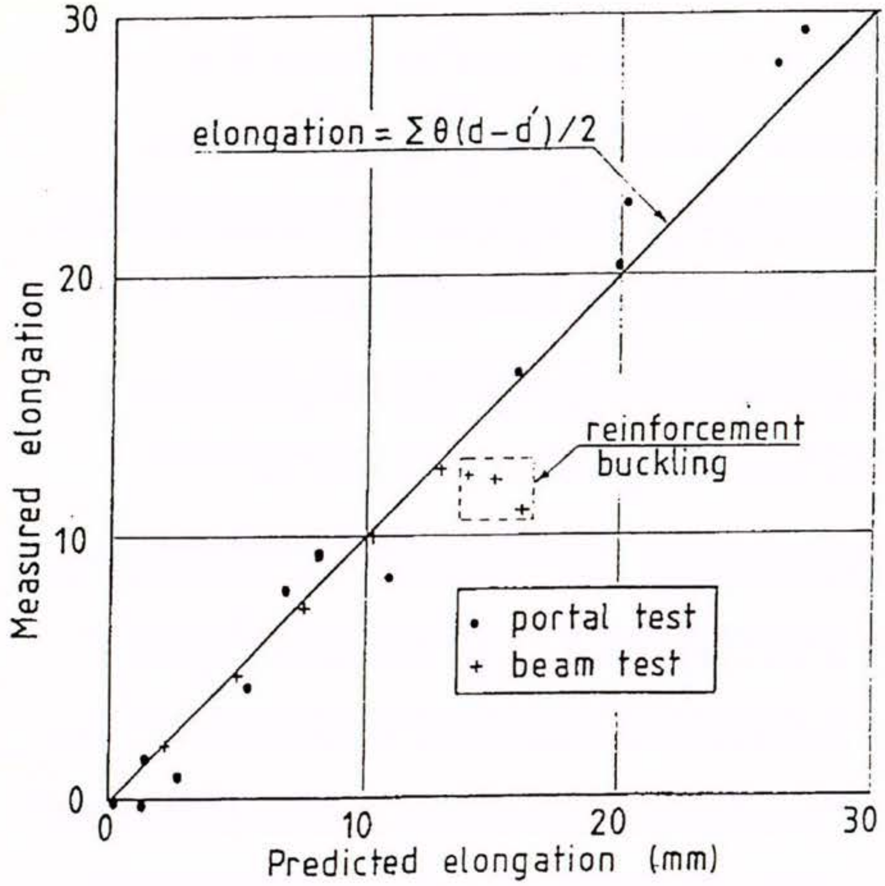

2.5 - Predicted and Measured Elongation in Beams forming Uni-Directional Plastic Hinges for the Portal Frame and Cantilever Beam shown

2.3.3 United States

Beam elongation has been reported at the University of California, Berkeley and at Rice University. Zerbe and Durrani [1989 and 1990] performed a series of tests on statically determinate beam-column connections and two-bay beam column subassemblies with and without slabs. The loads were applied to the columns as illustrated in Fig. 2.6. The elongation of the beam was restrained by the loading system since the tops of the columns were fixed in position relative to each other. Zerbe and Durrani compared elongation in the test on the two-bay unit with tests performed on individual internal and external statically determinate connections. The statically determinate connections were linearly added together for comparison and it was found that the two-bay unit gave a lower value of elongation. The Authors suggested that the difference in comparison between the two-bay unit and the sum of the individual connections was that the flexural stiffness of the columns partially restrained the elongation which resulted in axial compression in the main beams. They also observed significant cracking of the outer faces of the external columns which supported this conclusion. However it is likely that the fixing in position of the columns would be more significant in contributing to the difference. No such restaint was applied to the individual connections. Yielding of external column reinforcement, resulting from the restriction in elongation, occurred at 3.5% drift despite the column to beam flexural strength ratios being 1.88 for the internal connection and 2.41 for the external connections.

Qi and Pantazopoulou noted that the loading rig used by Zerbe and Durrani (1989) partially restrained elongation in the beam and influenced load distribution in the two bay unit, especially at large levels of interstorey drift. Hence in their testing of a similar subassembly, Qi and Pantazopoulou attempted to solve the problem of restraint by increasing the relative distance between the tops of the columns by amounts equal to the axial elongation of each span at the mid-beam level. This was achieved with the use of dynamic, actuators as shown in Fig. 2.7. However the loading rig adopted by these researchers still restrained the relative deflections of the tops of the columns since geometry requires this to be larger than the elongation of the beam. This produced additional column shear which was introduced to the beams as axial compression that increased with lateral drift as noted by the researchers. They noted that the residual beam deformations resulting from inelastic strains in the reinforcement, cracking of the concrete and bond deterioration all accumulated with increasing lateral drift, thus producing an overall expansion of the beams of the specimen. Maximum elongations in the two bays were recorded at 1.3% and 2.4% of the member depth at the conclusion of the test programme.

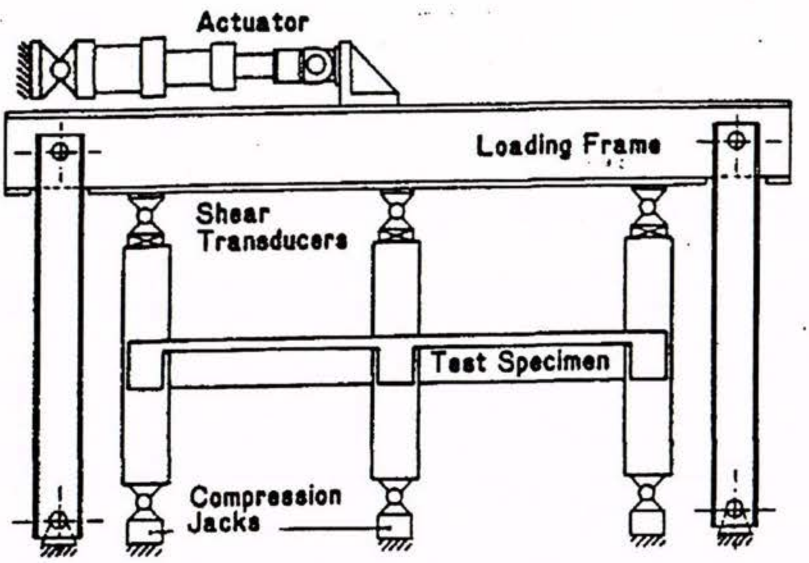

Fig. 2.6 - Zerbe and Durrani (1990) Schematic of Loading Frame

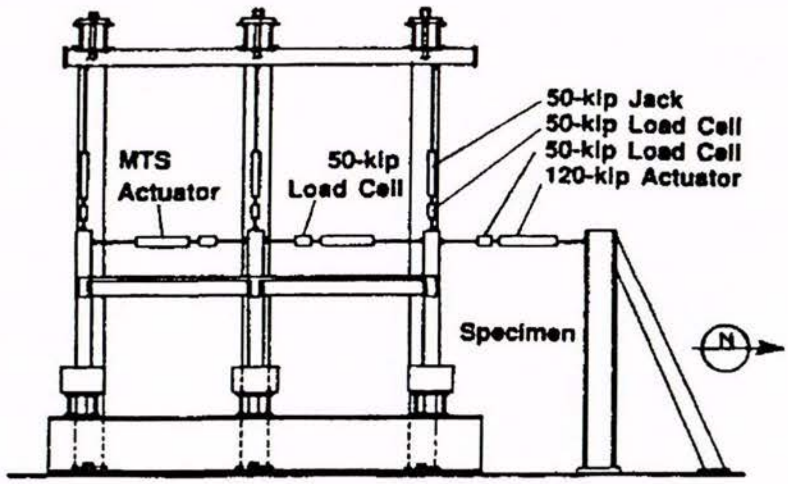

Fig. 2.7 - Qi and Pantazopoulou (1991) Schematic of Loading Frame

2.3.4 Japan

Elongation at the base of the structural wall of a full-scale seven-storey wall frame building, tested at the Building Research Institute (BRI) in Japan, has been reported by Wight (1984). Although the nature of the structural wall is different to the concrete beams previously discussed, it serves as a useful example of the type of problem that may be experienced when elongation occurs. The elongation in the plastic hinge, that formed at the base of the structural wall, caused a significant enhancement in the lateral strength expected of the structure due to increased compressive forces in the wall. This compression force was balanced by tensile forces in many of the columns in the structure.

Sakata and Wada tested one-twentieth scale concrete frame models to illustrate the effect of deformation on multi-bay medium-height structures. Because of the small size of the models [see Fig. 2.8 a)] they were able to devise a system of applying independent lateral loads to the columns of the test specimens without restraining the elongation of the longitudinal beams as shown in Fig. 2.8 b). Tests were performed under both monotonic and cyclic loading conditions. They showed that elongation can be expected to be larger in higher levels of a structure when compared to the lower levels as shown if Fig. 6.3 a). Some of the results of these tests are interpreted in Section 6.3.

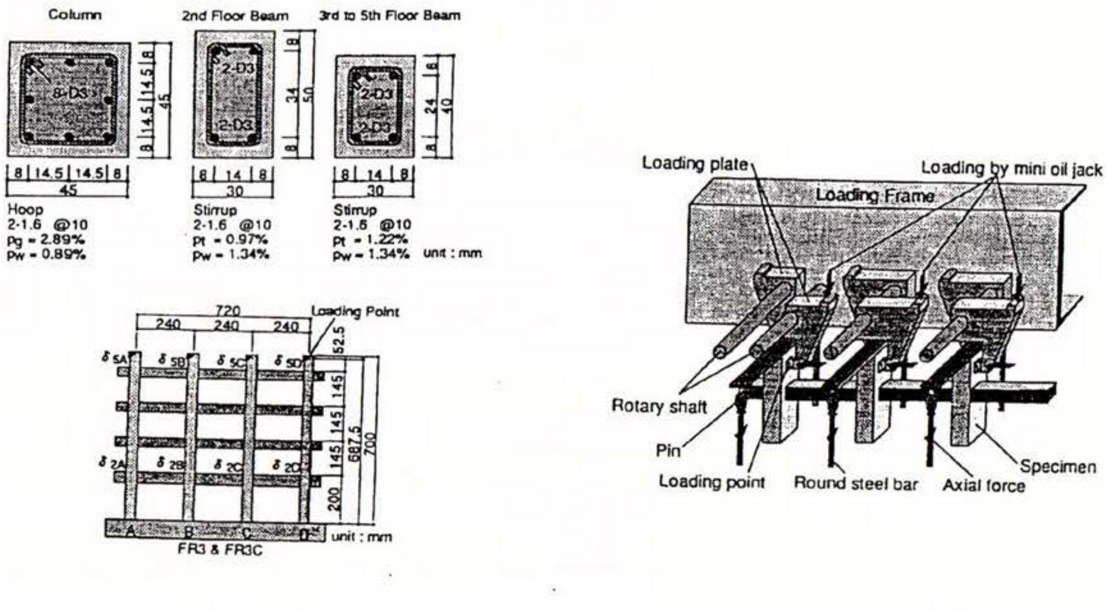

a) b)

Fig. 2.8 - Sakata and Wada Test Details: a) Reinforcement details; b) Loading Apparatus

2.4 ACTIONS WITHIN SLAB FROM BEAM ELONGATION

Cheung et al (1991) postulated that beam elongation caused the beam to go into compression and act as a strut which was resisted by the longitudinal slab reinforcement going into tension and acting as ties. The beams are considered incompressible through the mid-span regions adjacent to the plastic hinge zones. This strut and tie mechanism is shown in Fig. 2.9. The mechanism around the interior columns relies on sufficient anchorage of the longitudinal reinforcement within the slab for the steel to yield while the mechanism around the exterior column relies on the anchorage of the slab reinforcement in the transverse beams. As a result of this mechanism an increase in strength of the beam will occur.

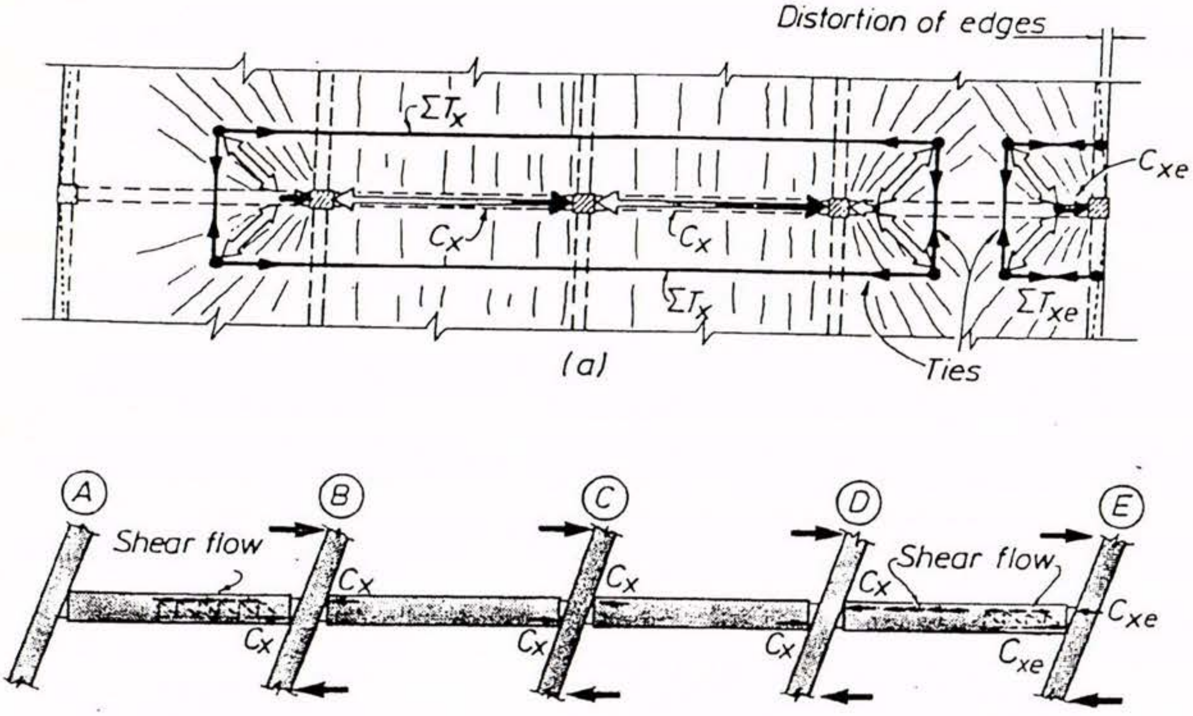

Fig. 2.9 - Strut and Tie Mechanism In Slab From Elongation [after Cheung et al (1991)]

2.5 PREVIOUS WORK ON EFFECTIVE SLAB WIDTH

The contribution of the strength of a slab in tension to the flexural behaviour of reinforced concrete beams has long been recognised. Many researchers have individually looked at this situation and most of this work has been summarised by Pantazopoulou and Moehle (1987). Researchers have suggested there is an effective width within which the longitudinal slab steel will contribute to the flexural strength of the beam. The New Zealand Concrete Code [NZS 3101 (1982)] used this concept for assessing the flexural strength of a beam by taking the effective width of slab as:

(i) four times the slab thickness for interior connections with transverse beams of similar dimensions to the main beam framing into the joint and two and a half times the slab thickness for interior connections without transverse beams framing into the joint, and

(ii) two times the slab thickness for exterior connections with transverse beams framing into the joint and the width of the column for exterior connections without transverse beams framing into the joint.

The work on the concept of an effective slab width has been summarised by Zerbe and Durrani (1990) who proposed the following design recommendations to account for the presence of a floor slab in the design of beam-column connections:

(i) reinforcement in a slab width equal to twice the total beam depth on each side of the beam should be considered effective in calculating the negative capacity of the beams, and

(ii) at exterior connections, if the torsional moment induced in the transverse beams by tension in the slab reinforcement within the effective slab width exceeds their torsional strength, the effective slab width for the design of exterior connections should be reduced to one beam depth on each side of the beam.

Cheung et al (1992) found that NZS 3101 (1982) underestimated the increase in flexural strength and hence recommended that the effective width for both the ideal and overstrength calculations for beam sections should be taken as the lesser of:

(i) one quarter of the beam span at each side from the beam centre line, or

(ii) one half of the distance to an adjacent parallel beam at interior columns, and one quarter of the distance to an adjacent parrallel beam at exterior columns at each side of the beam centre line.

Reinforcement considered effective should extend beyond an imaginary line at 45° degrees from the centre of the column to enable the tension forces in the reinforcement to develop.

Qi and Pantazopoulou (1991) observed that for interior connections at average lateral drifts exceeding 0.45% and exterior connections at average lateral drifts exceeding 2%, the longitudinal slab reinforcement at the faces of the support remained in tension regardless of the loading direction. Cheung, et al (1991) reported that these tension forces or membrane forces are the dominant forces which contribute to strength enhancement of the beam while actions from bending in slabs is not significant.

Cheung et al (1991) suggested that after the formation of plastic hinges these membrane forces impose large tensile strains in the longitudinal slab reinforcement on each side of the column which reduce further away from the beam. The tensile forces are transferred to the main beam via shear, as shown in Fig. 2.10 which develops diagonal compressive forces in the slab concrete. Hence tensile forces must be sustained by the transverse slab steel.

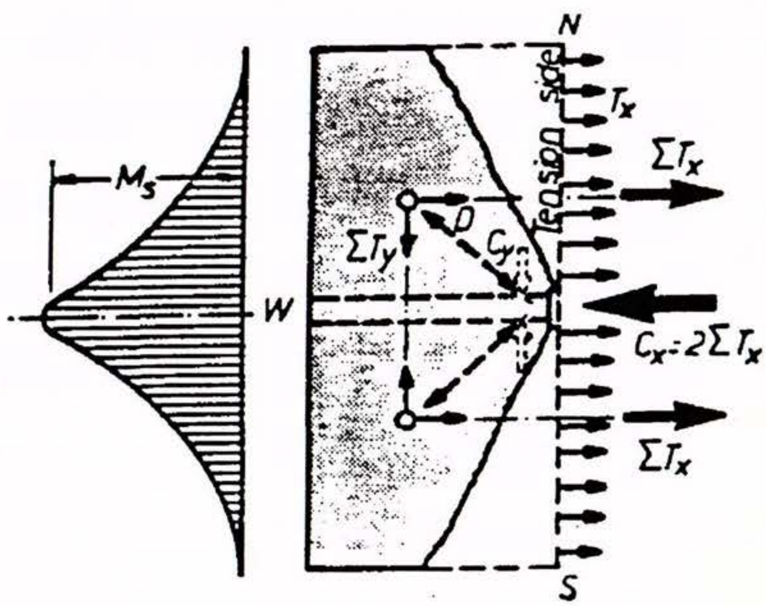

Fig. 2.10 - Mechanism of Force Transfer to Column at Interior Connection in Frame [after Cheung et al (1991)]

2.6 A DESIGN SOLUTION TO ELONGATION FOR PRECAST FLOOR SYSTEMS

Mejia-McMaster and Park (1994) recognised the potential for failure of the support of precast floor systems leading to collapse due to:

(i) seating lengths being too small in the direction of the span or tolerances not being met, and

(ii) imposed movements due to volume changes or the increase in span caused by elongation associated with plastic hinging of adjacent beams in ductile frames during earthquakes

The design of special reinforcement in the form of inclined hanger bars or saddle bars anchored in the hollows of precast slab units to carry these units in the event of beam failure or lateral movements of units off supports was tested. Such reinforcement can develop an alternative load-carrying path. Two test methods were used on various types of reinforcement configurations. Test A involved applying a vertical force to a precast unit with no bearing support so that vertical loads were resisted by the topping slab, containing a reinforcement mesh, and the special reinforcement connection. Test B involved first applying a horizontal force to the precast unit so that it moved laterally, fracturing the topping reinforcement mesh and clearing the support so that vertical forces could only be resisted by kinking of the tie bars. A vertical force was then applied to the precast unit until failure of the connection. These test methods are illustrated in Fig. 2.11 [after Mejia-McMaster and Park (1994)]. Results of these tests showed that this method of fixing can achieve the required capacity to withstand the large relative displacements imposed by the elongation of adjacent beams without the loss of structural integrity.

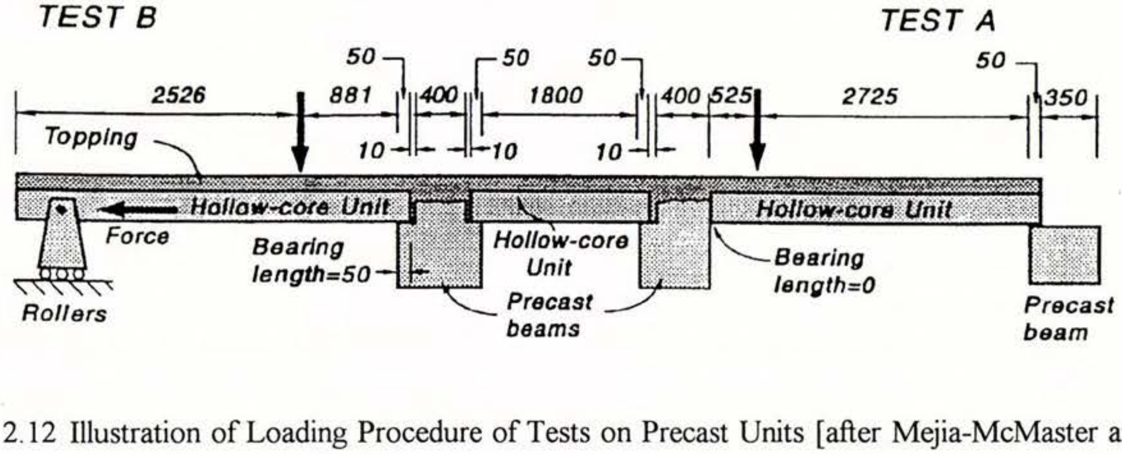

Fig. 2.12 Illustration of Loading Procedure of Tests on Precast Units [after Mejia-McMaster and Park (1994)]

2.6 SUMMARY

1. Elongation has been reported in a number of research projects. Elongation of 2% to 5% of the member depth can be expected in plastic hinges of a reinforced concrete ductile frame sustaining plastic hinges during seismic excitation.

2. The test set up and loading frames are important in the testing of multi-connection subassemblies. Some loading frames have been shown to restrict the amount of axial deformation that could occur.

3. Elongation of uni-directional plastic hinges can be predicted from the inelastic rotations sustained during cyclic loading. Elongation in reversing plastic hinges consists of a contribution from the inelastic rotations and from the permanent extension of the compression reinforcement. While the inelastic rotations can be predicted, it is very difficult to predict the amount of permanent extension in the compression reinforcement

4. Previous test results suggested that composite slabs have very little effect on the elongation behaviour of beam sections. That is, beams with composite slabs will elongate the same amount as beams without.

5. Suggestions of an effective width of slab contributing the flexural strength of beam are summarised.

CHAPTER 3

TEST PROGRAMME

3.1 INTRODUCTION

The test programme for this research project was designed primarily to investigate the effects of a reinforced concrete slab on the elongation occurring in the beams of moment resisting frames subjected to inelastic cyclic loading. To do this, two beam-column units were built and tested. In the first of these an internal frame with an insitu composite slab was constructed. The second unit was similar except that the slab was omitted. The structure sustained low gravity loads so that when it was subjected to cyclic lateral forces, reversing plastic hinges formed in the beams adjacent to the column faces. This chapter outlines the test programme beginning with the design of both units and concluding with the test procedure.

3.2 DESIGN CONSIDERATIONS

The units were designed to represent one level of an internal frame of a three-bay multi-storey building detailed in accordance with the New Zealand Code of Practice for the Design of Concrete Structures [NZS 3101 (1982)]. A scale factor of approximately one-third was used in the design to enable the units to be tested with existing equipment in the Test Hall. Figure 3.1 illustrates the likely position of the units in a multi-storey moment resisting frame. The absence of applied axial loads to the columns to simulate gravity loads was not considered to be significant in this test programme since it would produce the least desirable condition for the beam-column connection and have no effect on the beams where the inelastic deformation occurred.

To simulate the boundary conditions of the columns under seismic loading, cyclic lateral forces were applied to each column with loading jacks at a position representing the mid-height of the storey. This location represented the point of inflection of the columns in the building model shown in Fig. 3.1. The ratio of the applied lateral forces of internal columns to the external columns was two to one. The base of each column was fixed to the strong floor by a one-way pin joint, as illustrated in Fig. 3.2. The distance between the these joints and the beam was equal to the corresponding distance between the loading jacks and the beam.

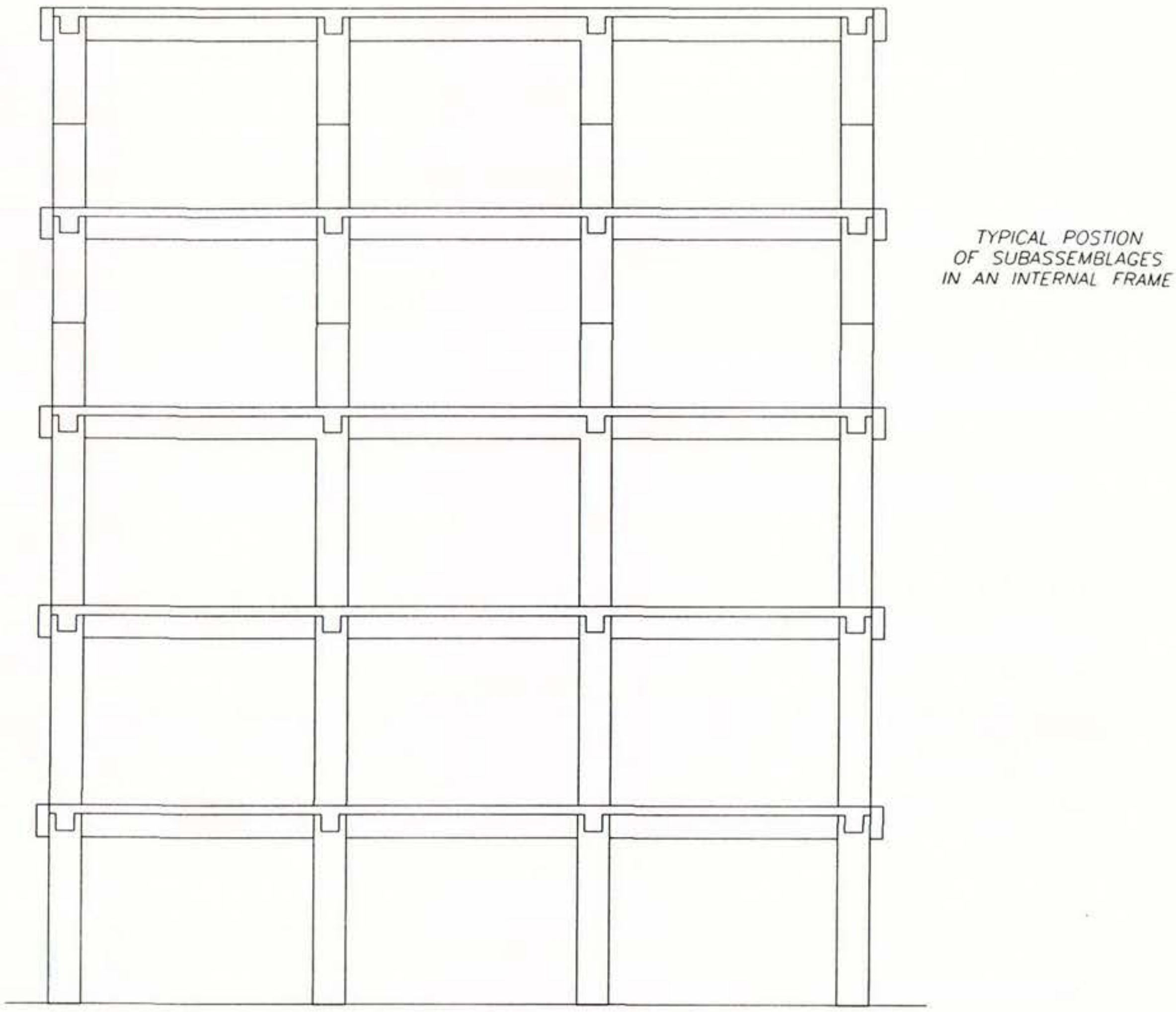

Fig. 3.1 - Position of Test Units in a Multi-Storey Moment Resisting Frame

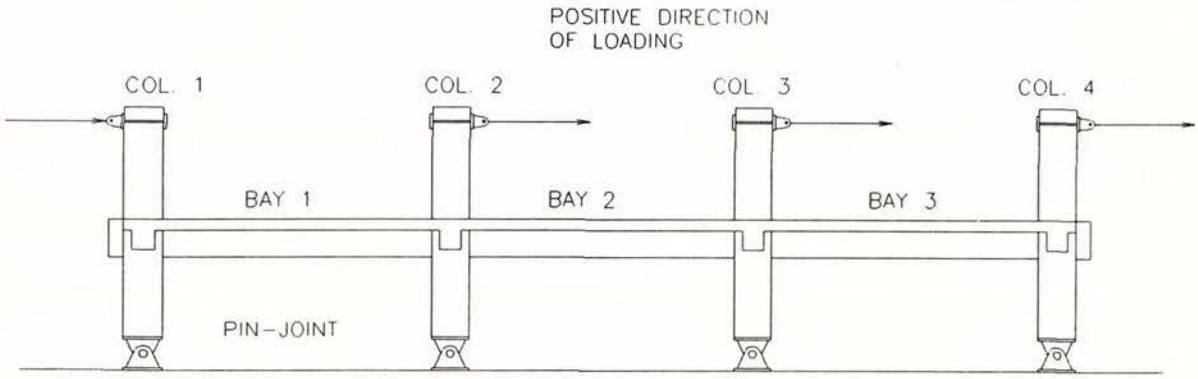

Fig. 3.2 - Schematic Setup of Both Test Units

3.3 DESCRIPTION OF UNIT 1: BEAM-COLUMN-SLAB UNIT

The main beam of this unit contained equal areas of top and bottom longitudinal reinforcement. The slab longitudinal reinforcement could act with the top reinforcement. The design considerations of NZS 3101 (1982) allow this additional slab reinforcement to be included in the calculation of the ideal flexural strength of the beam. As a result the negative ideal flexural strength was greater than the positive ideal flexural strength. In addition, as discussed in Section 2.5, NZS 3101 (1982) allows contributions of slab reinforcement for internal and external beam-column connections. These flexural strengths are presented in Table 3.1.

In calculating flexural overstrengths the nominal yield stress is usually factored by 1.25. This value is considered to be made up of two parts. First, an allowance of 10% is made since the nominal yield stress is likely to underestimate the actual yield stress. The second part, 15%, allows for strain hardening of the steel after yielding. For the calculation of flexural overstrengths in this project an overstrength factor of 1.15 was used since the actual yield stress of the reinforcement was known. The negative flexural overstrength was calculated assuming the contribution from all longitudinal reinforcement in the entire slab width. These flexural overstrengths are presented in Table 3.1. The transverse beams were included to support the slab and to provide restraint against possible torsional rotations.

The units were designed so that under cyclic loading reversing plastic hinges would form in the beams adjacent to the column faces. To ensure a "weak-beam strong-column" design, as recommended by NZS 3101 (1982), the ideal flexural strength of the internal columns was made 30% stronger than the flexural overstrengths of the beam. The corresponding value for the external columns was 88%. The main longitudinal flexural reinforcement in the beam consisted of five D10 bars running the full length of the unit in both the top and bottom of the section. The longitudinal flexural reinforcement of the column consisted of twelve D12 bars as shown in Fig. 3.3. Four additional D10 bars were placed in each internal column extending 400 mm above and below the joint zone to ensure this region remained elastic. The transverse beams contained three D10 bars in both the top and bottom regions as shown in Fig. 3.3.

To ensure that yielding of the beam longitudinal reinforcement of the main beam did not penetrate into the beam-column joint, additional bars were welded to four out of the five longitudinal flexural bars passing through both the top and bottom of the joint zone. This restricted the inelastic deformations to the potential plastic hinge zones adjacent to the column faces. This detail is illustrated in structural drawing of the unit which can be found in Fig. 3.3.

In addition the beam-column joint was substantially over-designed so that deformations in these regions were kept to a minimum. Five sets of 4-legged D6 stirrups were placed in each joint zone as detailed in Fig. 3.3.

Table 3.1 Ideal Flexural Strengths and Flexural Overstrengths of Unit 1

Location		Strength (kNm)
Column Ideal Flexural Strength	Internal Column	52.5
	External Column	45.0
Beam Ideal Flexural Strength	Positive Ideal	27.2
	Internal Connection Negative Ideal	34.65
	External Connection Negative Ideal	31.7
Beam Flexural Overstrength	Positive Overstrength	31.2
	Negative Overstrength	51.4

The calculated lateral force required to cause the ideal flexural capacity of the beam to be reached adjacent to the internal columns, $F_i^{(int)}$, was 47.6 kN. The corresponding values for the beam adjacent to the exterior columns, $F_i^{(ext)}$, were 27.2 kN and 31.7 kN for the positive and negative ideal flexural capacity of the beam respectively. The average value of these two values, which coincided with half of $F_i^{(int)}$ above was used in the elastic cycles to ensure the two to one force ratio was maintained. Similar calculations were made to find the overstrength lateral forces to enable the flexural overstrength capacity of the beam to be reached. A summary of these lateral force calculations are presented in Table 3.2.

Table 3.2 Ideal and Overstrength Column Lateral Force Capacities of Unit 1

Location	Ideal Capacity (kN)		Overstrength Capacity (kN)	
	Positive	Negative	Positive	Negative
Internal Column	47.6	47.6	62.8	62.8
External Column	21.2	24.2	227.2	31.7

To model the slab reinforcement deformed 4 mm diameter bars (D4) were used. When delivered, the yield stress of the steel was unacceptably high and the extension to failure was very small. By heat treating it, more acceptable values of yield stress and extension to failure were achieved. This involved heating the steel to 600° Celsius for half an hour and then annealing it to achieve a definite yield plateau in the stress-strain curve. Two batches of this steel were used in the unit with the second batch having a yield stress and extension to failure much larger than the first. However, though the same heat treatment was used for the second batch, which contained just a few bars, the yield stress was not reduced to the same extent as the first batch. These bars were placed in the centre of each slab in the transverse direction where it was expected to have very little influence on the behaviour of the unit. None of this second batch of reinforcement in the slab yielded.

The shear reinforcement, consisting of 3.125 mm diameter wire, which was used for the potential plastic hinge zones, was heat treated to achieve more realistic reinforcement characteristics as described above for the slab reinforcement. The remainder of the beam shear reinforcement was left untreated as these zones were designed to remain essentially elastic throughout both tests. The material properties are further described in Section 3.5.1.

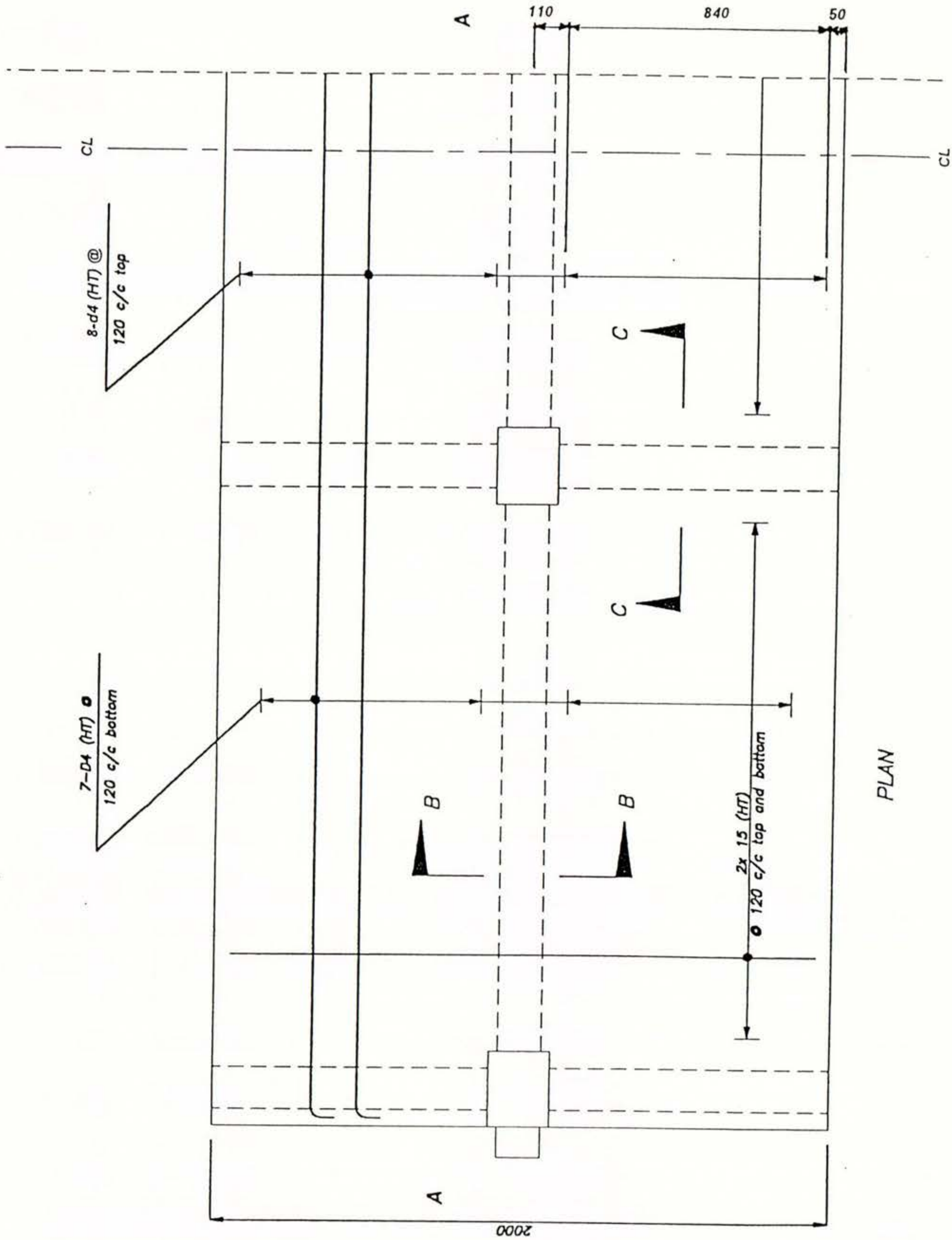

Fig. 3.3 - Reinforcing Details of Beam-Column-Slab Unit a) Plan

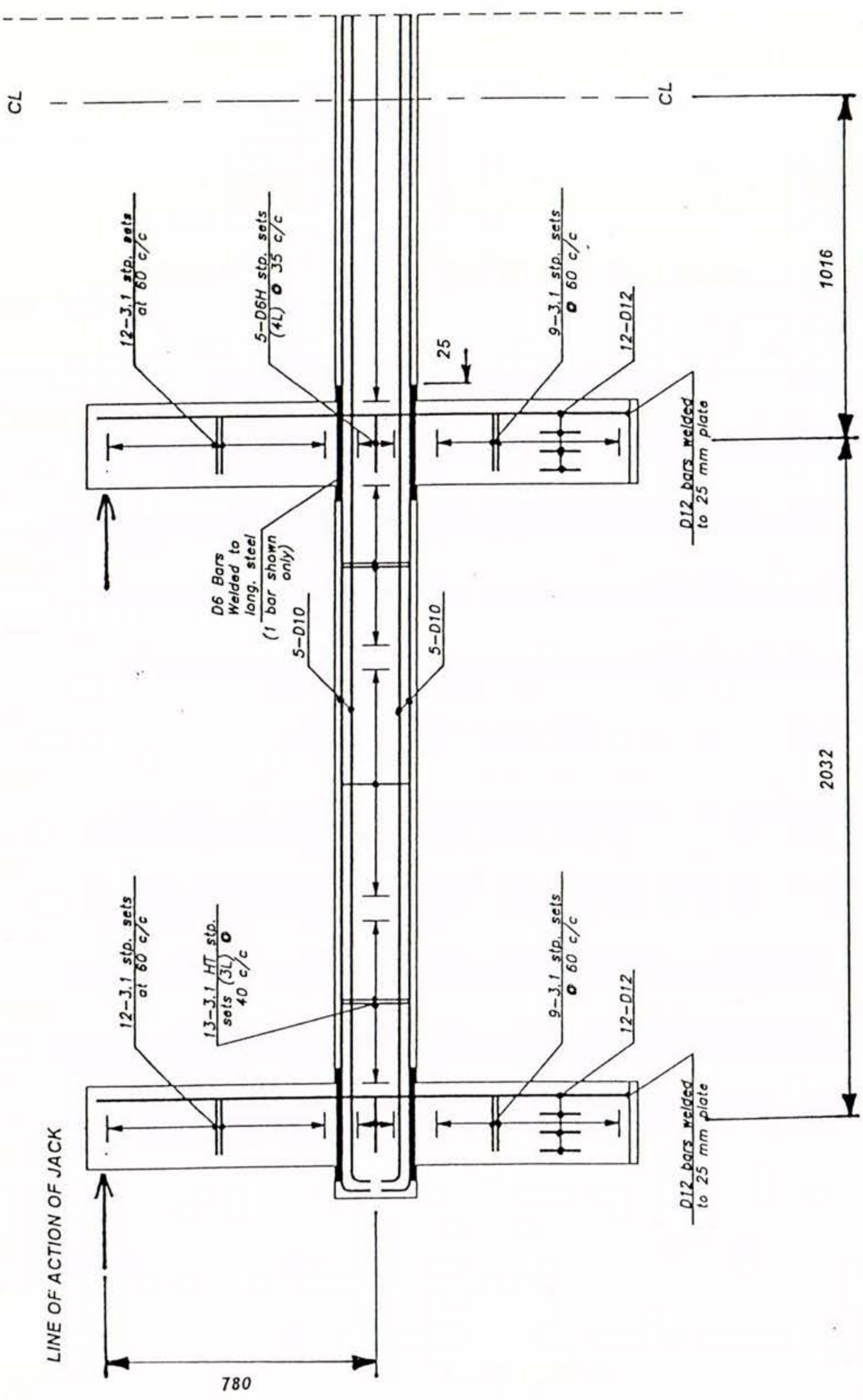

Fig. 3.3 - Reinforcing Details of Beam-Column-Slab Unit b) Section A-A

3.4 DESCRIPTION OF UNIT 2: BEAM-COLUMN UNIT

Except for the omission of the slab and transverse beams this unit was kept identical to Unit 1 to enable direct comparisons to be made. The detailing of this unit is shown in Fig. 3.4. The positive and negative ideal flexural capacities of the beam section were identical. As in the previous unit, additional D6 bars were welded to the beam flexural reinforcement where this passed through the joint zones to prevent their yielding progressing into the joints. The flexural overstrength of the beam was calculated assuming a 15% overstrength factor as discussed in Section 3.3. The column ideal flexural strength was 200% and 87.5% stronger than the beam ideal flexural strengths for the internal and external columns respectively. The ideal flexural strengths and overstrengths are presented in Table 3.3.

Table 3.3 Ideal and Ultimate Flexural Strengths of Unit 2

Location		Strength(kNm)
Column Ideal Flexural Strength	Internal Column	52.5
	External Column	45.0
Beam Ideal Flexural Strength		25.7
Beam Flexural Overstrength		29.2

The internal column lateral force required to cause the ideal flexural capacity to be reached, $F_i^{(int)}$, was 39.2 kN. The external column lateral force required, $F_i^{(ext)}$ was half this at 19.6 kN. These lateral forces as well the lateral forces required for the beam to reach the calculated flexural overstrength capacity are presented in Table 3.4.

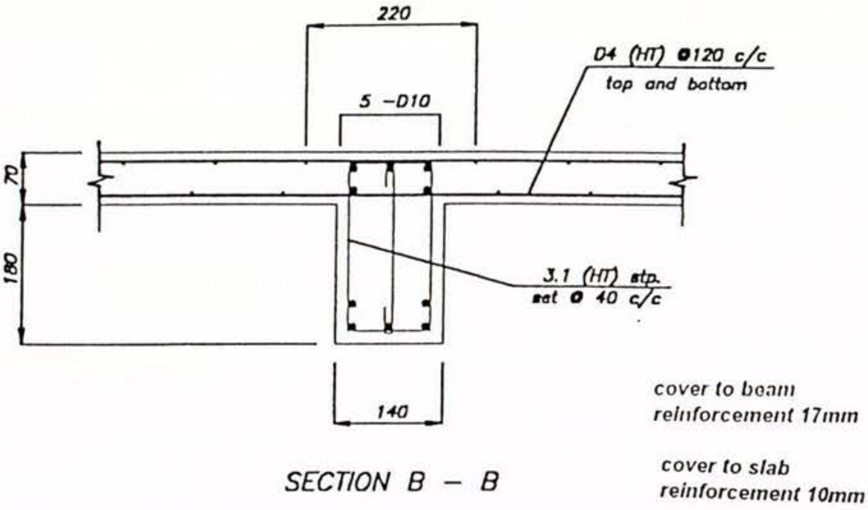

c)

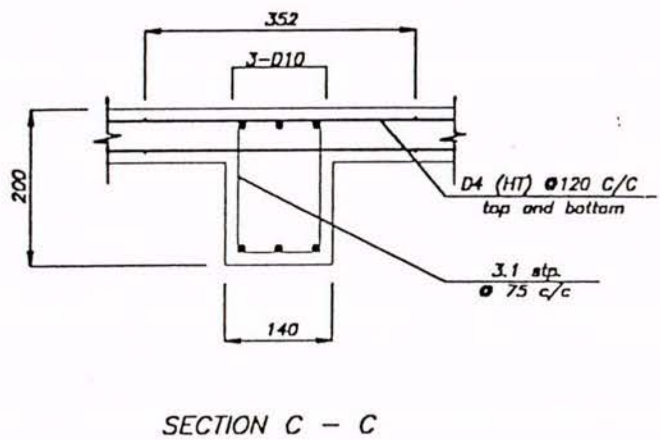

d)

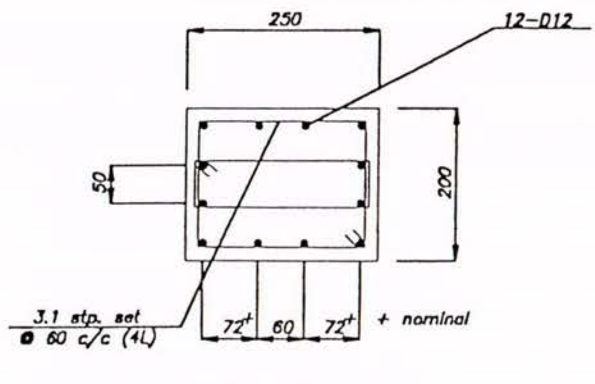

e)

Fig. 3.3 - Reinforcing Details of Beam-Column-Slab Unit; c) Section B-B Detail of Main Beam, d) Section C-C Detail of Transverse Beams, and e) Section D-D Detail of Columns

Table 3.4 Ideal and Overstrength Column Lateral Force Capacities of Unit 2

Location	Ideal Capacity (kN)	Overstrength Capacity (kN)
Internal Column	39.2	44.5
External Column	19.6	22.3

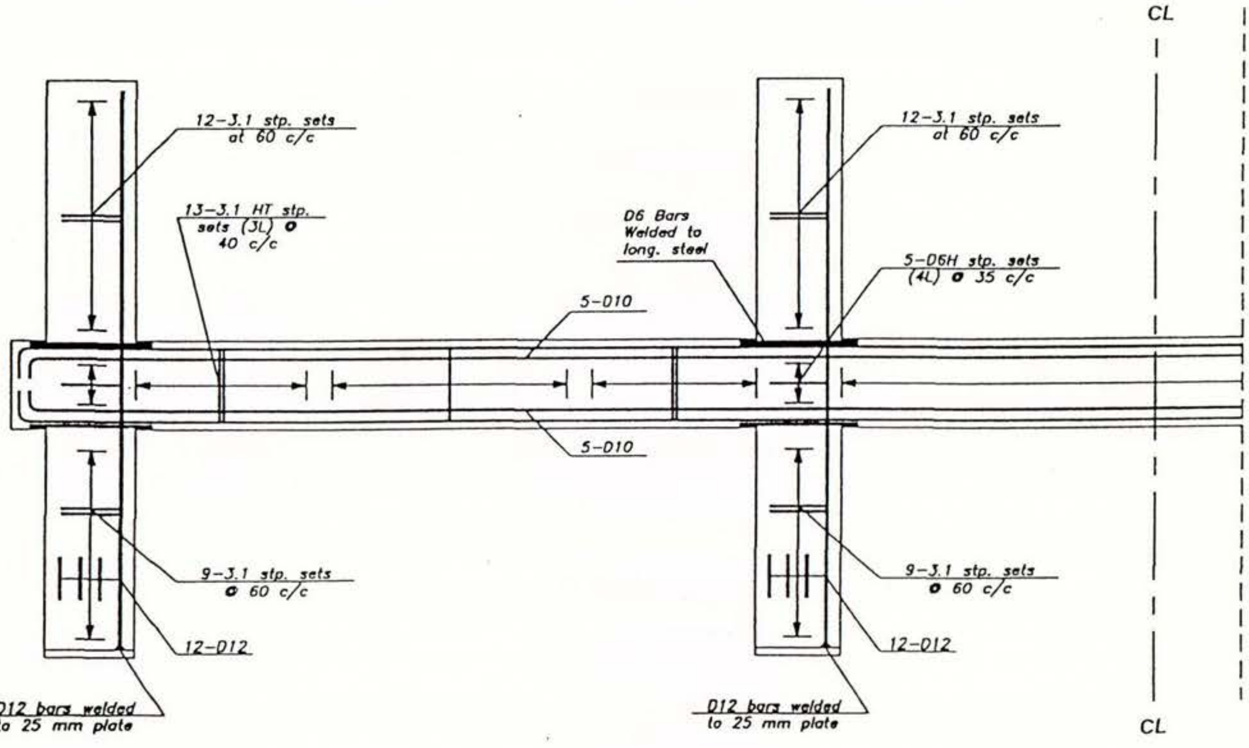

Fig. 3.4 - Reinforcing Details of Beam-Column Unit

3.5 TESTING OF MATERIALS

3.5.1 Reinforcing Steel

Axial tensile tests were carried out on samples of all the reinforcement used to determine the stress-strain relationships. The 4 mm deformed steel (D4) and the 3.125 mm diameter wire (Φ3.125) were tested on the Hounsfield H25KM axial loading unit located in the Strength of Materials Laboratory in the Department of Mechanical Engineering. The unit had a 20 tonne loading capacity and a 50 mm gauge length extensometer was used to measure the strain of each specimen. Not all specimens tested broke inside the measurement zone of the extensometer. However, enough did fail in this region to get repeatability of the stress-strain relationships and these are presented in Table 3.5. The stress and strain at specific locations as presented in Table 3.5 are defined in Fig. 3.5.

Tests on the beam-column joint zone reinforcement (D6) and the longitudinal flexural reinforcement (D10 and D12) were performed on the Avery universal testing machine located in the Test Hall of the Department of Civil Engineering. The joint and longitudinal flexural reinforcement for both units came from the same batch. These results are also presented in Table 3.5. All of the stress-strain curves for the successful tests are given in Appendix A.

3.5.2 Concrete Compression Testing

Cylinder crushing tests were carried out on test cylinders prepared for each pour used in the two test units. They were tested using the Contest Concrete Testing Machine located in the Civil Materials Laboratory. A total of 7 tests were carried out on specimens from Unit 1 and four from Unit 2. These results are presented in Table 3.6.

Table 3.5 - Reinforcing Steel Stress-Strain Properties for Tests Units

Description	f_y (MPa)	f_s (MPa)	ε_y	ε_s	ε_f
R3.125 stirrup steel	754 755	758 759	0.005 0.006	0.033 0.033	0.065 0.060
R3.125 (HT) stirrup steel	295 300	372 378	0.059 0.061	0.295 0.303	0.393 0.400
D4 (HT) Batch 1 slab reinforcement	356 359	414 415	0.058 0.060	0.175 0.184	0.177 0.203
D4 (HT) Batch 2 slab reinforcement	600 651	641 651	0.019 0.016	0.066 0.084	0.086 0.094
D10 Beam reinforcement	330	457	0.0019	0.151	(i)
D12 Beam reinforcement	317	480	0.0062	.236	(i)

(i) = Test specimen unloaded before failure

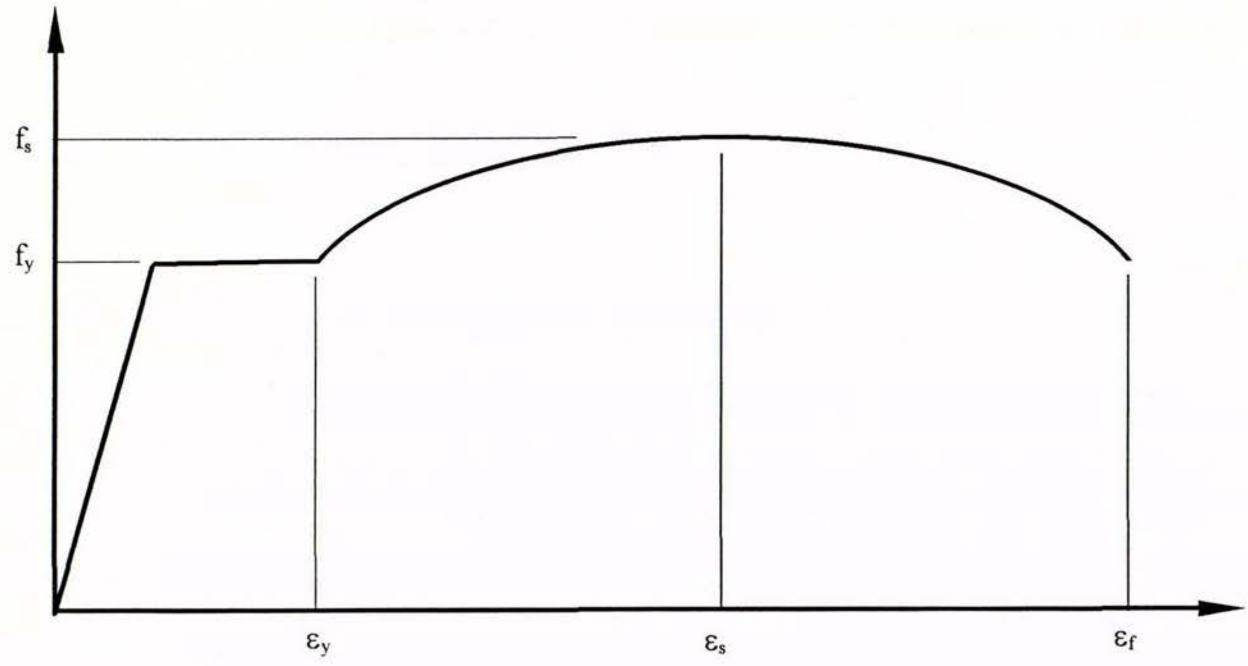

Fig. 3.5 Idealised Reinforcing Steel Stress-Strain Curve

Table 3.6 - Concrete Properties

Location	Number of Tests	Slump (mm)	Age at Test (Days)	Comp. Strength f_c' (MPa)
Unit 1				
Bottom of Columns	2	100	99	35
Slab, Main and Transverse Beams	3	85	90	36
Top of Columns	2	80	83	36
Unit 2 Whole Unit	4	80	74	33

3.6 CONSTRUCTION OF UNITS

3.6.1 Formwork

The beam and column formwork for both units was constructed using 12.5 mm thick particle board stiffened by 50 mm by 50 mm timber batten framing. The slab formwork was propped off the floor to prevent sagging during casting. Unit 1 was cast in a vertical position while Unit 2 was cast 'on its side' and turned through 90° before being tested.

3.6.2 Reinforcement

The vertical longitudinal flexural steel in the columns was welded to 25 mm plates at the base of the columns. Each plate had threaded studs welded to the underside so that the one-way pin joints at the base of the columns could be bolted to them. This detail is illustrated in Fig. 3.6. The beam and column reinforcement cages were constructed first and then lifted into the formwork. Standard reinforcing ties and 17 mm plastic concrete spacers were used to ensure the correct position and cover for the longitudinal reinforcement in the main beams and columns.

The D4 slab steel was cut in 2 m lengths to be heat-treated and it was then butt welded to achieve the required length. Ten millimetre deep precast concrete spacers were used to ensure the correct cover for the bottom reinforcement was maintained. The top steel was tied in place to the bottom formwork at the correct height to stop it moving during pouring. The reinforcement of both units is shown in Figs. 3.3 and 3.4.

3.6.3 Concreting of Units

Unit 1 was cast in three pours. The first pour involved concreting the lower portion of the columns to the level of the underside of the main beam. The concrete mix for this pour included cement, sand and crusher fines (Stevenson's PAP 7) and water. In addition water reducer and superplasticiser was used to get a slump of approximately 100 mm. This ensured that the concrete could be poured from the top of the column reinforcement into the formwork. In the second the concrete in the slab, longitudinal and transverse beams and the beamcolumn joints was cast. The concrete was purchased from a ready mix company. It had a maximum aggregate size of 10 mm and a slump of 85 mm. Construction joints between pours two and three were formed approximately 80 mm above the top of the slab level. The final pour completed the upper portion of the columns. Steel wire strops were anchored 400 mm into the tops of the columns and looped to enable the unit to be lifted to have the hinges fitted.

Unit 2 was cast on its side in one pour. The concrete for this pour was purchased from a ready mix company. The maximum aggregate size was 10 mm and the slump was 80 mm. The exposed concrete in both units was kept wet with hessian fabric and wet sacks for a period of seven days. During this period the units were covered with polythene sheeting and additional water was poured onto the hessian fabric to ensure it remained wet.

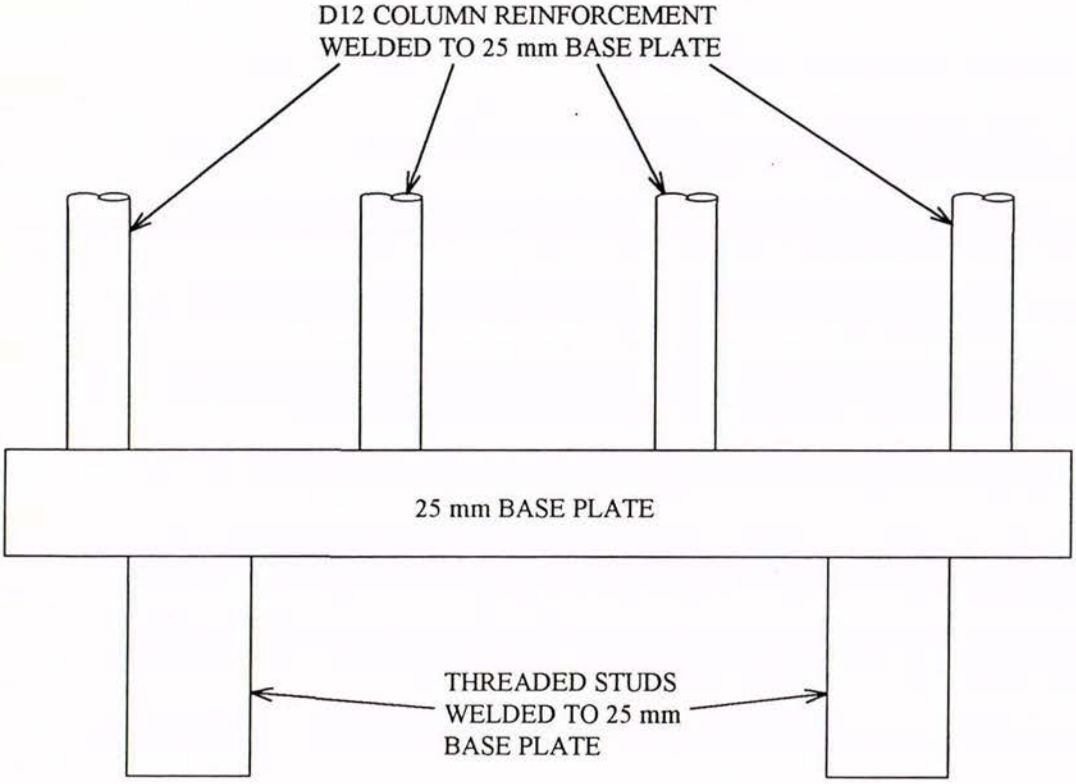

Fig. 3.6 - Column Base Plate Details

3.7 LOADING FRAMES AND COLUMNS

Different loading frames were used for each of the units. These are shown in Fig. 3.7. The main consideration in the design of the loading frames was the need to apply independent lateral forces to all four columns as described in Section 3.2. The cyclic lateral forces were applied to the columns by two 5 tonne reversing hydraulic jacks for the external columns and two 10 tonne reversing hydraulic jacks for the internal columns. Each hydraulic jack was operated by hand using two way hydraulic hand pumps.

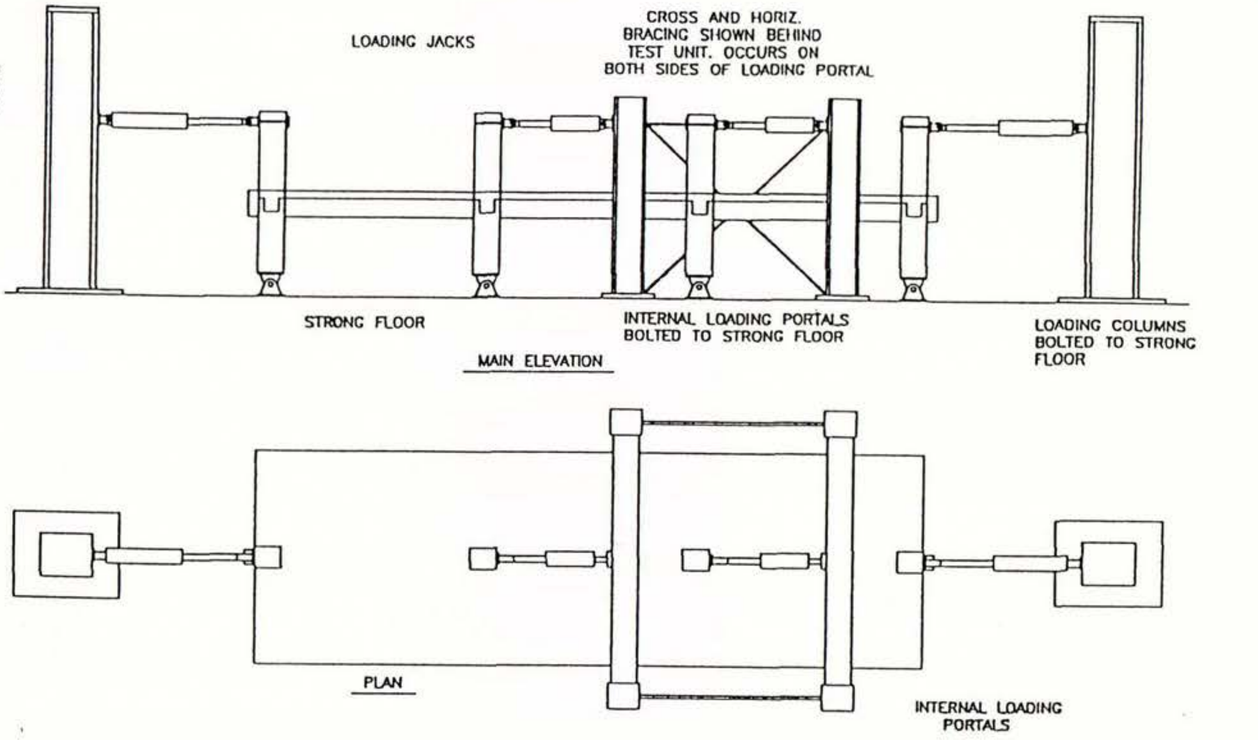

Fig. 3.7 a) - Loading Frame Detail; Unit 1

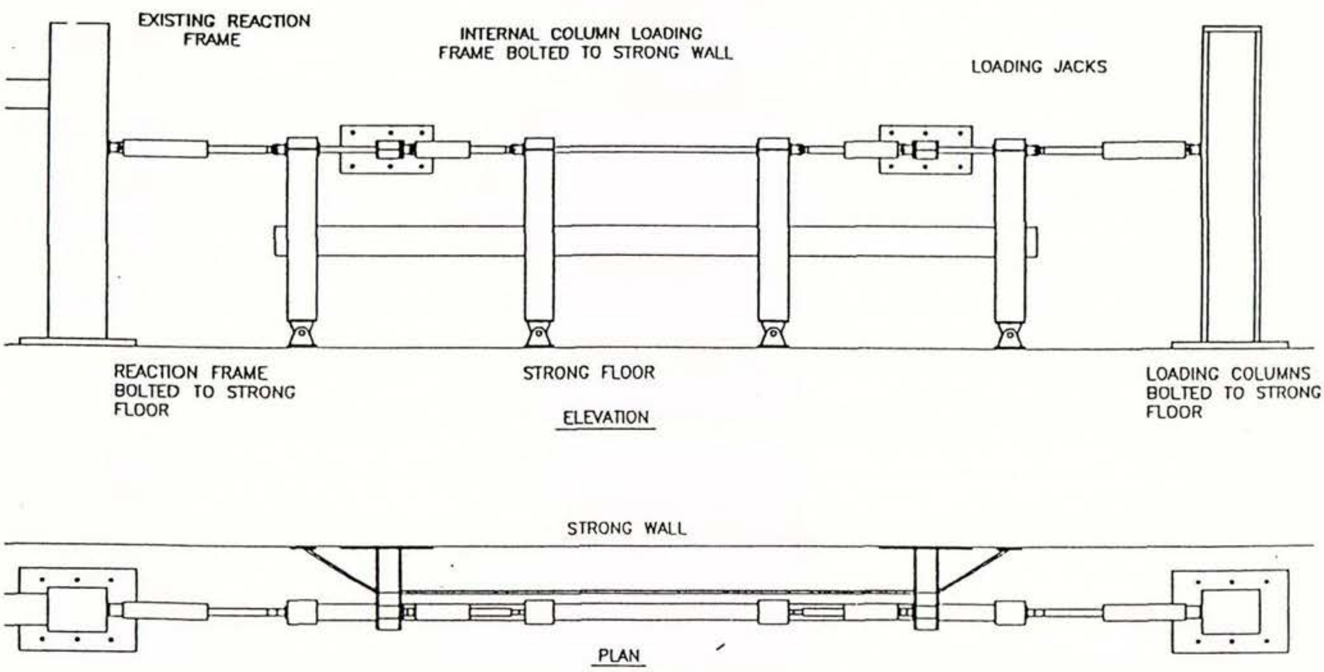

Fig. 3.7 b) - Loading Frame Detail; Unit 2

3.8 INSTRUMENTATION

Except for the measurements of the slab deformations in Unit 1, measurements of the various parameters explained in this section were similar for both units. Hence the following discussions are written primarily to define the instrumentation in both units. Deformations in the columns were not measured, but it was clear from the crack pattern that they remained elastic. The column deformations were calculated. The moment of inertia, I, was calculated assuming a cracked transformed section while the modulus of elasticity for the concrete was calculated Eqn. 3.1 from the Concrete Code [NZS 3101 (1982)].

$$E_c = 4700\sqrt{f'_c} \qquad \textbf{(3.1)}$$

3.8.1 Measurement of Lateral Forces Applied to the Columns

These were measured using load cells which were coupled to the reversing hydraulic jacks. They had previously been calibrated on the MTS Structural Test Machine in the Civil Materials Laboratory in both tension and compression.

3.8.2 Measurement of Displacements

Linear Variable Displacement Transducers (LVDTs) were used to measure the displacement of each column and the deflection of the centre-line of the main beam at each end of the units. They were calibrated previously on the MTS Structural Test Machine in the Civil Materials Laboratory. Hand measurements were taken at each of the above six measurements points at cycle peaks and at the zero force position as a check on the LVDTs.

3.8.3 Measurements of Beam Deformations

One top and bottom longitudinal bars on one side of the beam had studs tack welded to them after fabrication of the reinforcement cages so that beam deformations could be measured from these points. 30 x 17 x 6 mm steel plates were welded to the same longitudinal bars at the column faces for mounting the instrumentation. They extended into the column to reduce the buckling of the reinforcing bars at large inelastic deformations which would have affected the readings. These details are shown in Fig. 3.8 a) and b).

Aluminium discs were fixed to the steel studs and plates by allen screws [see Fig. 3.8 a)]. Steel rods to these these discs and the portal displacement transducers as shown in Fig. 3.8 c). A sliding rod system was fitted at each portal transducer to restrict shear displacements across the portal.

These portal transducers were used on both units to measure the components of deformation in the main beam. These components were:

(1) elongation of the main beam,
(2) rotations throughout the main beam,
(3) flexural deformation of the main beam,
(4) shear deformation within each main beam plastic hinge, and
(5) extensions along the top surface of the slab at various positions for the beam-column-slab unit.

The flexural and shear deformations were calculated separately for each bay as a component of the mid-span lateral displacement. This enabled them to be compared with the interpolated measurements from the two mid-height LVDT readings.

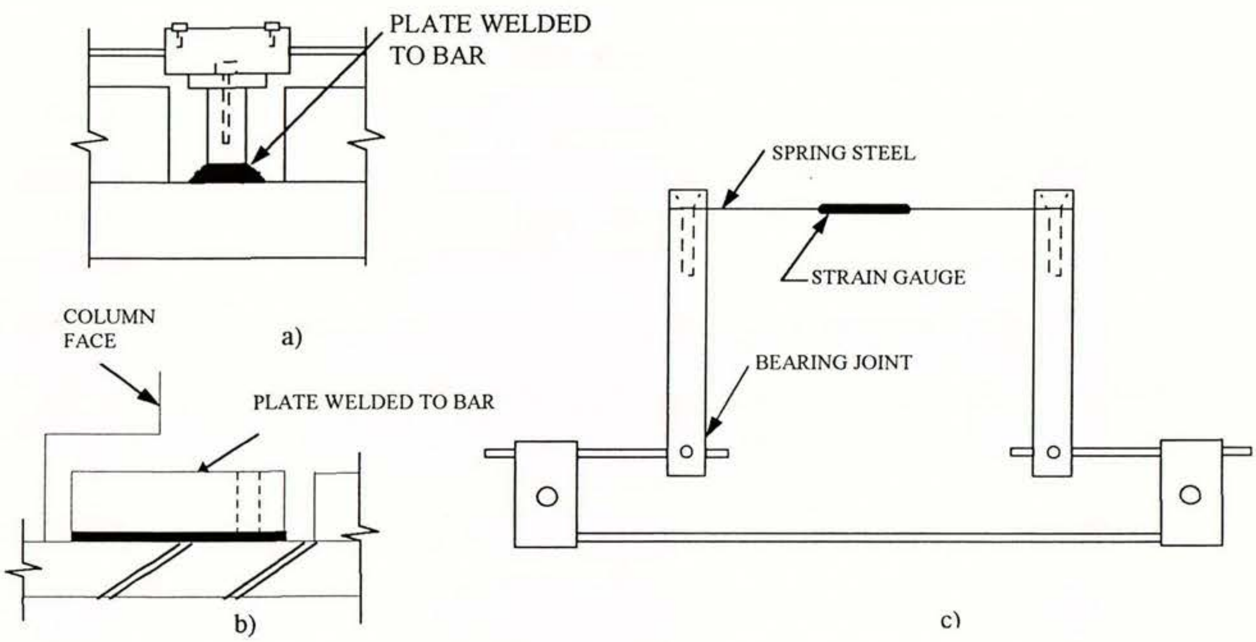

Fig. 3.8 Details of Mounting Studs, a) and Plates, b) and Portal Displacement Transducers c)

The instrumentation used for Unit 1 is shown in Fig. 3.9. Measurements were taken in four discrete segments of beam in each bay. These were the two potential plastic hinge zones and two segments between these with their boundary at the mid-span region. The elongation at the centre-line of each segment of the main beam could be calculated from the extension of the top and bottom of each segment from Eqn. 3.2;

$$\delta l = k_t \delta_t + k_b \delta_b \tag{3.2}$$

Where, δl is the beam elongation,

δ_t and δ_b are the extensions of the top and bottom portal transducers,

k_t and k_b are weighted average factors to take account of the distance from the portals to the centre of the mid-height of the beam.

For unit 1 $k_t = 0.435$ and $k_b = 0.565$ while both factors equal 0.5 for unit 2.

Assuming the columns are rigid, then lateral deflection of the mid-span of each bay due to flexural deformation and elongation, δ_{fl}, is given by Eqn. 3.3. This methodology is illustrated in Fig. 3.10 a) and b).

$$\delta_{fl} = \frac{(\theta_1 + \theta_2)\, h_c}{2} \tag{3.3}$$

where, θ_1 and θ_2 are the rotations of the columns and

h_c is the distance from the base of the columns to the beam centre-line.

From the geometry of Fig. 3.10 a) then θ_1 and θ_2 are given by Eqn. 3.4 a)and b).

$$a) \quad \theta_1 = \frac{\Delta_1}{L} \qquad\qquad b) \quad \theta_2 = \frac{\Delta_2}{L} \tag{3.4}$$

where, Δ_1 and Δ_2 correspond to Fig. 3.10 a) and

L is the distance between the column centre-lines.

The rotations of the discrete segments can be used to calculate Δ_1 and Δ_2 as shown in Fig. 3.10 b). Δ_1 and Δ_2 are give by Eqn. 3.5 a) and b).

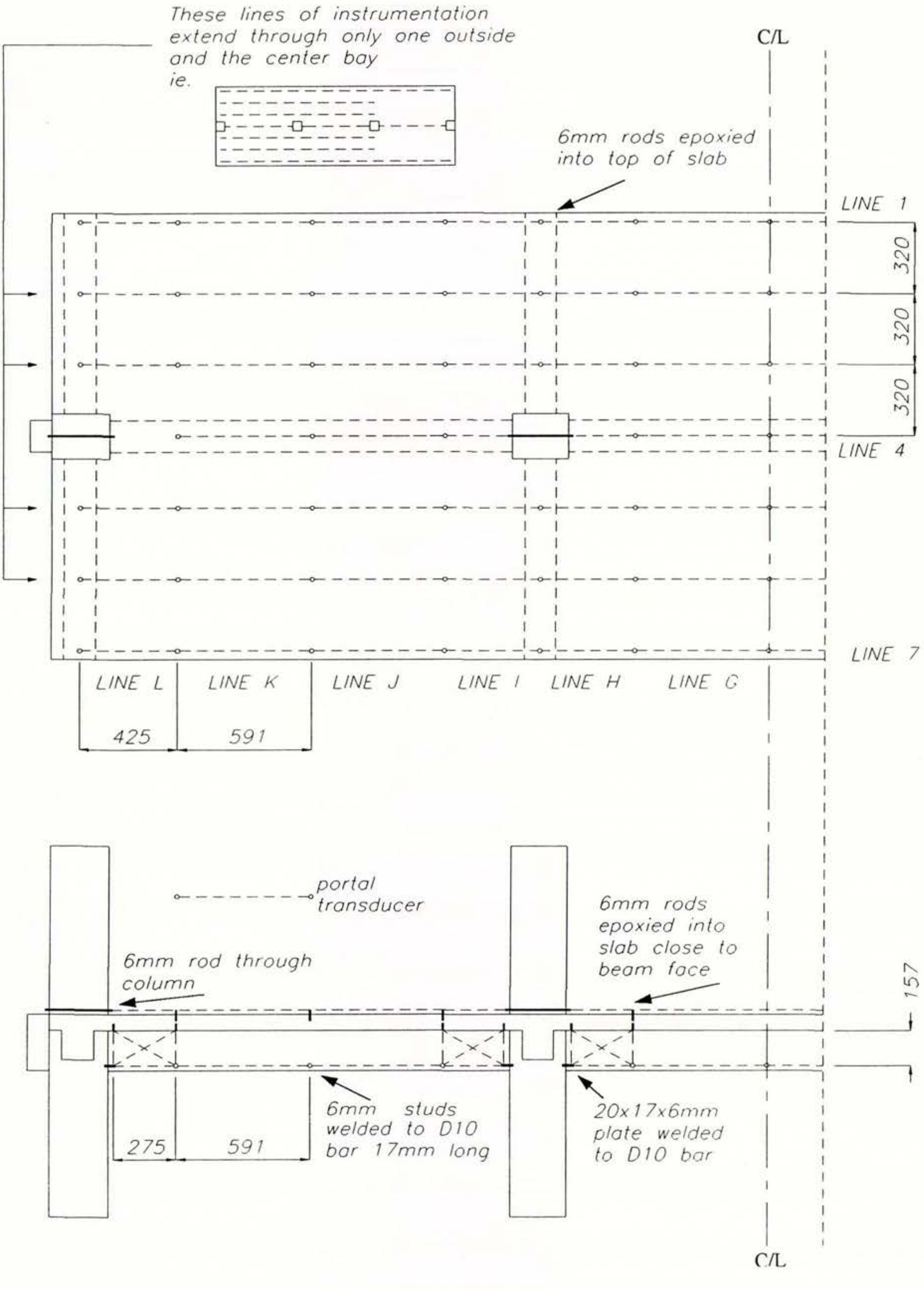

Fig. 3.9 - Instrumentation Setup of Beam-Column-Slab Unit

$$\Delta_1 = \theta_a x_a + \theta_b x_b + \theta_c x_c + \theta_d x_d \qquad \text{a)}$$

$$\Delta_2 = \theta_a(L - x_a) + \theta_b(L - x_b) + \theta_c(L - x_c) + \theta_d(L - x_d) \qquad \text{b)} \; \textbf{(3.5)}$$

where, θ_n is the rotation of each segment and

x_n is the distance to the centroid of each segment as shown in Fig. 3.10 b).

The rotation, θ_n, of each segment of beam is given by Eqn. 3.6:

$$\theta_n = \frac{\delta_t - \delta_b}{h} \qquad \textbf{(3.6)}$$

where h = the distance between the top and bottom portal transducers.

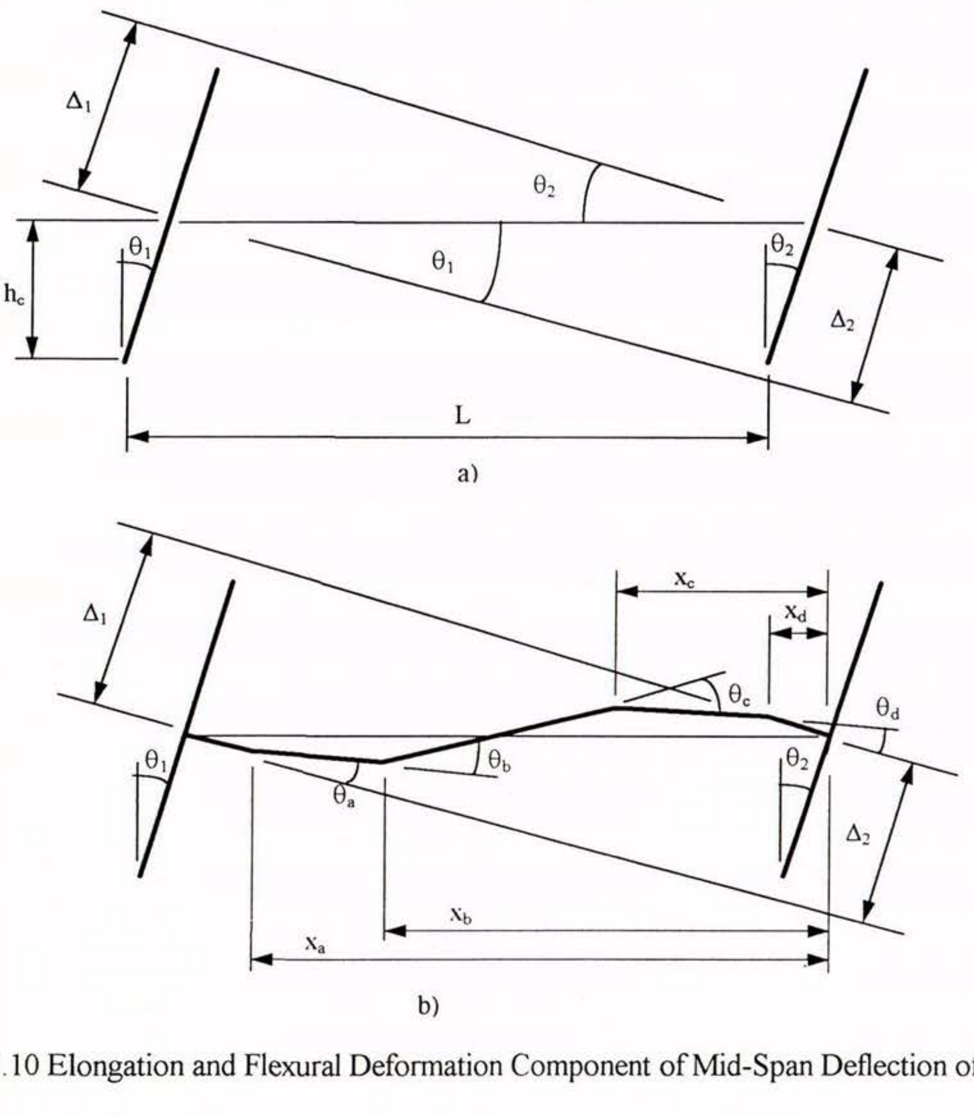

Fig. 3.10 Elongation and Flexural Deformation Component of Mid-Span Deflection of Each Bay

The lateral deflection of the mid-span of each bay due to shear deformation of the beam can be calculated from the sum of the beam deformations recorded in each segment. By considering Fig. 3.11, Eqn. 3. 7 can be obtained.

$$\delta_s = (s_a + s_b + s_c + s_d)\frac{h_c}{L} \qquad \textbf{(3.7)}$$

where s_n is the shear deformation of each segment.

The shear deformation of each segment, s, is calculated using the diagonal portal transducers so that it is given by;

$$s = \frac{(\delta_{di} - \delta_{di}')}{2\cos\alpha} \qquad \textbf{(3.8)}$$

where, δ_{di} and δ_{di}' = the diagonal portal extensions in each segment and
α = the angle the diagonal portal transducers makes with the horizontal portal transducers.

The deformations in the Joint zone of Unit 1 were not measured because of the existence of the transverse beams.

In Unit 2 deformations throughout the main beam and the beam-column joint zones were measured using the instrumentation set-up shown in Fig. 3.12. Each of the components of deformation (flexural deformation, elongation and shear deformation) were calculated in the same way as above. A limited number of deformation measurements were made by a vernier gauge as a check for possible errors in the transducers. No errors were found.

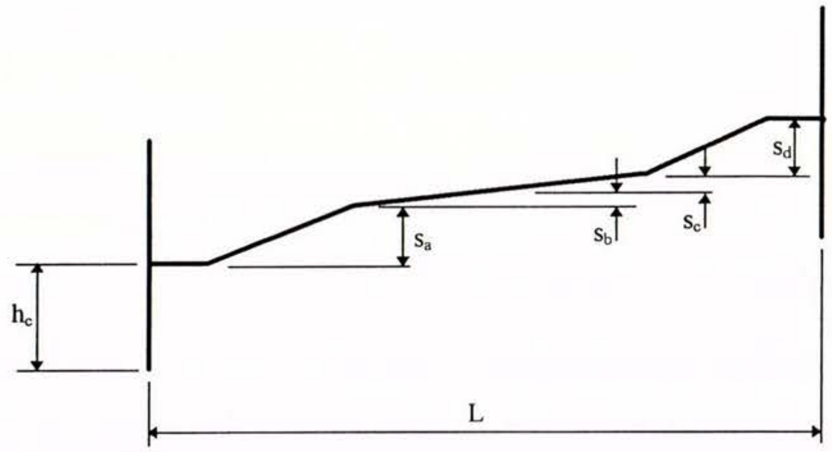

Fig. 3.11 Shear Component of Mid-Span Deflection of Each Bay

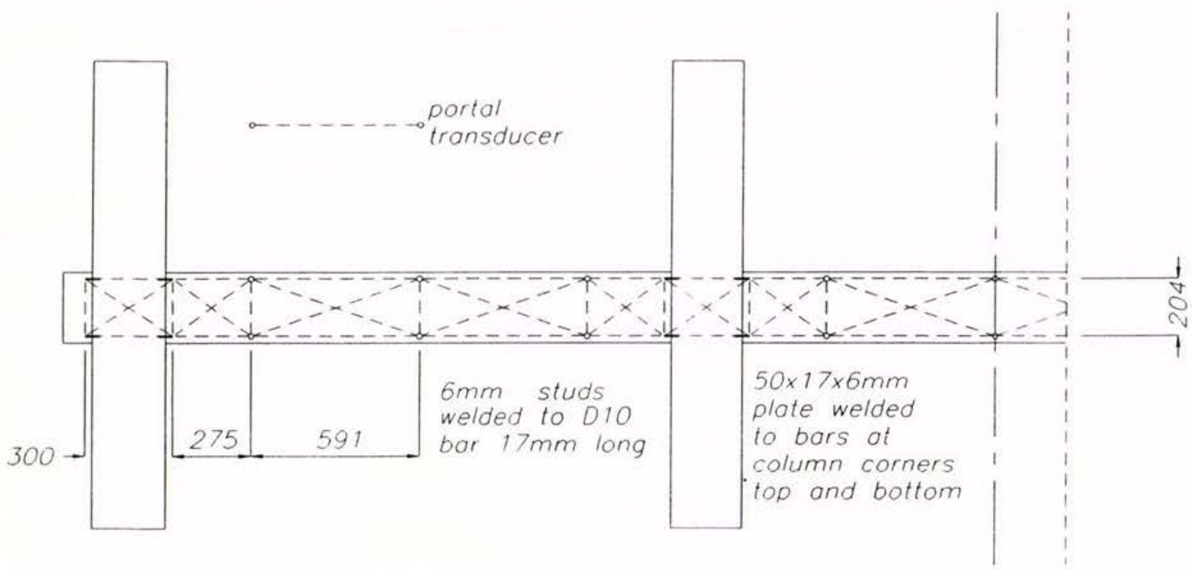

Fig. 3.12 - Instrumentation Setup of Beam-Column Unit

3.9 TEST SEQUENCE AND PROCEDURE

Cyclic forces were applied to the loading jacks on each column in small increments using hand pumps. At each load increment all instrumentation was scanned by the data-logging system and at cycle peaks hand measurements were taken. Photographs to record the crack patterns were also taken. Prior to unloading a second scan of the instrumentation was taken. Generally there was a delay of about forty minutes between these sets of readings and some relaxation of forces occured during this interval.

The procedure used at the University of Auckland in many previous tests was followed. The main beam lateral displacement at mid-span of the centre beam was taken as the reference for controlling the testing. The test units were initially subjected to two cycles of lateral forces equivalent to three-quarters the ideal lateral load capacity, F_i, of the unit. From these force controlled cycles the first yield, or ductility one displacement, was predicted by extrapolating linearly from the cycle peak force and displacement to the lateral ideal force. Following the load controlled cycles the units were subjected to inelastic displacement controlled cycles to predetermined values of displacement ductility. Two complete loading cycles were performed at each ductility level as illustrated in Fig. 3.13. Testing was completed when the unit would not sustain 80% of its theoretical lateral force capacity.

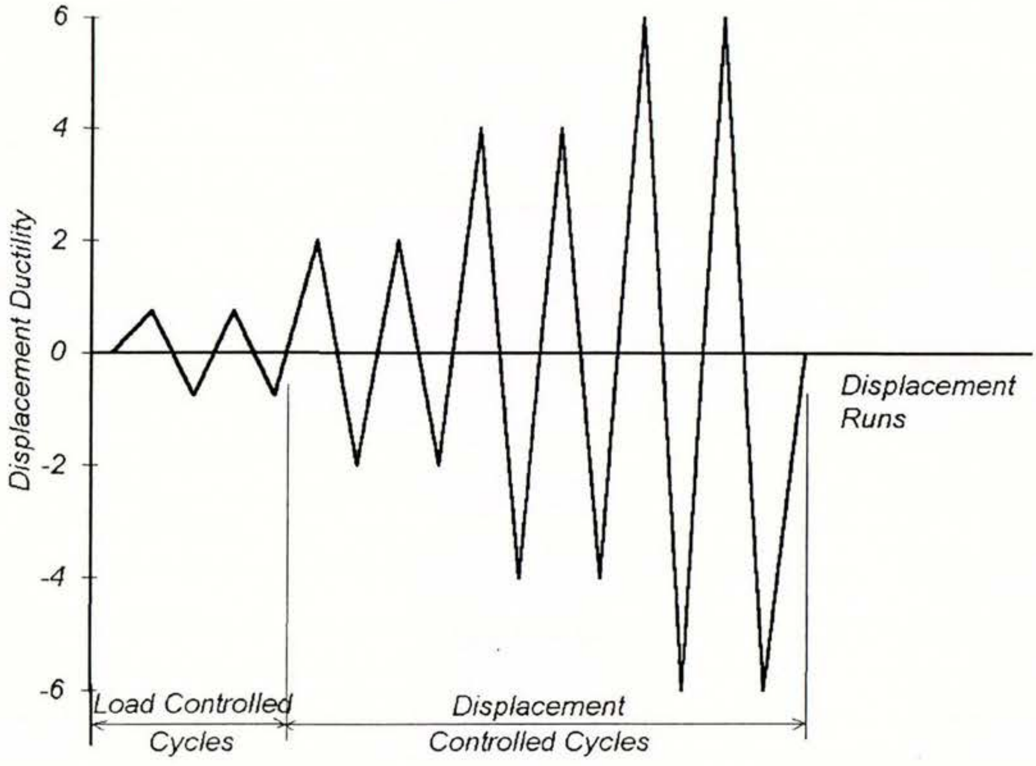

Fig. 3.13 - Loading Sequence For both Tests

3.10 SUMMARY

This chapter describes the design and construction for two beam-column units representing an upper level of a three bay internal frame. The units were designed according to NZS 3101 (1982). Specific consideration was given to the effect of composite slabs on the elongation of reinforced concrete beams. Descriptions of each unit including materials, construction and instrumentation are given. Sufficient ductility was achieved for the D4 and Φ3.125 reinforcement by heat treating.

The test procedure and sequence used for testing the two units is described with particular reference to the method in which the tests were conducted under quasi-static displacement controlled inelastic cyclic loading conditions.

CHAPTER 4

TEST RESULTS OF UNIT 1: BEAM-COLUMN-SLAB UNIT

4.1 INTRODUCTION

This chapter presents test results from unit 1. It includes the force-displacement response for each column and the overall force-displacement response for the unit. By comparing elongation measurements with the results from the unit without the slab, the effect of the slab on the elongation of the main beam could be determined. The concept of the effective width contribution of the slab is discussed in relation to the distribution of extensions from the centre of the slab. These results are presented in terms of the displacement ductility as defined in Section 3.9.

4.2 GENERAL BEHAVIOUR

The initial elastic cycles of the test were performed over a period of two days. Reduction of results and extensions of the portal transducers was carried out over the following ten days with the inelastic cycles being performed over the following eight days. In total the entire testing from the commencement of the elastic cycles to the completion of the ductility six cycles took approximately three weeks.

All four columns of the unit appeared to behave elastically and only fine flexural cracks on the tension faces were observed. The transverse beams also appeared to remain elastic, although a limited amount of diagonal cracking was noted in the beams extending from the external columns, as shown in Fig.s 4.1 a) and b). This cracking was first noted during the $\pm 4\mu$ cycles. All of the cracks appeared to extend from the intersection of the column with the top surface of the slab and project downwards at approximately 45° - 60° to the horizontal so that they reach the bottom surface at about one transverse beam depth away from the column face.

Fig. 4.1 - Cracking in Transverse Beams Extending from External Columns

These cracks were all no wider than 0.5 mm at the end of the test. There was no evidence of torsional failure in the transverse beams such as was reported by Pantazopoulou and Moehle (1987).

During the half cycle to the peak displacement ductility of +4μi, a wide crack formed in the slab in the middle bay as shown in Fig. 4.2. It's formation was accompanied by a loud noise which was likely to have been caused by the fracture of some of the longitudinal reinforcement in the slab on one side of the main beam, see Fig. 4.2. The crack allowed the unit to bow out of plane slightly which in turn caused the further opening of the crack on one side of the slab. At the end of the test the concrete on either side of the crack was carefully broken back to expose the longitudinal bars running across it. All top and bottom longitudinal bars (a total of 15) had all fractured on this side of the slab. Further discussion of the effect of this crack can be found in Section 4.4.2.

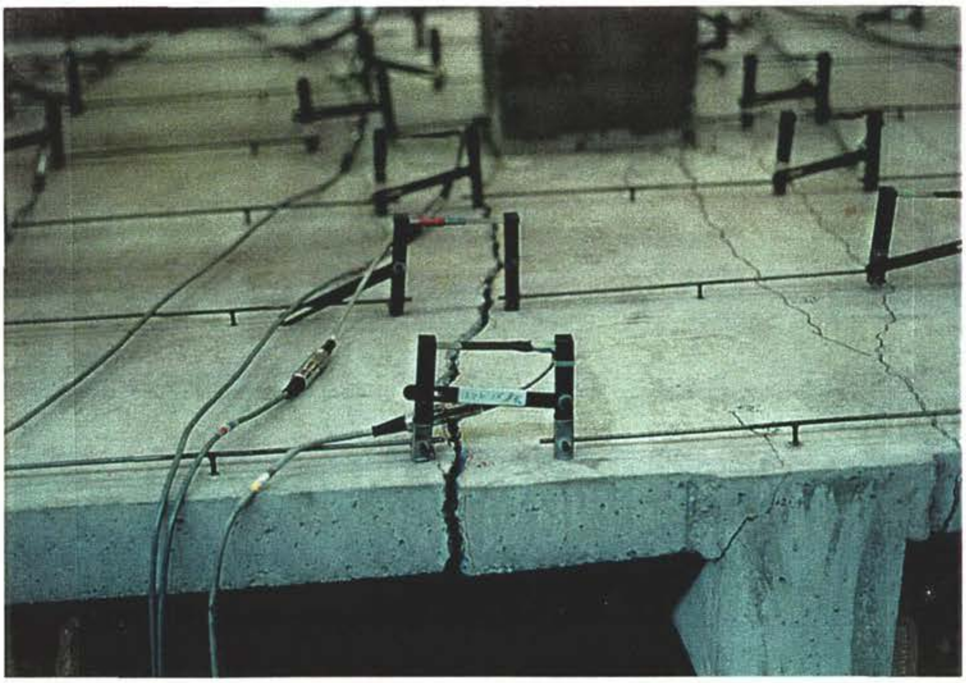

Fig. 4.2 - View of main wide crack at time of occurrence (during +4μi).

Cracking in the main beam was concentrated in the hinge zones with only minor cracks forming in the mid-span regions. Diagonal shear cracking was well defined by the completion of the ±2μ cycles. In these cycles the cracks in the beams' compression zones did not fully close, indicating an overall residual elongation of the longitudinal reinforcement in the main beam. The main cracking was established and stabilised during the first cycle of each ductility level and only minor crack development occurred in the second cycle of each ductility level. The progression of cracks at various stages throughout the test is shown in Fig.s 4.3 a), b), c), and d) for the external plastic hinge zone of beam 1 (at column 1 - see Fig. 3.2).

a)

b)

Fig. 4.3 - Progression of Cracks at Joint 1 of Beam-Column-Slab Unit

c)

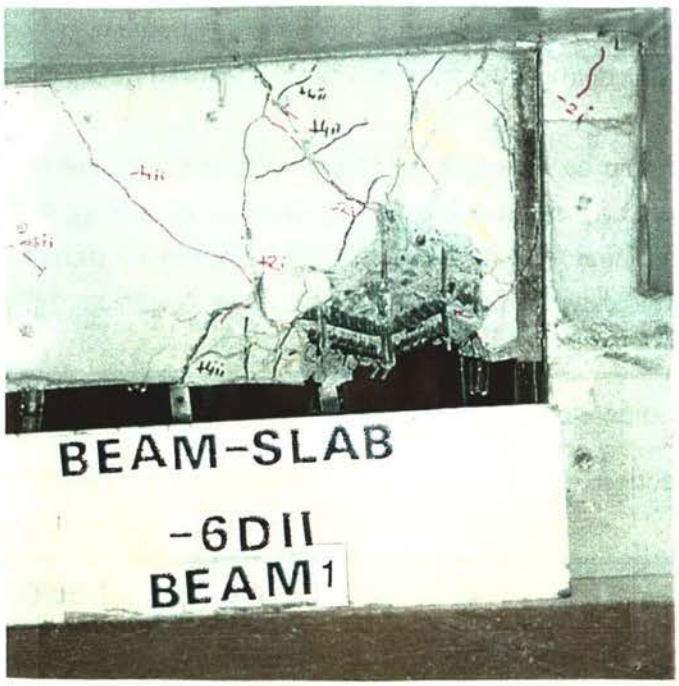

d)

Fig. 4.3 - Progression of Cracks at Joint 1 of Beam-Column-Slab Unit

During load stage +6μii the displacement of column 4 exceeded the travel limit of the instrumentation. This would have jeopardised both the column displacement measurement and the mid-depth beam measurement. It was decided that the unit should be unloaded so that the problem could be rectified. This effected the force-displacement response of the columns and overall unit together with the elongation measurements. The pattern of the unloading and subsequent reloading can be seen in Figs. 4.4 to 4.7 and Fig. 4.9. The reloading path did not follow the unloading path as might be expected.

4.3 FORCE DISPLACEMENT RESPONSE

4.3.1 Individual Column Response

The force-displacement response for each individual column is shown in Fig.s 4.4, 4.5, 4.6 and 4.7. The continuous relaxation of forces that occurred, resulted in the force-displacement response appearing irregular, particularly just prior to the peak of each run. The relaxation of forces when the large crack (discussed in Section 4.2) formed can be seen during the half cycle to the peak of displacement ductility +4μi. On columns 2 and 3, a significant reduction in the applied lateral forces occurred at this point. Redistribution of these forces simultaneously caused an increase in the applied lateral force on column 4 to accommodate the reduced forces in columns 2 and 3.

From Fig.s 4.4 to 4.7 it can be seen that the column displacements are not symmetrical in each direction. The movement of the first column in the direction of loading was the smallest and the movement of the last column was the greatest. This pattern of movements applied to both directions of loading, as indicated in Table 4.1.

Table 4.1 - Comparison of Column Displacements at the Peaks of Cycle ±4μi

Cycle	Direction	Column 1 Displ. (mm)	Column 2 Displ. (mm)	Column 3 Displ. (mm)	Column 4 Displ (mm)
+4μi	⇒	43.1	49.3	50.6	74.5
-4μi	⇐	-51.0	-41.7	-28.5	-19.6

This pattern was due to the elongation of the beams between each column and is discussed in Section 4.4.1.

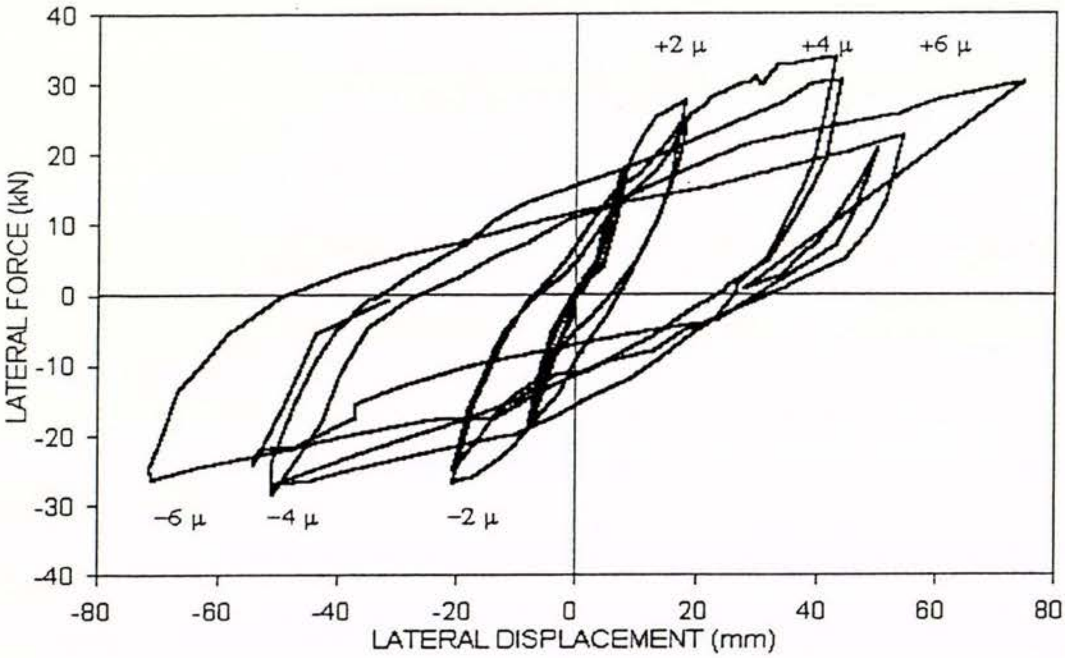

Fig. 4.4 Force-Displacement Response of Column 1 of Unit 1

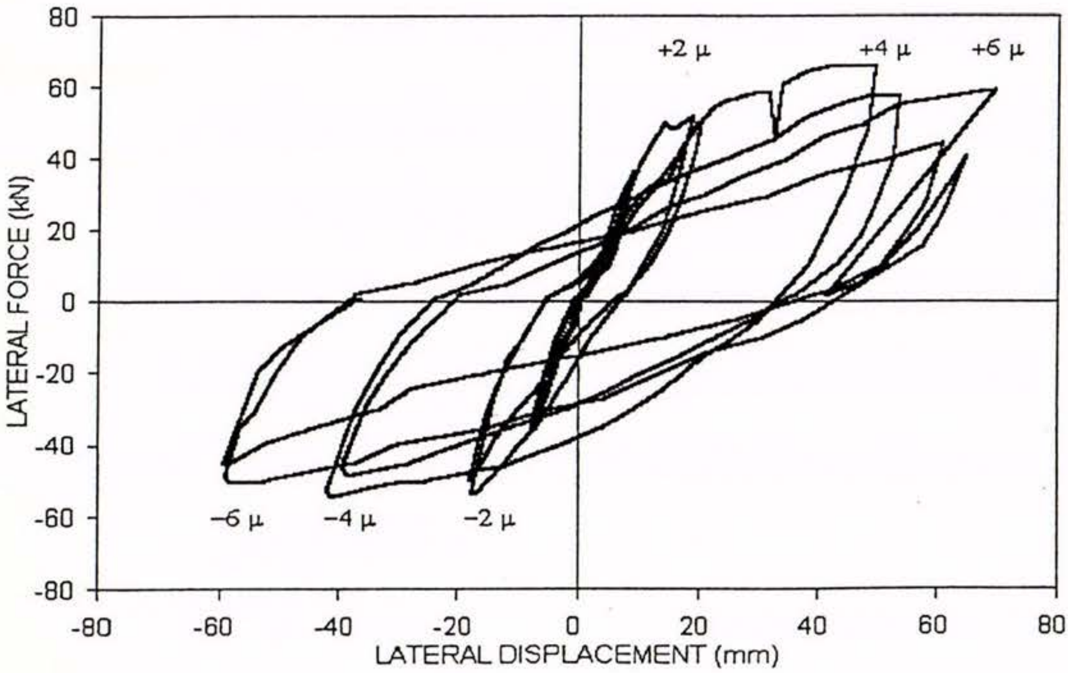

Fig. 4.5 Force-Displacement Response of Column 2 of Unit 1

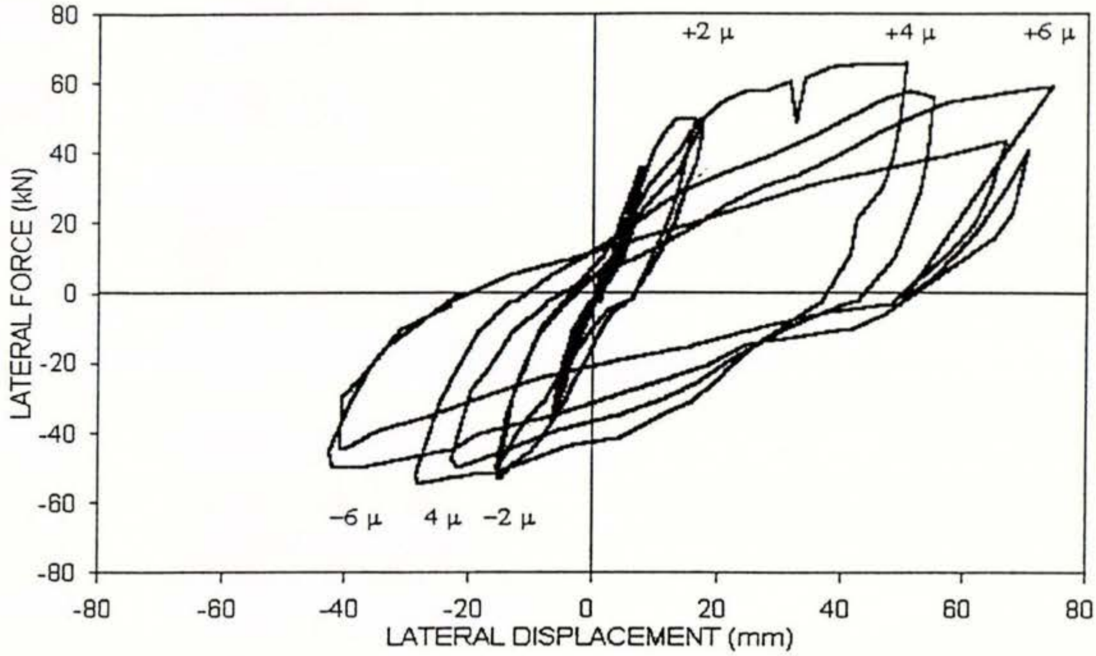

Fig. 4.6 Force-Displacement Response of Column 3 of Unit 1

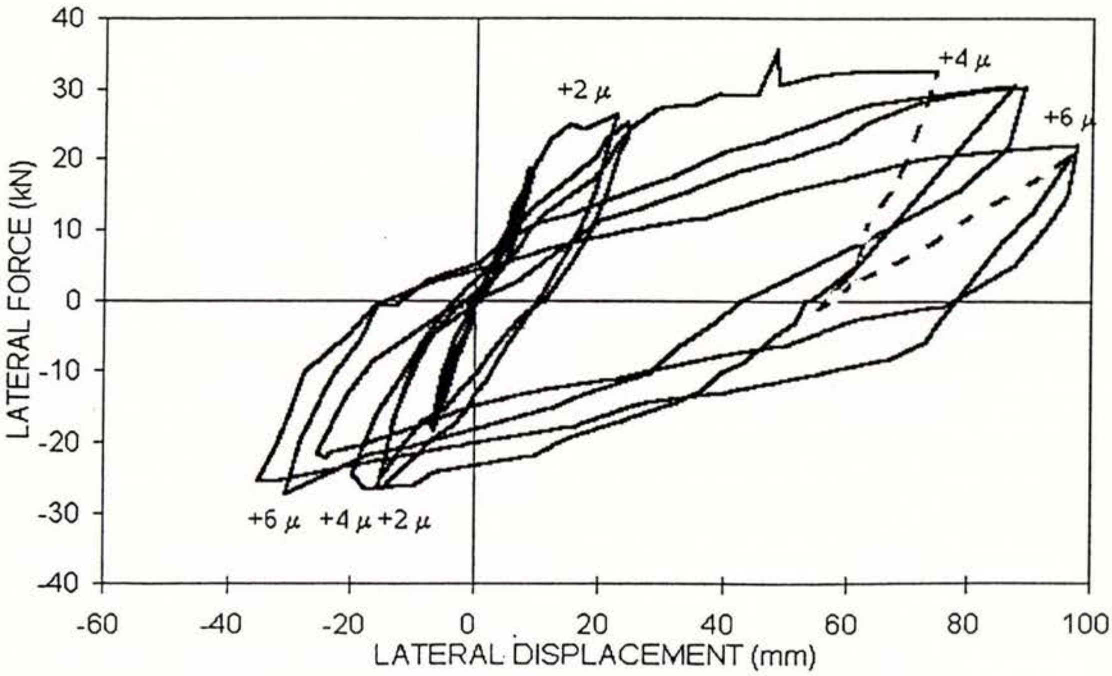

Fig. 4.7 Force-Displacement Response of Column 4 of Unit 1

4.3.2 Overall Response of Unit 1

The theoretical sum of the applied lateral forces required to cause yielding (ideal conditions), ΣF_i, was 142.8 kN. One way of gaining an impression of the overall response of the unit was to plot the sum of the applied lateral forces against the control displacement as defined in Section 3.9. However this does not give a true force-displacement response from which the stiffness of the unit can be quantified since these two measurements were at two different levels.

The elastic response is shown in Fig. 4.8. The unit appears to have been softer in the second cycle than in the first cycle. This behaviour can be attributed to the initial cracking that occurred in the first cycle. The extrapolated ductility one displacement, Δ_1 was 5.2 mm corresponding to an interstorey drift of 0.67%. This was found as described in Section 3.9.

The lateral force-displacement response for the whole test is shown in Fig. 4.9. In the first inelastic cycle to a ductility factor of $\pm 2\mu$, ΣF_i was exceeded by 7.7% in the positive direction and 12.5% in the negative direction.

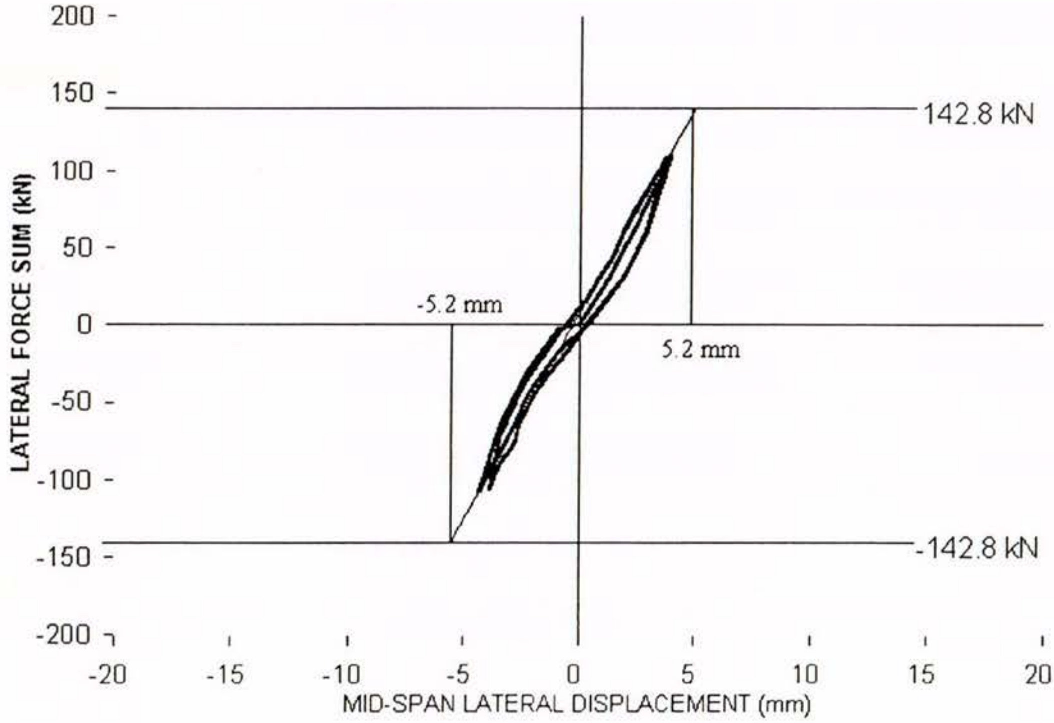

Fig. 4.8 Lateral Force-Displacement Response of Unit 1 During Cycles in the Elastic Range

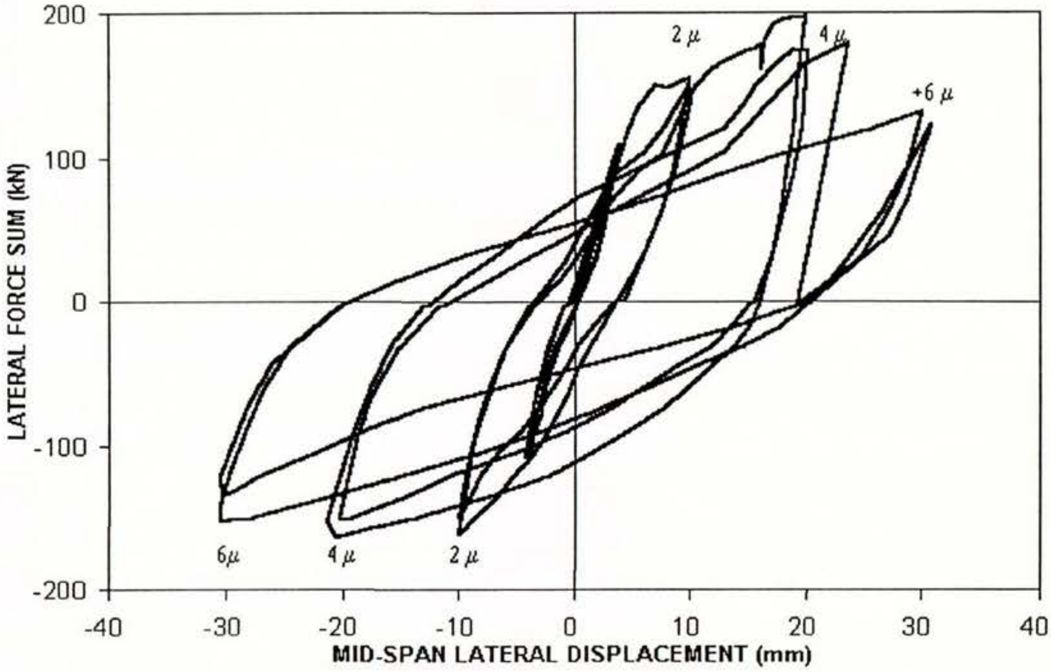

Fig. 4.9 Lateral-Force Displacement Response on Unit 1

The applied lateral forces reached in the second cycle at all ductility levels were found to be less than in the first cycle. Generally, the crack pattern formed in the first cycle at each ductility level, with these cracks continuing to open in the second cycle.

The maximum overstrengths were recorded in the first ±4μ cycle. They were $1.39\Sigma F_i$ in the positive direction and $1.14\Sigma F_i$ in the negative direction of loading. In Fig. 4.9 the point where the large crack in the slab formed is visible in the loading to the peak of +4μi. The reduction in the applied lateral forces from the first cycle to the second cycle was more significant during the ±4μ cycles because of the existence of the wide crack.

Near the end of the test, loading to the peak of +6μii, the lateral force carrying capacity had reduced to 67% of the maximum recorded in that direction. At this point one final half cycle, -6μii was performed to complete the cycle. This reached 82% of the maximum lateral force carrying capacity in that direction. Pinching of the hysteresis loops shown in Fig. 4.9 occurred as a result of the significant reduction in stiffness of the unit.

4.4 ELONGATION

4.4.1 Beam Elongation

The recorded elongation of the whole length of the unit is shown in Fig. 4.10 a) in terms of displacement ductility and in Fig.4.10 b) as a function of the sum of the applied lateral forces. The initial elongation in the elastic cycles was small and due to the flexural cracking of the main beam in the regions adjacent to the column faces. In addition, the flexural cracks caused the release of concrete shrinkage stresses that developed after curing, which may have contributed to the recorded elongation. The maximum elongation recorded in the elastic cycles was 0.83 mm, recorded at the peak of -3/4 μii (the three-quarter ductility displacement, $\Delta_{0.75}$, was -4.26 mm).

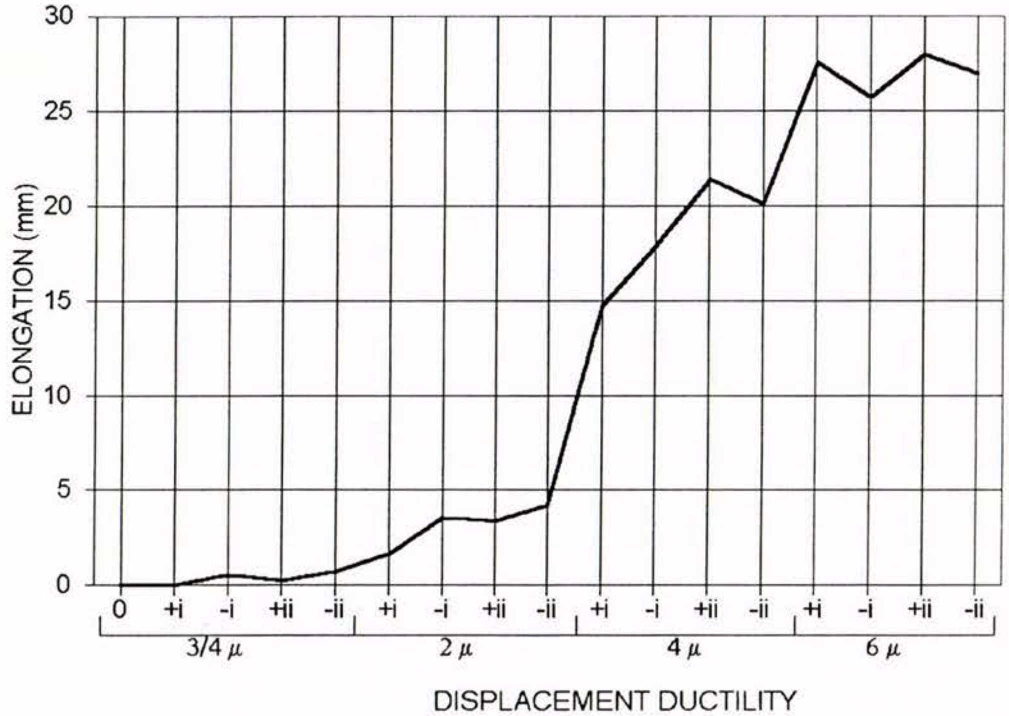

Fig. 4.10 a) Elongation of Unit 1 in Terms of Displacement Ductility

Fig. 4.10 b) Total Elongation of Unit 1 as a Function of the Sum of the Applied Lateral Forces

In the first inelastic cycle (±2μi), the elongation increased slightly, approximately 1 mm per bay. The cumulative nature of beam elongation in reversing plastic hinges was apparent at this stage as seen in Fig 4.10 b). The maximum elongation recorded in the ±2μ cycles was 4.19 mm at the peak of the half cycle to -2μii (ductility two displacement, Δ_2, was -9.98 mm). In the ±4μ cycles a significant increase in elongation occurred to an interstorey drift of 2.56%. From both Fig.s 4.10 a) and 4.10 b) for the ±2μ and ±4μ cycles, it is clear that the elongation in each ductility level occurred mostly in the first cycle of that ductility level. At this point most of the new cracks were formed in the plastic hinge zones. In the second cycle at each ductility level only minor cracks formed and the existing cracks just became wider with the elongation concentrated in these areas. The maximum elongation recorded in the ±4μ cycles was 21.43 mm at the peak of the half cycle to +4μii (ductility four displacement, Δ_4, was 20.27 mm).

At the commencement of the ±6μ cycles a further significant increase in elongation occurred. At this point the interstorey drift was 3.85% and during the unloading mid-way through the +6μi half cycle, buckling of the longitudinal reinforcement in the external plastic hinge zones of the main beam began to occur. With this buckling, the length of the compression zone longitudinalreinforcement reduced which also caused the elongation of the unit to reduce. Any increase in interstorey drift resulted in greater buckling in the external plastic hinge zones rather than an increase in elongation. Hence the maximum recorded elongation occurred during rather than at the peak of the half cycle to +6μi. This was 31.54 mm when the average main beam displacement was 23.83 mm (interstorey drift = 3.05%).

When the beam elongation is divided into its separate beam components, as shown in Fig,4.11, it can be seen that for ductility levels up to ±4μ the centre bay contributed less to the elongation of the whole unit than the outside bays. This was due to the cumulative elongation of the unit causing the plastic hinges adjacent to the external columns to undergo larger rotations than the plastic hinges adjacent to the internal columns. Observations of deformations of the internal plastic hinge zones support this. The greater rotations of the external plastic hinges caused the outside bays to elongate more. This did not occur during the ±6μ cycles because of the buckling that was taking place in the external plastic hinge zones.

4.4.2 Elongation of the Top of the Slab

The elongation of the top of the slab for the whole unit could be looked at as the sum of the measurements in the longitudinal direction. The comparison of this overall elongation is shown in Fig. 4.12 with lines 1, 4 and 7 corresponding to those illustrated in Fig. 3.9. It can be seen in Fig. 4.12 that for the elastic displacement cycles the deformation of the slab was approximately the same at each of the positions measured. In this figure the presence of the large crack occurring adjacent to transverse beam 3 in bay 2 is evident. Results from line 7, the extreme section of the slab most affected by the crack, shows a greater increase in elongation than the other lines during the ±2μ cycles. This suggests that the unit was probably deforming out of plane, creating larger tensile strains in that portion of the slab. The crack extended almost to the centre of the slab (line 4) and by the completion of the ±4μ cycles the centre of the slab was deforming the same amount as the outside section of the slab (line 7). Elongation of the slab on the opposite side of the main beam was considerably less due to the reduction in tensile strains in the longitudinal steel brought about by the out-of-plane behaviour.

Analysis of the results of the portal transducers crossing the large crack (summarised in Fig. 4.14) show that the elongation across this region ranged from 10 mm to 15 mm. Since the crack originally formed as a flexural crack at a much lower level of ductility, the strain in the reinforcement would have been localised within the crack causing some of the bars to fracture. As noted previously (see page 51), at the end of the test all the longitudinal bars on this side of the beam had been fractured.

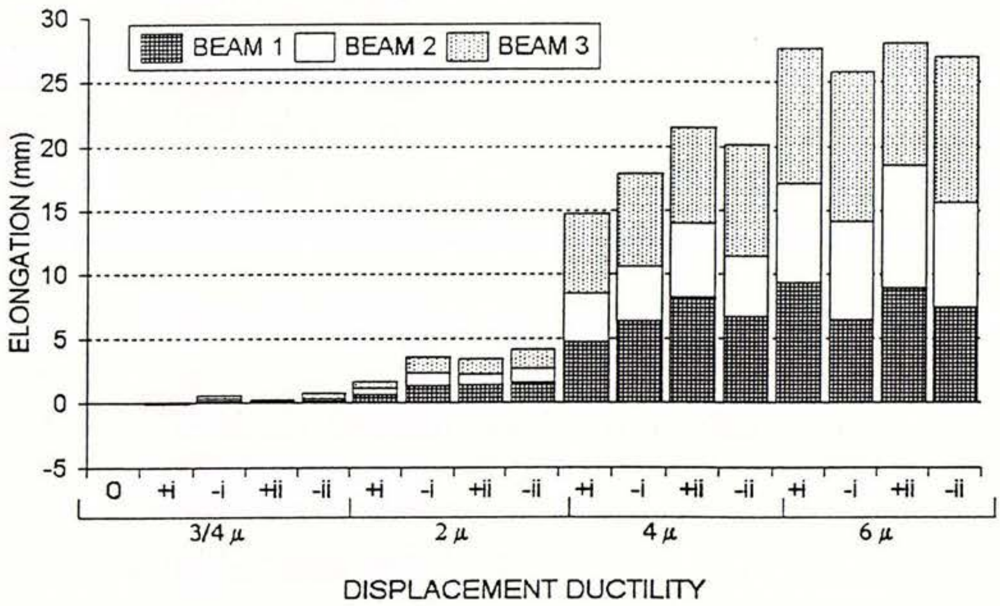

Fig. 4.11 Elongation of Each Bay of the Main Beam of Unit 1

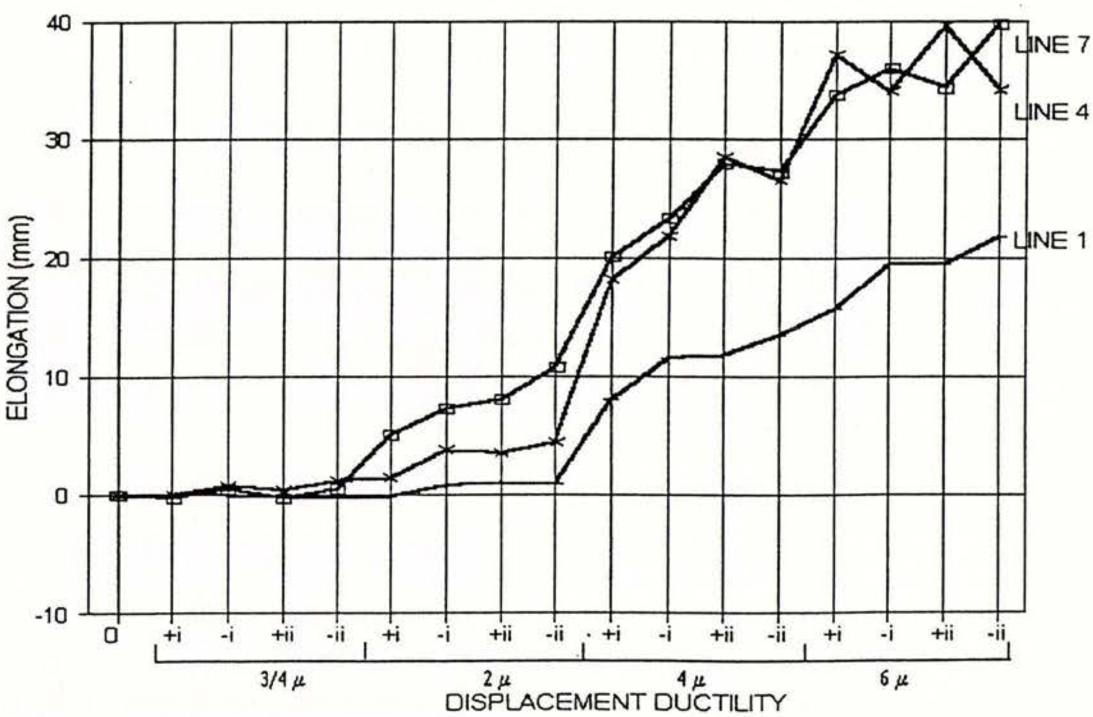

Fig. 4.12 Longitudinal Distribution of Elongation Along the Top of the Slab

4.5 EFFECTIVE WIDTH OF SLAB

The distribution of elongation across the slab gives an indication of the effective width contribution at different sections of the top of the slab. This transverse distribution was studied across the regions extending from each plastic hinge zone. The regions were Lines A,D,E,H,I and L as per Fig. 3.9. Note that lines A,D, and E are not shown and are to the right of the centreline in Fig. 3.9. The results for the elongation of the final cycle of each ductility level for each line are shown in Fig.s 4.13 to 4.16. Each figure contains results for both the positive and negative loading directions. The transverse elongation distribution for the remaining sections of the slab were also measured but it was found that in these regions the elongation was usually less than 1 mm even after the $\pm 6\mu$ cycles. The gauge to the extreme right of the centre line of the slab shown in Fig. 4.16 was believed to be faulty.

The distribution of crack widths are illustrated in Appendix B. Crack widths were taken only at the centre and extreme sections of the slab. When these figures are considered it can be seen that a significant portion of the measured extensions shown in Fig.s 4.13 to 4.16 can be attributed to cracking of the slab close to the transverse beams. This suggests that tensile forces exist in all of the longitudinal slab reinforcement across the slab and hence this reinforcement would have been effective in contributing to the increased flexural capacity of the unit.

The flexural and shear deformation are shown as components of the mid-span lateral deflection for each bay in Fig. 4.17 a), b) and c). The mid-span deflection for each bay was calculated as linear interpolations between the two L.V.D.T. readings at each end of the test unit. Significant closure errors were observed between these linear interpolations and the computed deflection due to shear and flexure. The instrumentation to measure shear in each plastic hinge zone did not extend the full effective depth, d-d', of the beam. It is believed that this may have significantly underestimated the shear component of the mid-span deflection. The assumption that the mid-span deflection of each bay could be linearly interpolated may also have contributed to the closure errors.

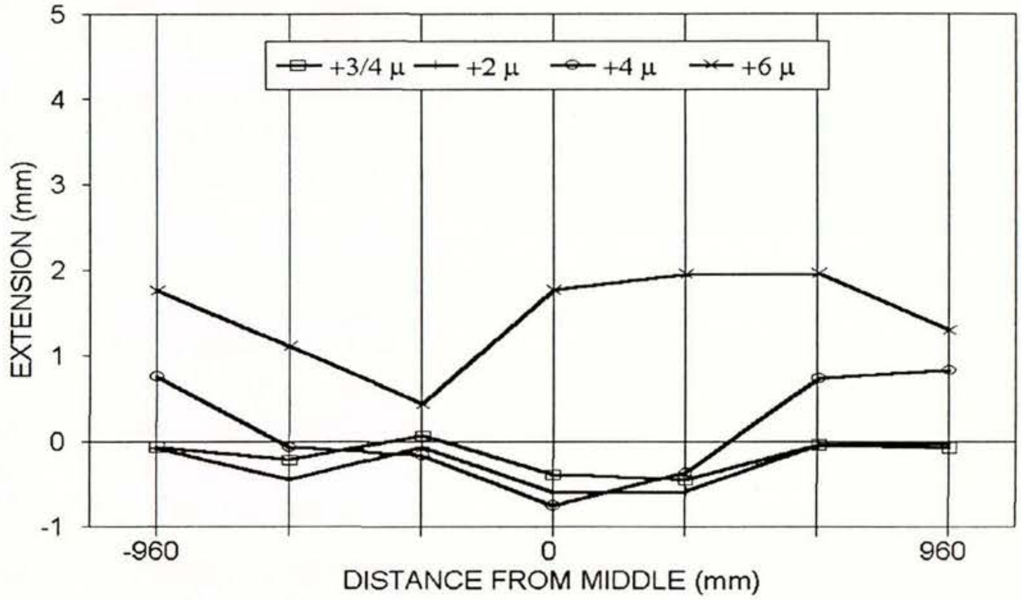

a) Positive Direction of Loading

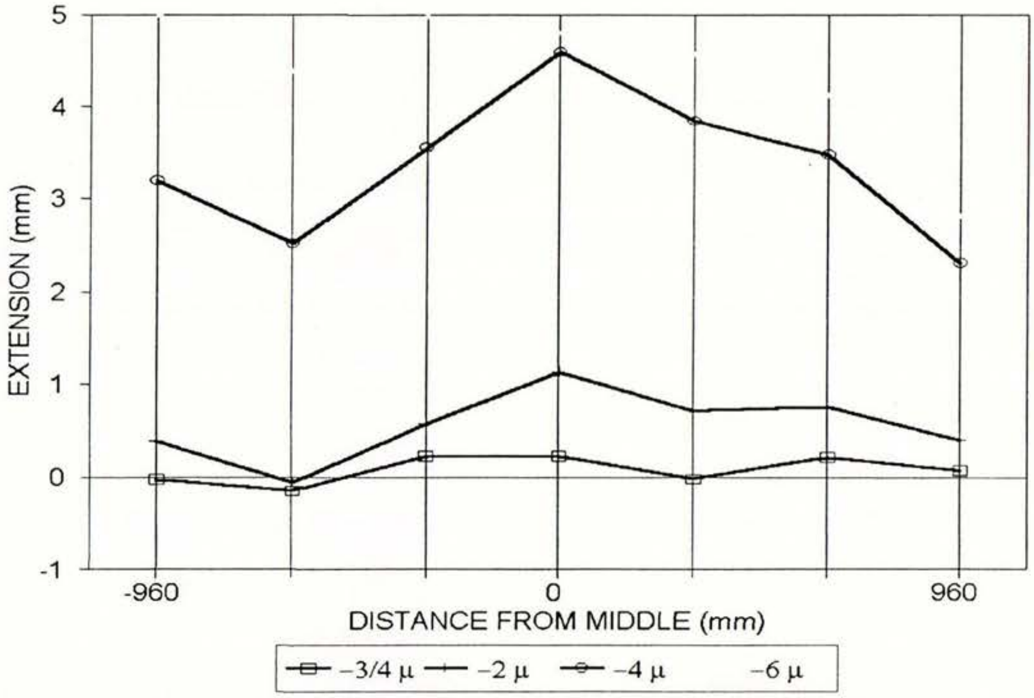

b) Negative Direction of Loading

Fig. 4.13 Transverse Distribution of Slab Elongation; Line E

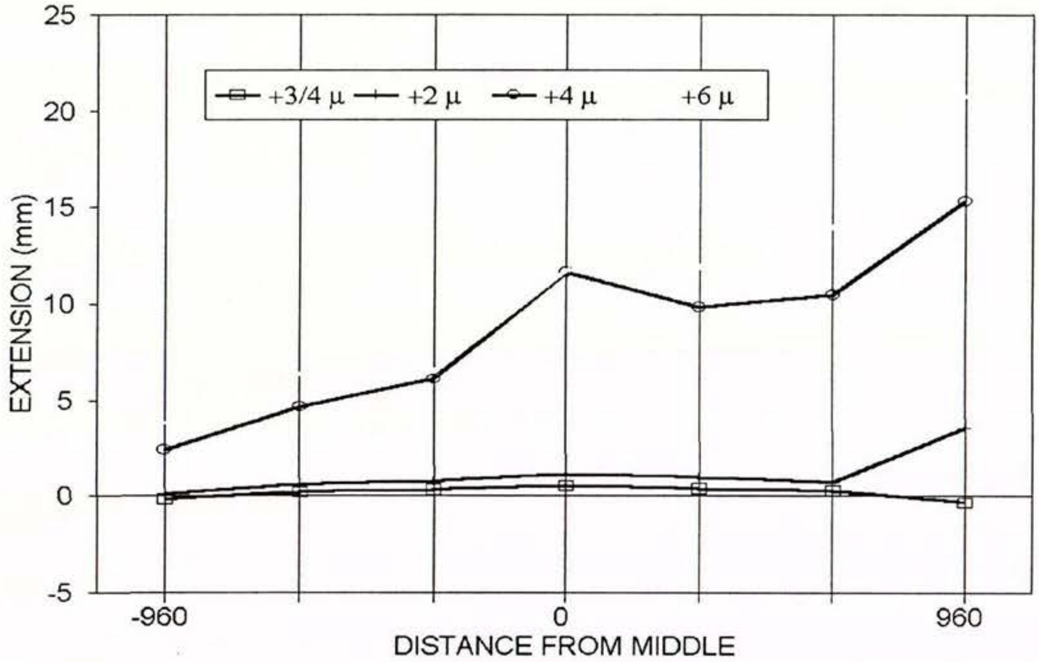

a) Positive Direction of Loading

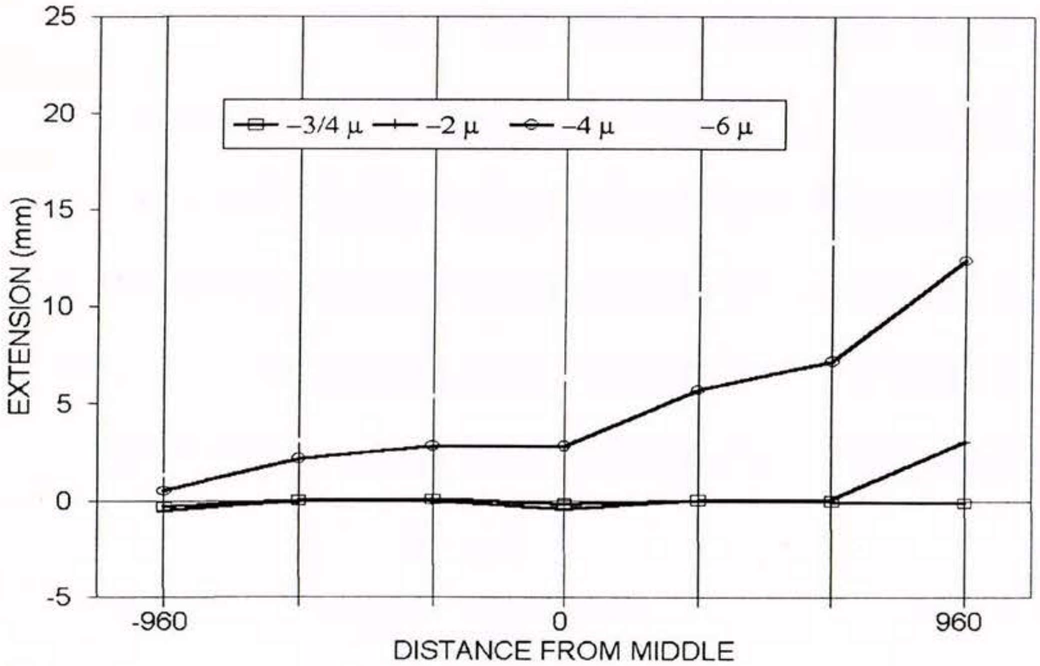

b) Negative Direction of Loading

Fig. 4.14 Transverse Distribution of Slab Elongation; Line H

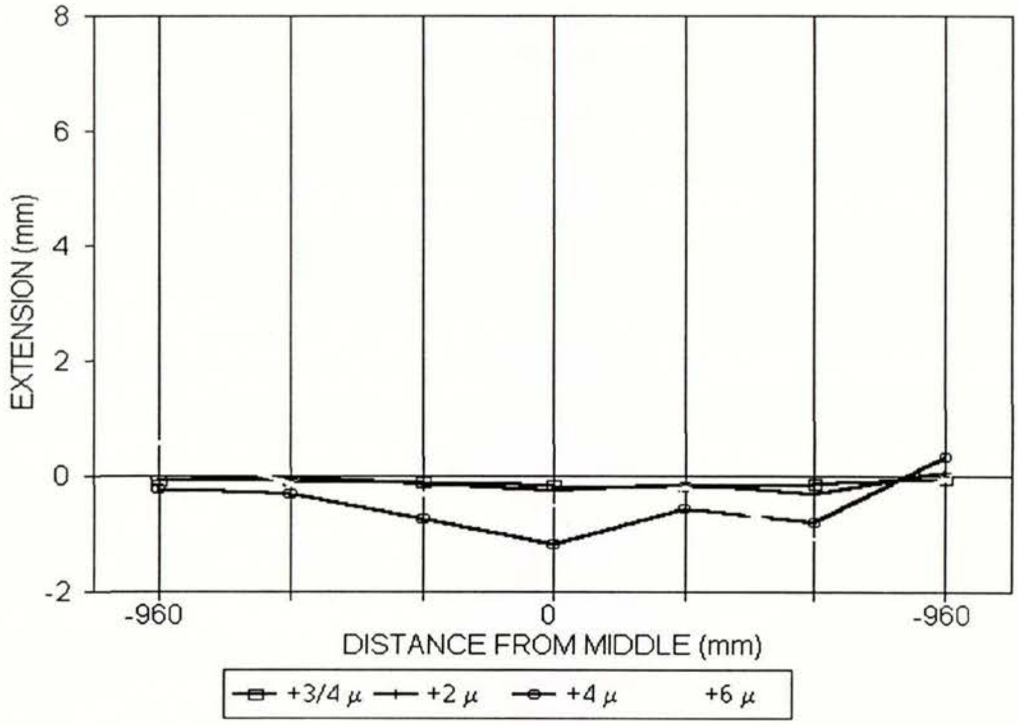

a) Positive Direction of Loading

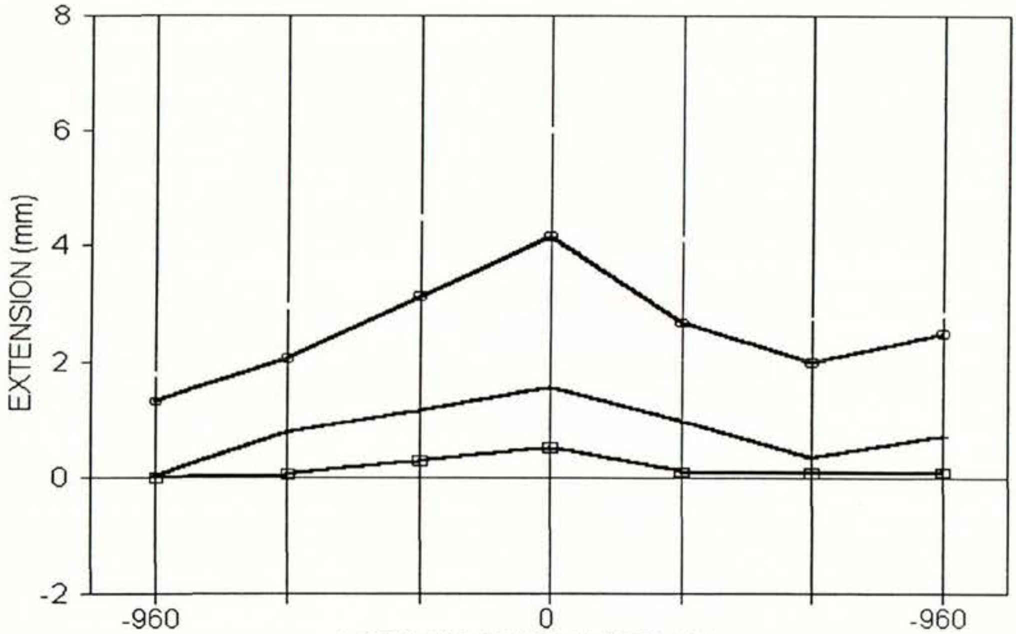

b) Negative Direction of Loading

Fig. 4.15 Transverse Distribution of Slab Elongation; Line I

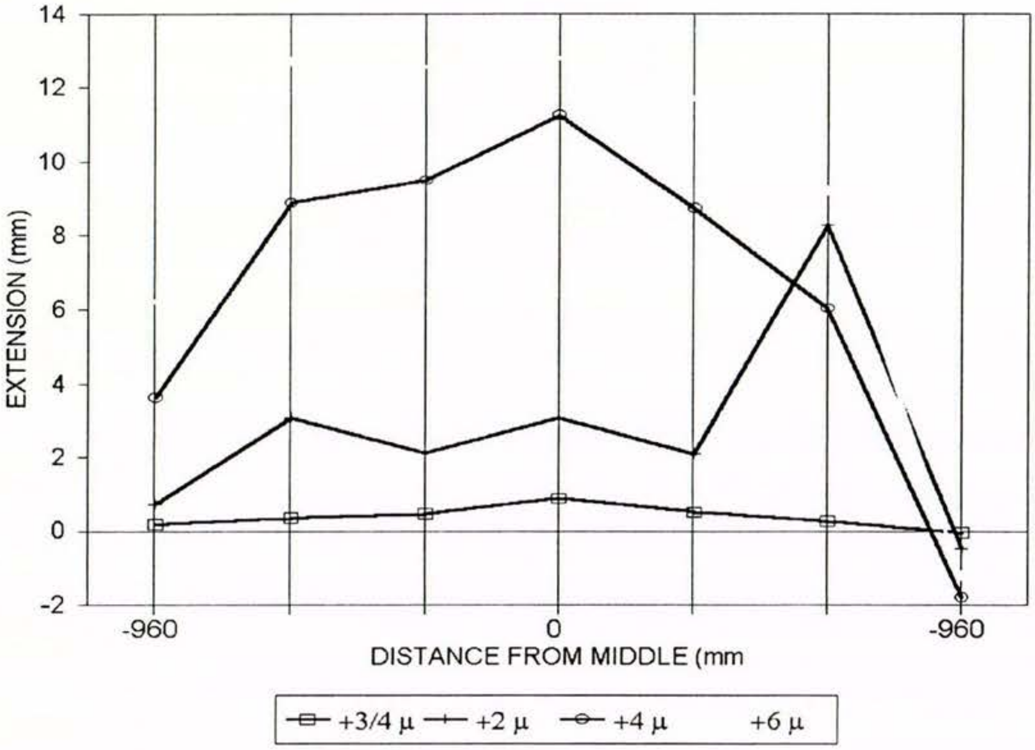

a) Positive Direction of Loading

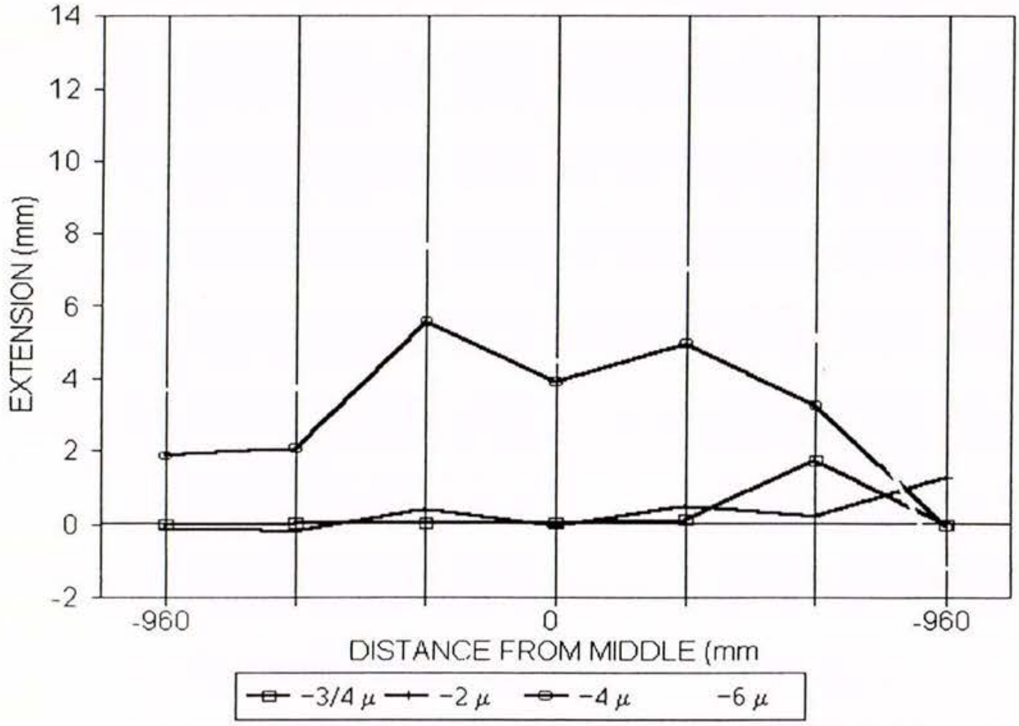

b) Negative Direction of Loading

Fig. 4.16 Transverse Distribution of Slab Elongation; Line L

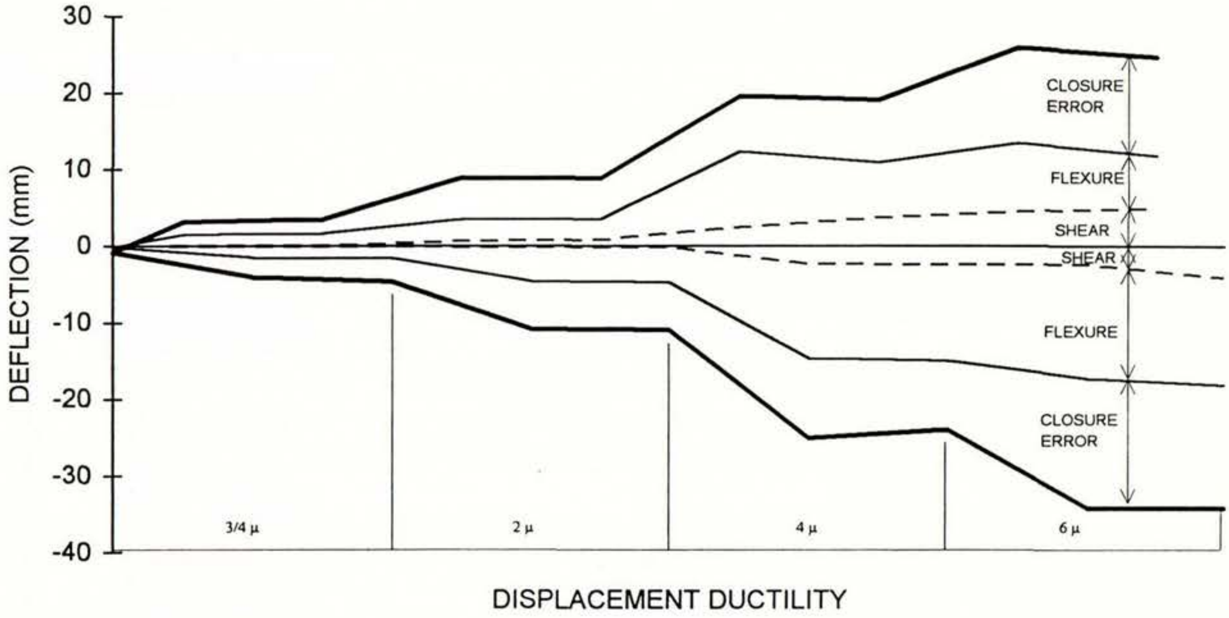

Fig. 4.17 a) Components of Bay 1 Mid-Span Displacement

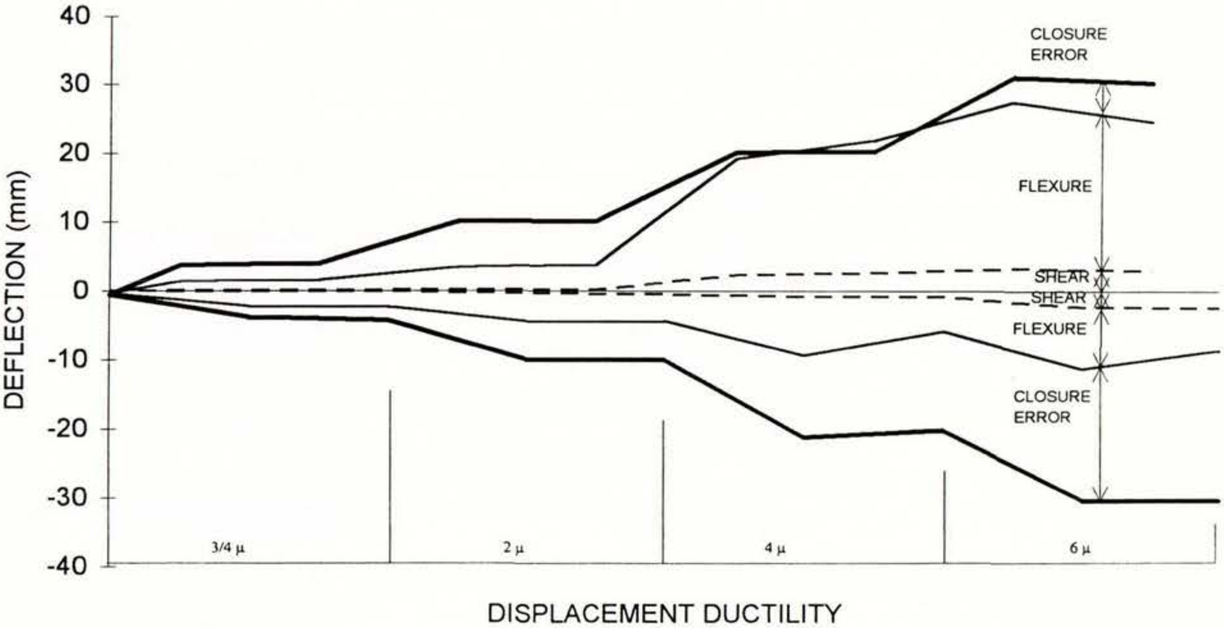

Fig. 4.17 b) Components of Bay 2 Mid-Span Displacement

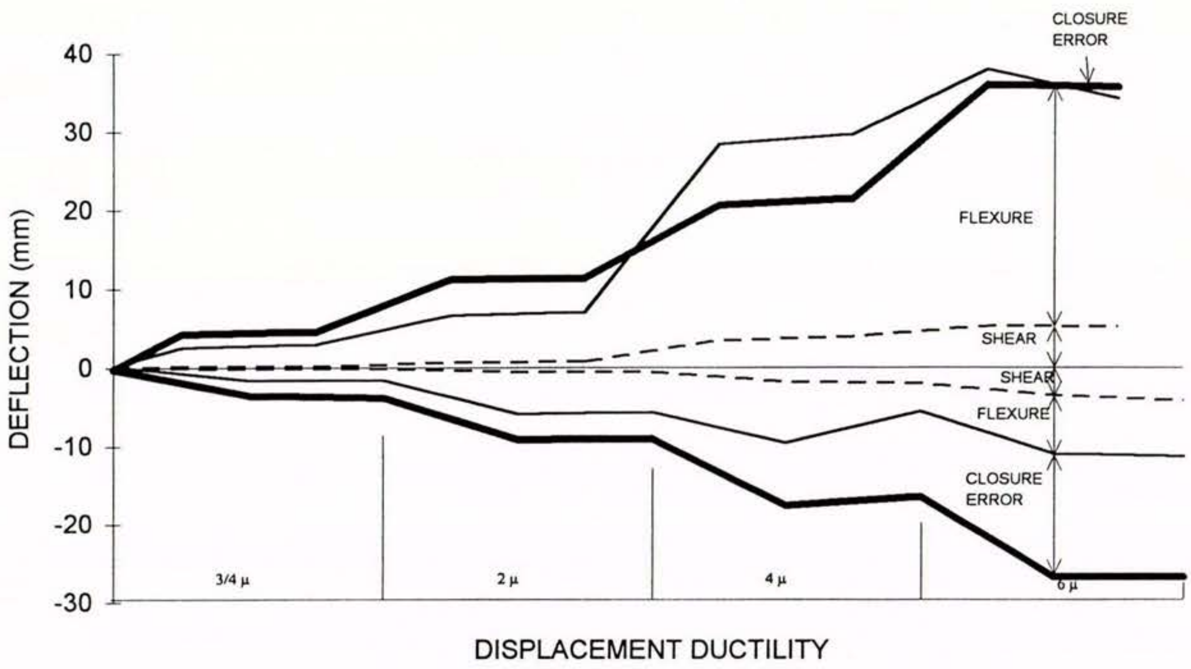

Fig. 4.17 c) Components of Bay 3 Mid-Span Displacement

4.6 SUMMARY

Unit 1 was tested under displacement-controlled cyclic loading conditions so that inelastic behaviour occurred. The unit exceeded the calculated overstrength laterally applied forces under displacement controlled loading to a ductility factor of 4μ.

Observations of significant plastic hinging adjacent to all beam-column connections were recorded. Elongation of these plastic hinges was measured and reached a maximum of 31.54 mm at a displacement ductility of 6μ, which corresponded to an interstorey drift of 3.85%. Elongation of the central bay was found to be less than the outside bays due to the additional rotations imposed on the plastic hinges adjacent to the external columns.

Elongations of the top of the slab were recorded. It was observed that outer transverse sections of the slab were effective in contributing to the flexural strength of the beam.

CHAPTER 5

TEST RESULTS OF UNIT 2: BEAM-COLUMN UNIT

5.1 INTRODUCTION

This chapter presents test results from Unit 2 which was made to observe the behaviour of a multi-bay frame undergoing elongation of the main beam when subjected to cyclic loading. In particular the results of this test, when compared with the results obtained from the previous unit, can be used to indicate the effect of the slab on the elongation of the unit described in Chapter 4. In addition the general behaviour and force-displacement response for the columns and the overall unit is presented.

5.2 GENERAL BEHAVIOUR

The force controlled elastic cycles were made over a period of two days. Reduction of the results and extensions of the portal transducers was then carried out over the following five days. The inelastic cycles were carried out over the following seven days.

The four columns appeared to behave elastically throughout the test. Fine flexural cracks were observed on the column faces in the first inelastic cycle and this crack pattern continued to grow throughout the test. At the peak displacement of the final inelastic half-cycle (-6μii) there were approximately six cracks on the tension sides of each column and all cracks were less than 0.5 mm wide.

Cracking in the main beam was concentrated in the plastic hinge zones, with only minor cracking occurring in the mid-span regions. Steeply inclined diagonal shear cracking occurred close to the column faces in all of the plastic hinge zones. The main diagonal cracks appeared to be initiated by the first or second vertical shear stirrup from the column faces. These cracks were approximately vertical through the middle third of the depth of the plastic hinge and then spread out at an angle of about 45° to the top and bottom surfaces of the main beam. Progression of the cracking is shown in Figs. 5.1 a) to g) for the external joint at column 1.

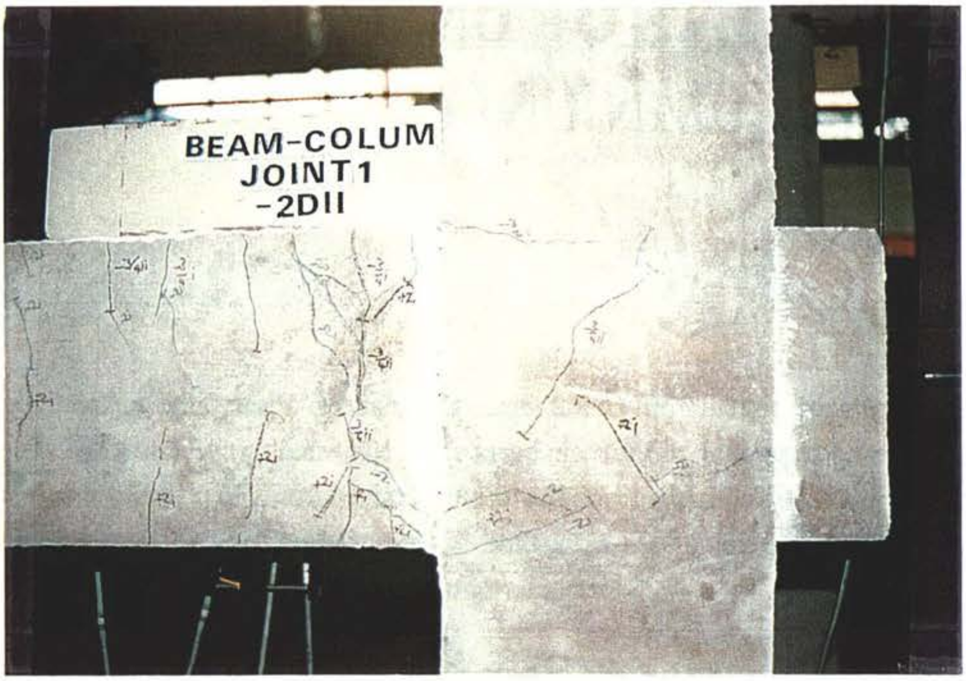

a)

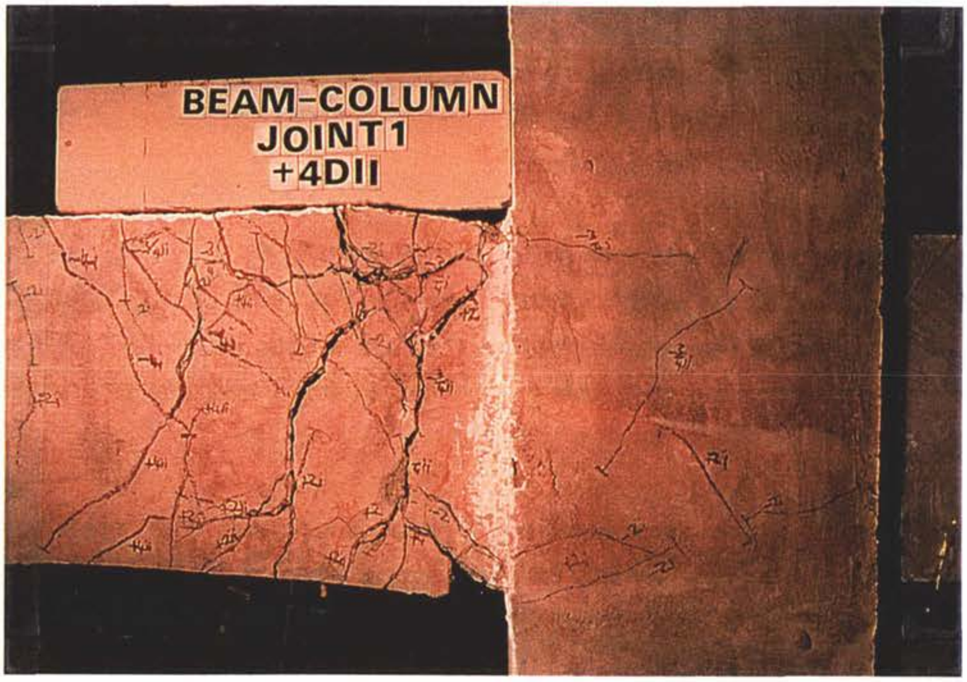

b)

Fig. 5.1 - Cracking of Beam-Column Unit at Joint 1 Adjacent to Column 1

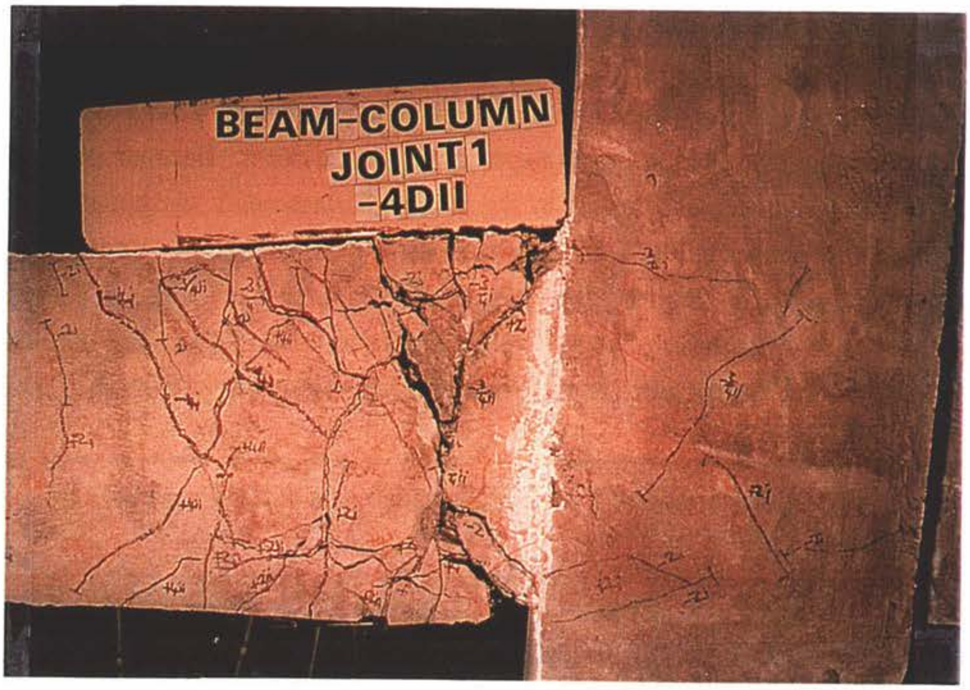

c)

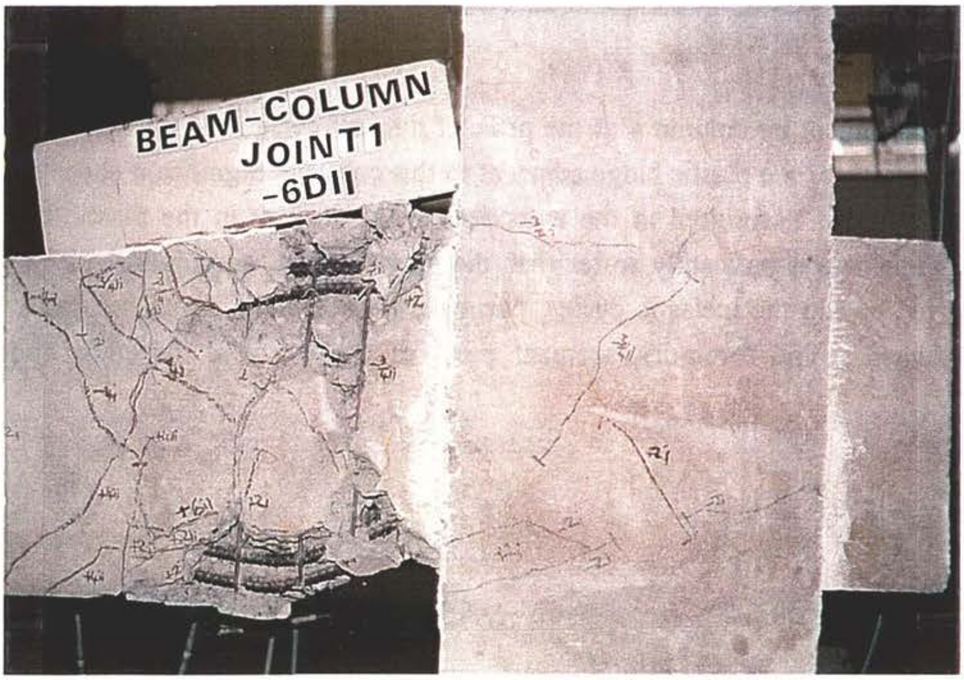

d)

Fig. 5.1 - Cracking of Beam-Column Unit at Joint 1 Adjacent to Column 1

5.3 FORCE DISPLACEMENT RESPONSE

5.3.1 Individual Column Response

The force-displacement response of each column is presented in Fig.s 5.2 to 5.5. In the test the lateral displacement was controlled at the mid-span of the centre beam. Because of the elongation of the whole beam, significant differences in the lateral displacements of the tops of the four columns occurred, as is shown in Fig. 5.6. Comparisons of the column deflections at the peaks of 4μi are presented in Table 5.1. Figure 5.7 shows, in an exaggerated manner, the pattern of these differences as previously discussed in Section 4.3 for the beam-column-slab unit. The significance of elongation on additional the rotations of the external columns is apparent from this Table 5.1.

Table 5.1 - Comparison of Column Displacements at the Peaks of ±4μi

Cycle	Direction	Column 1 Displ. (mm)	Column 2 Displ. (mm)	Column 3 Displ. (mm)	Column 4 Displ (mm)
+4μi	⇒	26.2	48.7	65.0	72.1
-4μi	⇐	-87.5	-57.7	-41.7	-24.3

The large displacement by column 4 at the peak of the half cycle to -6μii was a result of the significant softening of the plastic hinge adjacent to this column. Significant shear deformation as observed in Fig, 5.1, resulted in the extension of the stirrups in the plastic hinge zone. Because this unit was significantly softer than the previous unit, continuous relaxation of the forces occurred during the inelastic cycles, particularly once the lateral force capacity of the unit was reached. The force-displacement plots of the columns therefore appear quite irregular.

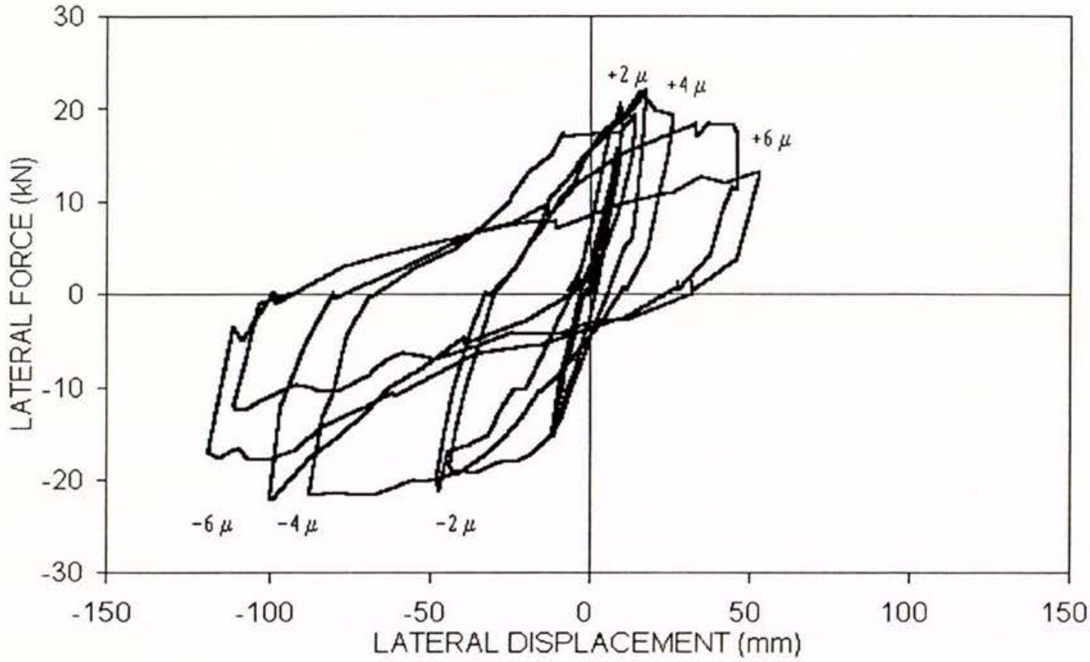

Fig. 5.2 Force-Displacement response of Column 1 of Unit 2

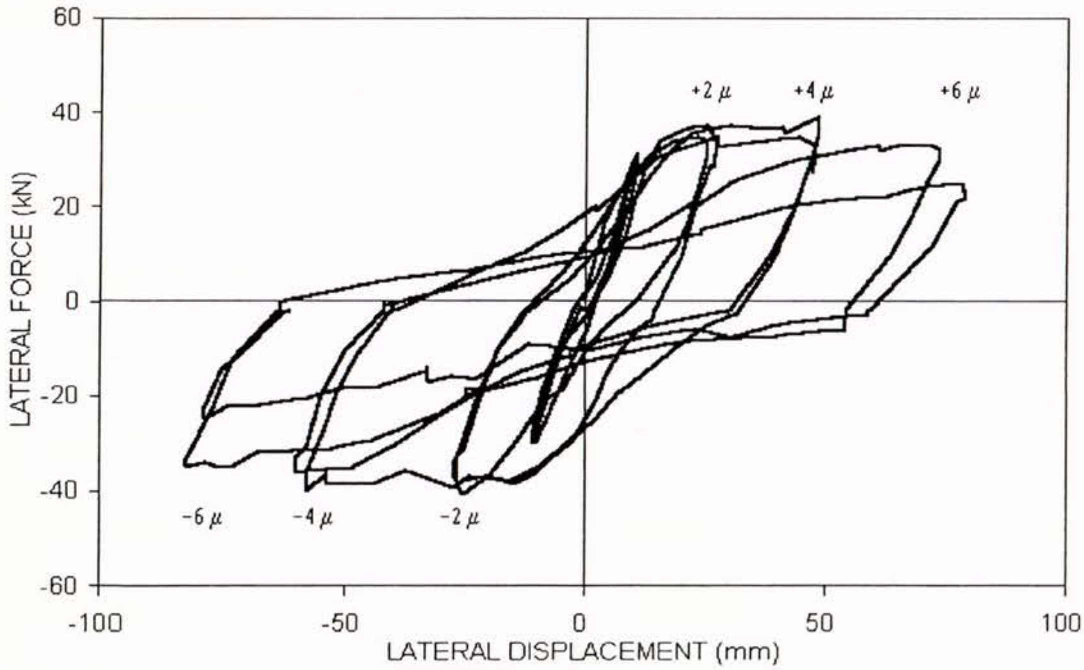

Fig. 5.3 Force-Displacement Response of Column 2 of Unit 2

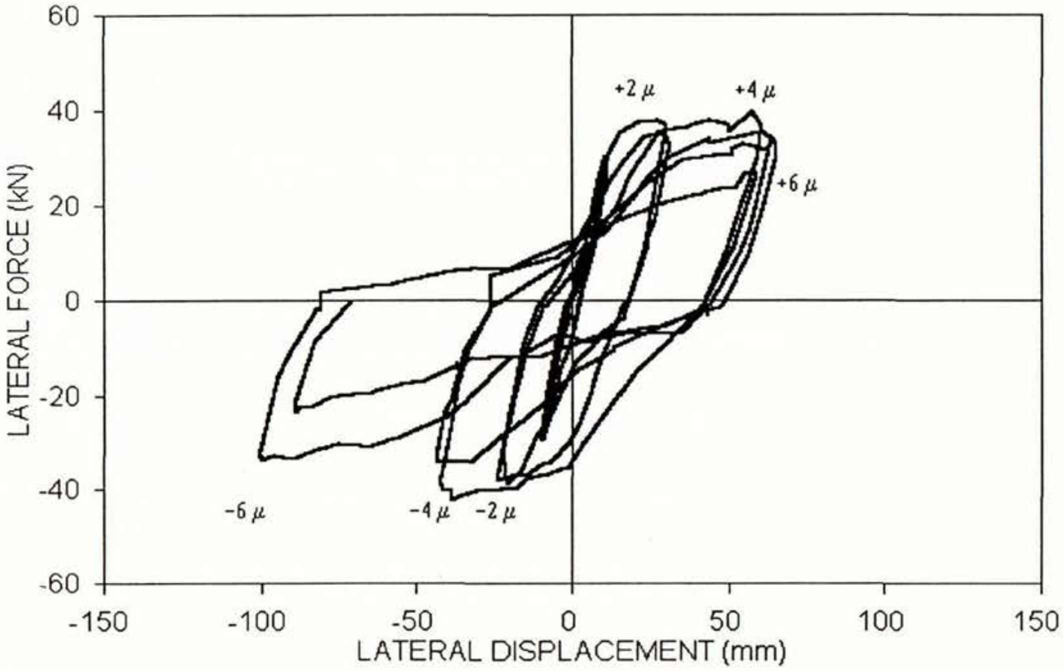

Fig. 5.4 Force-Displacement Response of Column 3 of Unit 2

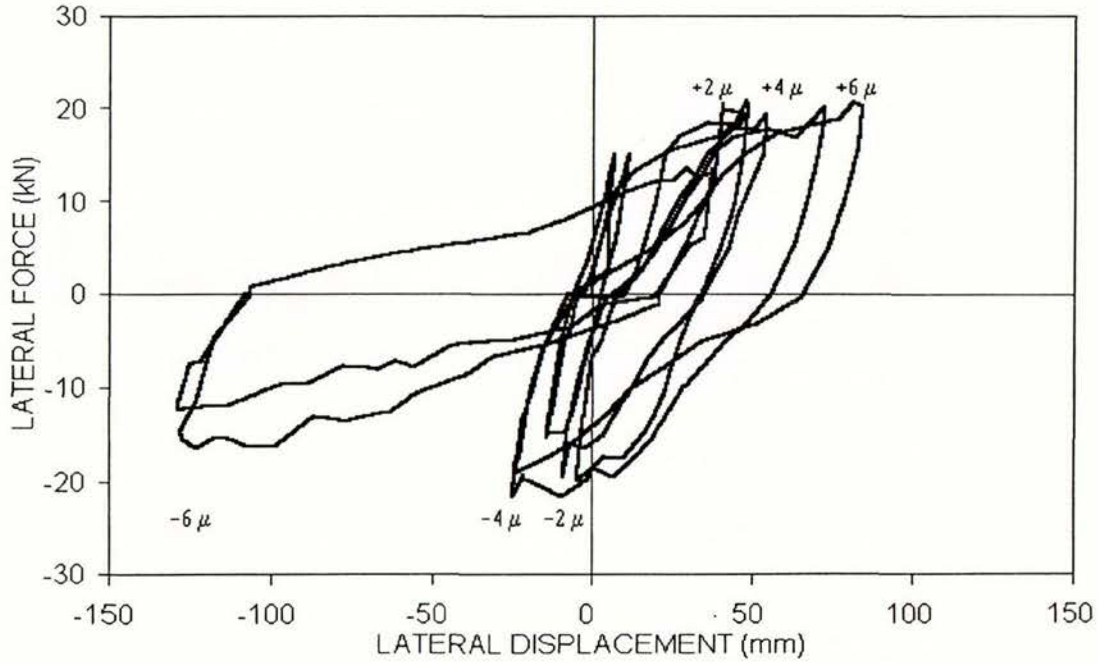

Fig. 5.5 Force-Displacement Response of Column 4 of Unit 2

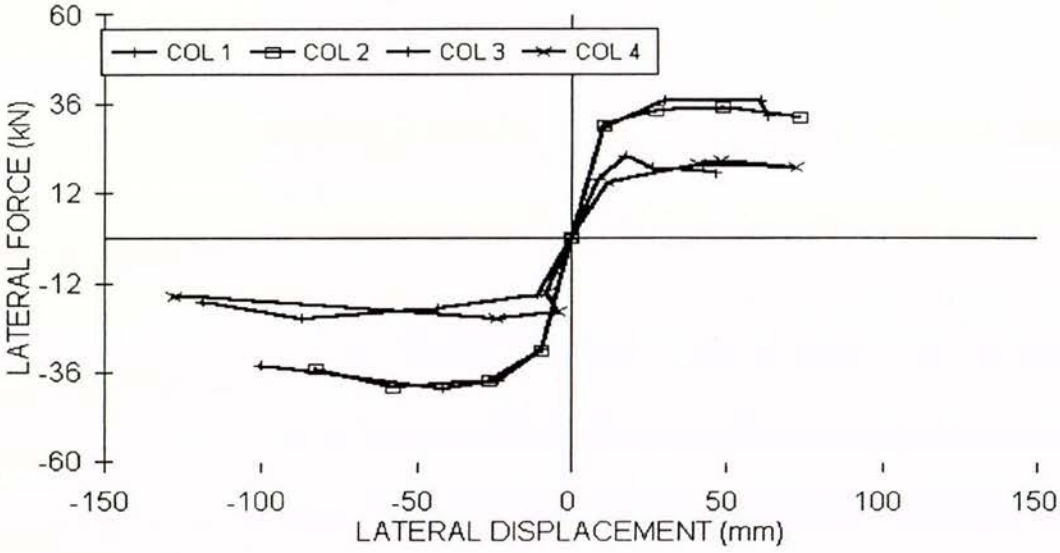

Fig. 5.6 Peak Lateral Force-Displacement values Compared for All Columns Unit 2

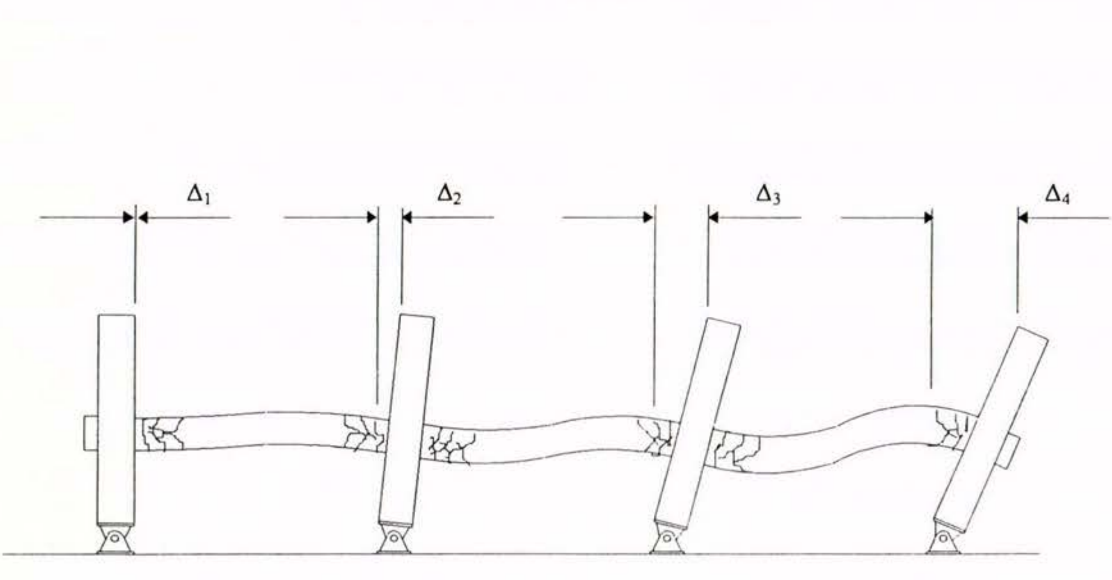

Fig. 5.7 - Illustration of Differences in Lateral Displacements of the Four Columns

5.3.2 Overall Response of Unit 2

The theoretical sum of the applied lateral forces corresponding to the ideal strength, ΣF_i was 117.6 kN. Figure 5.8 shows the force-displacement response for the elastic cycles in terms of the sum of the applied lateral forces versus the lateral displacement of the mid-span of the main beam at mid-depth. The extrapolated ductility one displacement was 7.4 mm corresponding to an interstorey drift of 0.95%. The unit became softer during the second elastic cycle due to the initial cracking in the first cycle.

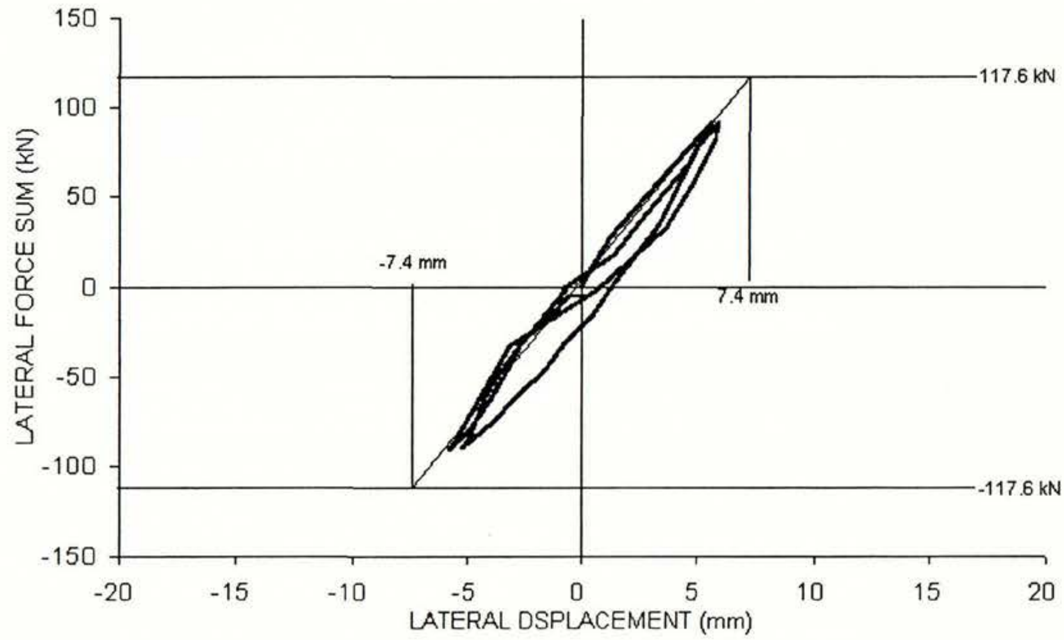

Fig. 5.8 Lateral Force Displacement Response of Unit 2 During Cycles in the Elastic Range

The force-displacement response for the whole test is shown in Fig. 5.9. During the $\pm 2\mu$ cycles the loading of the unit reached $0.97\Sigma F_i$ (in both directions). The maximum lateral forces for the positive and negative direction of loading of $1.00\Sigma F_i$ and $1.05\Sigma F_i$ respectively, were reached in the first $\pm 4\mu$ cycle. During the $\pm 4\mu$ cycles, pinching of the force-displacement response occurred so that the dissipation of energy was reduced as seen in Fig. 5.9. Buckling of the main reinforcement, as seen in Fig. 5.1, in the plastic hinge zones began to occur during the $\pm 6\mu$ cycles. This also contributed to the pinching of the force-displacement response. Significant degradation of the moment-capacity of the plastic hinge zone occurred during the

$\pm 4\mu$ cycles resulting in a reduction of the laterally applied forces. In the final $\pm 6\mu$ cycle only 66% and 61% of ΣF_i was reached in the positive and negative directions respectively. This rapid degradation in strength was a consequence of the very large rotations imposed on the plastic hinge zones which resulted in considerable damage (see Fig. 5.1). This damage caused the concrete in the plastic hinges to spall, exposing the longitudinal reinforcement and allowing it to buckle.

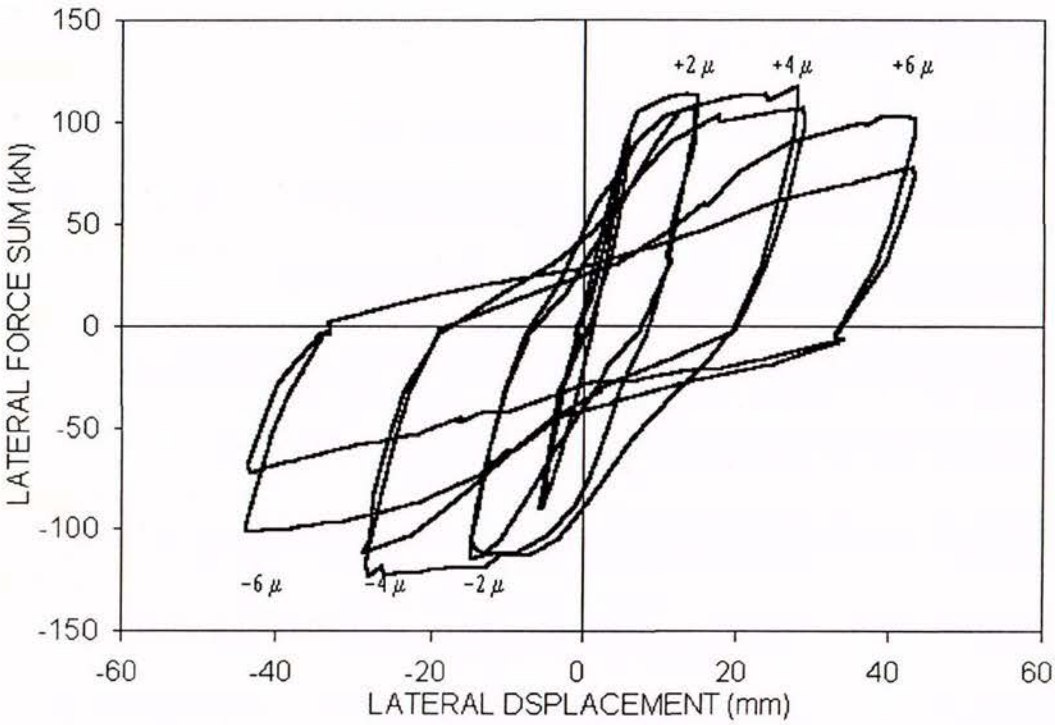

Fig. 5.9 - Lateral Force Sum - Displacement Response of Beam-Column Unit

5.4 ELONGATION

Measurements for the longitudinal beam were carried out in the same way as the Unit 1. In addition the deformation of the joint zones was also measured. This was found to be small and was a result of the columns and beam-column joint zones being proportioned so that they would remain elastic. The overall recorded elongation is plotted in Fig.s 5.10 a) in terms of displacement ductility and in Fig. 5.10 b) against the sum of the applied lateral forces. The initial elongation was a result of the flexural cracking that occurred along the beam. In addition, shrinkage of the concrete that occurred after curing placed the longitudinal reinforcement in compression. This was released when the specimen first cracked and would have contributed to the initial recorded elongation. The maximum elongation recorded in the elastic cycles was 2.2 mm at the peak of the +3/4μii cycle to a lateral displacement of 5.9 mm at the mid-span of the longitudinal beam.

An appreciable increase in elongation occurred during the first inelastic ±2μ cycle. This was due to the large increase in rotation imposed on each of the plastic hinge zones. The maximum recorded elongation during the ±2μ cycles was 16.0 mm at the peak of the +2μii cycle, corresponding to a lateral displacement of 14.6 mm at the mid-span of the longitudinal beam. During these cycles the interstorey drift was 1.87 %. During the ±4μ cycles most of the elongation developed in the first cycle. A small amount of buckling of the longitudinal reinforcement in joints 1 and 4 occurred during the positive direction of loading of the second ±4μ cycle as seen in Fig. 5.10 b), which resulted in a reduction in elongation. The maximum recorded elongation during the μ = ±4 cycles was 34.1 mm at the peak of the -4μii cycle corresponding to a lateral displacement of -28.8 mm at the mid-span of the longitudinal beam. The interstorey drift at the peak of this cycle was 3.69%.

During the ±6μ cycles there was a small increase in elongation. The maximum recorded elongation during the test occurred during the positive loading direction of the first ±6μ cycle as shown if Fig. 5.10 b). It was 35.0 mm corresponding to a lateral displacement of 21.0 mm at the mid-span of the longitudinal beam. From this point onwards a significant amount of longitudinal reinforcement buckling developed and the elongation plot became erratic. The elongation reduced to as low as 25.1 mm just after the peak of the -6μii cycle. Figure 5.10 a) shows the overall continuous decrease in elongation during the ±6μ cycles.

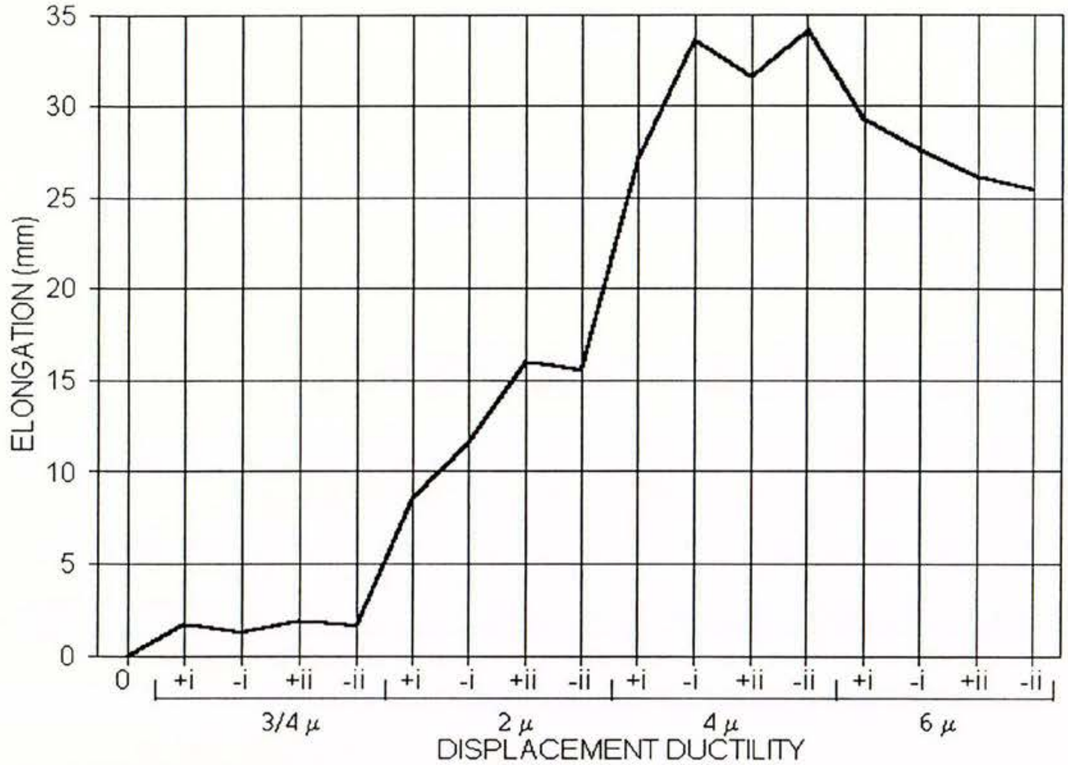

Fig. 5.10 a) - Elongation of Beam-Column Unit in Terms of Displacement Ductility

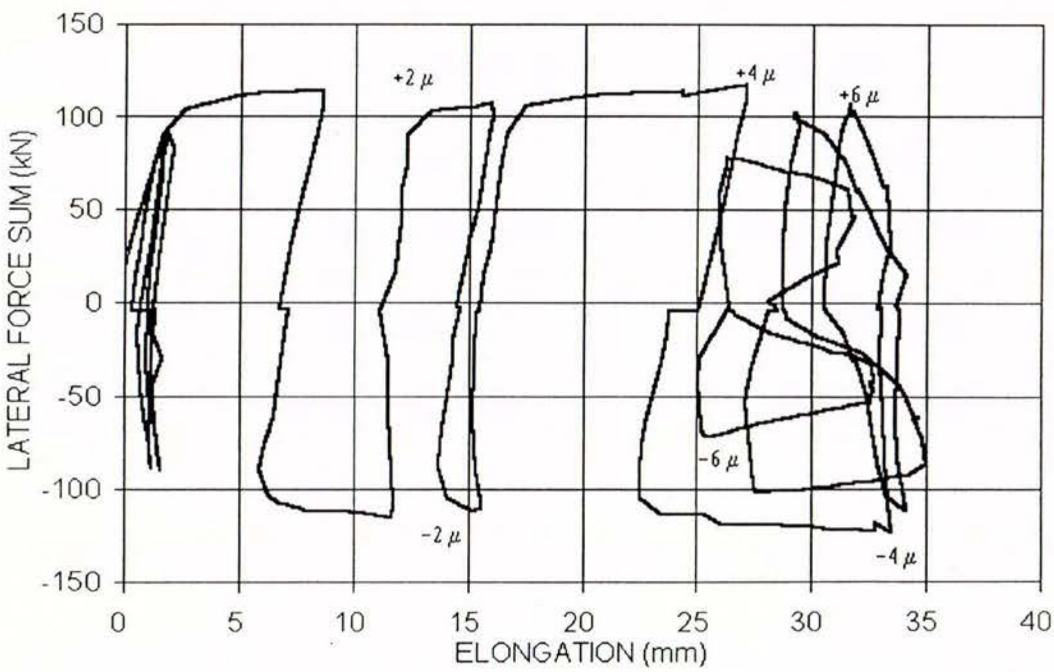

Fig. 5.10 b) Total Elongation of Beam-Column Unit as a Function of Applied Lateral Force Sum

Figure 5.11 shows the elongation divided into the components of Eqn. 2.2 as illustrated in Fig. 2.3, plotted against displacement ductility. It can be seen for the elastic cycles that the rotations resulted in a small increase in length of the tension zone longitudinal reinforcement of the beam. This was partially negated by the reduction in length of the compression zone reinforcement throughout the length of the beam. In the first inelastic half-cycle this pattern still existed since no force reversals had occurred. However, the yielding of the longitudinal steel in the tension zones of the beam caused a significant increase in elongation. The first force reversal in the inelastic range illustrated the significant contribution of the permanent extension of the compression zone reinforcement, *e*, which accounted for a third of the total elongation measured throughout the length of the beam. After a sufficient increase in ductility and a number of full reversals to the end of the $\pm 4\mu$ cycles, *e* accounted for over half of the total elongation measured throughout the length of the beam. During the $\pm 6\mu$ cycles as previously discussed, considerable buckling of the longitudinal flexural reinforcement of the beam occurred. This resulted in a significant reduction of the permanent extensions of the compression zone reinforcement, *e*, so that most of the measured elongation was a result of the imposed rotations of the plastic hinges.

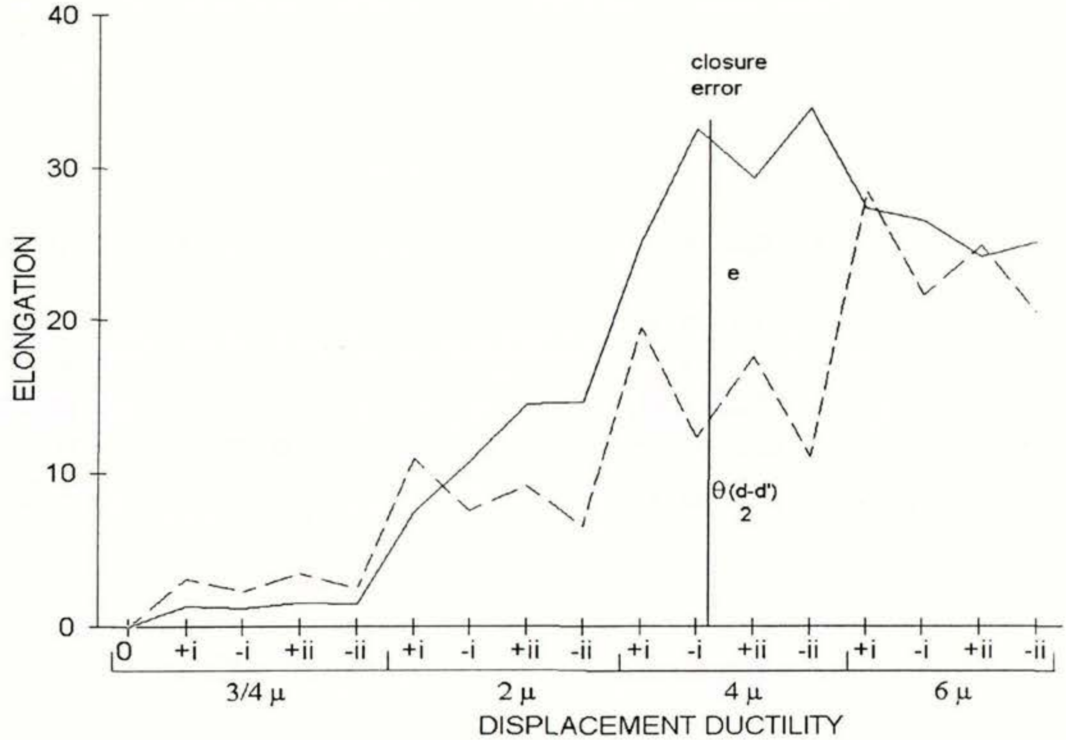

Fig. 5.11 Rotation and Compression Reinforcement Extension Components of Elongation for Unit 2

A difference in the measurements of elongation of the top and bottom beam gauges occurred. Figure 5.12 illustrates in an exaggerated way how the elongation of the longitudinal beam caused each of the four columns to have a residual "tilt" at the end of testing. For this to occur the top flange of the beam had to increase in length by a greater amount than the bottom flange. This mode of deflection caused the elongation on the top surface to be 5 mm greater than the corresponding value on the bottom surface in the ductility 4 cycles (see Fig. 5.13).

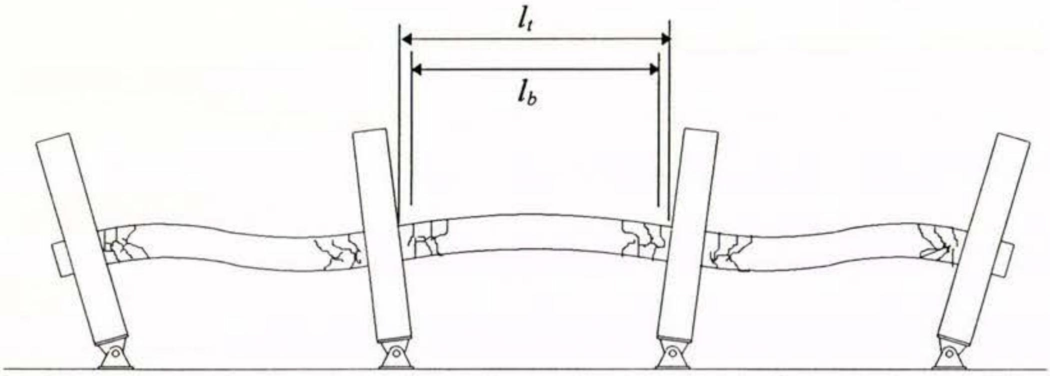

Fig. 5.12 - Schematic of Elongation Variation from Top and Bottom Flanges of Longitudinal Beam in Beam-Column Unit

The elongation was calculated for each separate bay (with joint deformation also separated) and plotted in Fig 5.14. It is evident that the central bay contributed less to the elongation of the whole unit than the two external bays. This can be explained by the considerably higher deflections through which the two external columns passed (1 and 4) compared with the two internal columns (2 and 3). Because of this, plastic hinges adjacent to the external columns of the longitudinal beam were forced to rotate more than the plastic hinges adjacent to the internal columns. Hence this caused the external bays to have larger elongations. This occurred up until the end of the 4μ cycles. During the 6μ cycles, buckling of the longitudinal steel, particularly in the plastic hinge zones adjacent to the external columns became significant. The considerable decrease in elongation in the +6μi and +6μii cycles of the exterior bays can be seen in Fig. 5.14. The reduction occurred to an extent that the internal bay showed a larger elongation than the exterior bays in the +6μi half cycle.

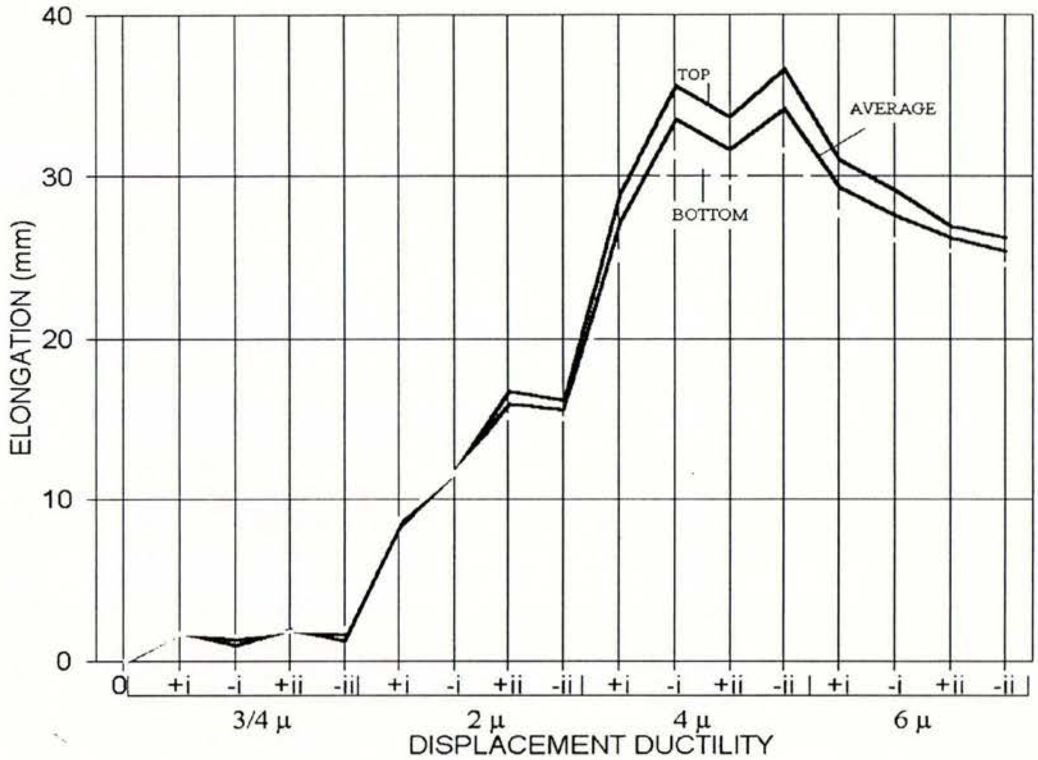

Fig. 5.13 Elongation of Top and Bottom Flanges of Unit 2

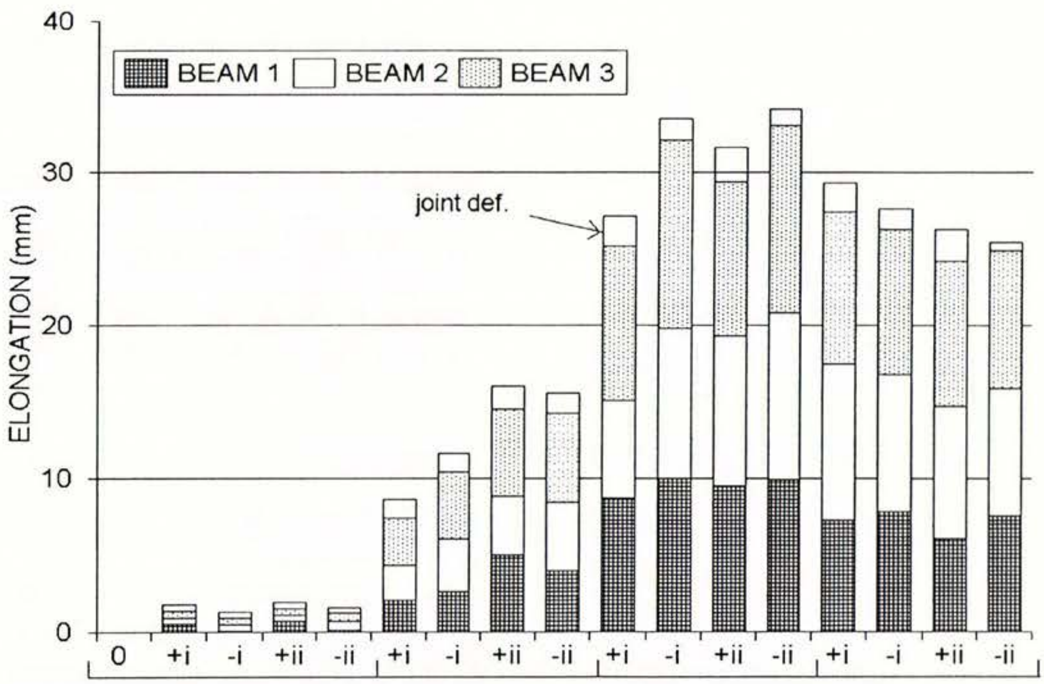

Fig. 5.14 Elongation of Each Bay of the Main Beam of Unit 2

The flexural and shear deformation are shown as components of the mid-span lateral deflection for each bay in Fig. 5.15 a), b) and c). As for unit 1, closure errors were observed between the computed mid-span deflection for shear and flexure and the linear interpolations of the mid-span deflection of each bay. In this unit the instrumentation to measure shear deformation extended the full effective depth, d-d', of the beam. However the computed shear deflection was only marginally greater than in unit 1. The closure error for this test was quite consistent for each bay throughout the test and generally follows the pattern of the flexural deformation. This suggests again that the closure error may be attributed to the measurement of shear deformation.

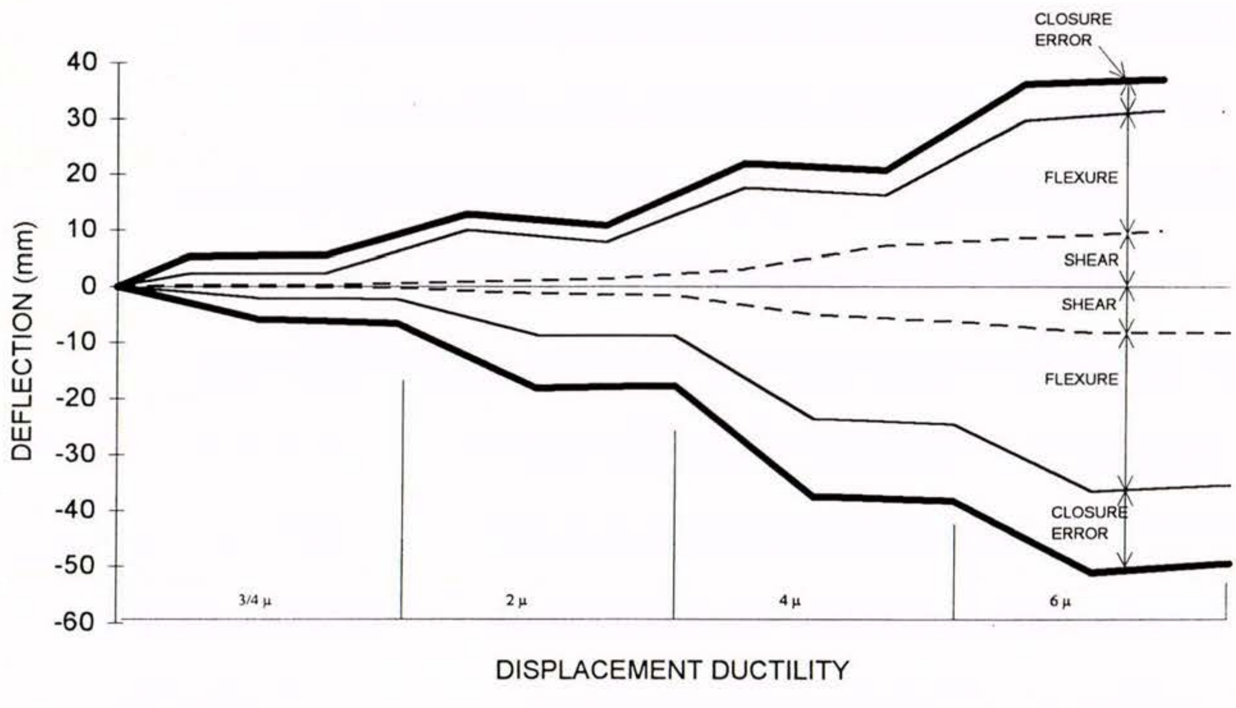

Fig. 5.15 a) Components of Bay 1 Mid-Span Displacement

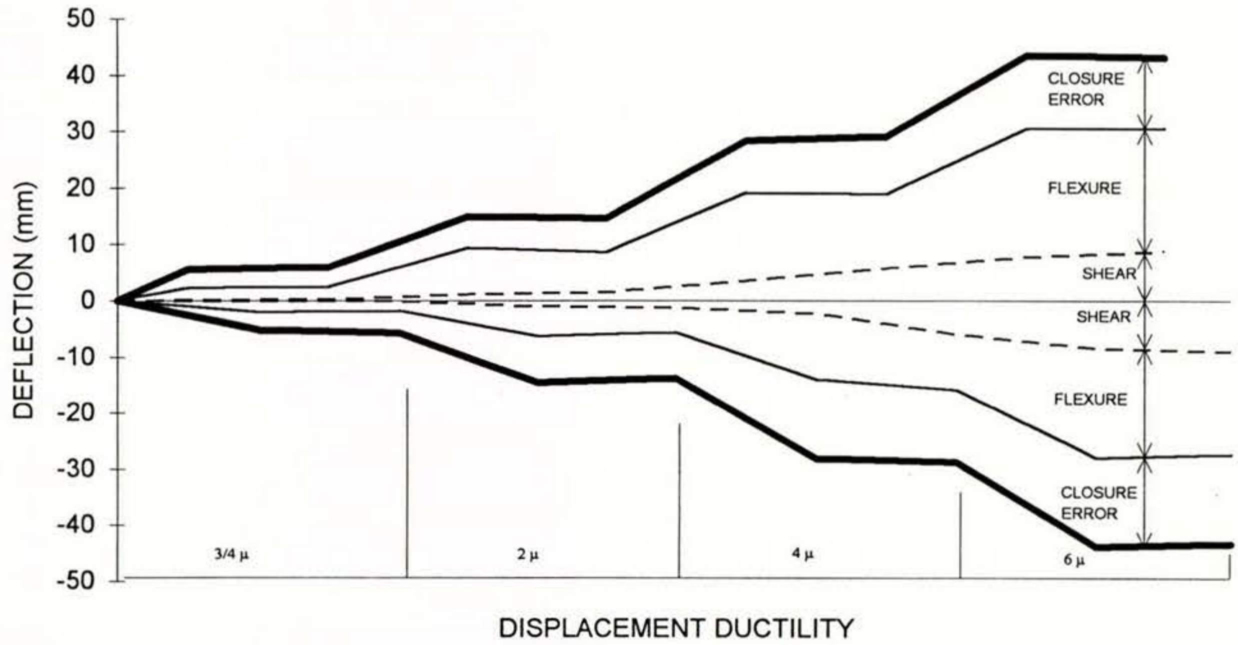

Fig. 5.15 b) Components of Bay 2 Mid-Span Displacement

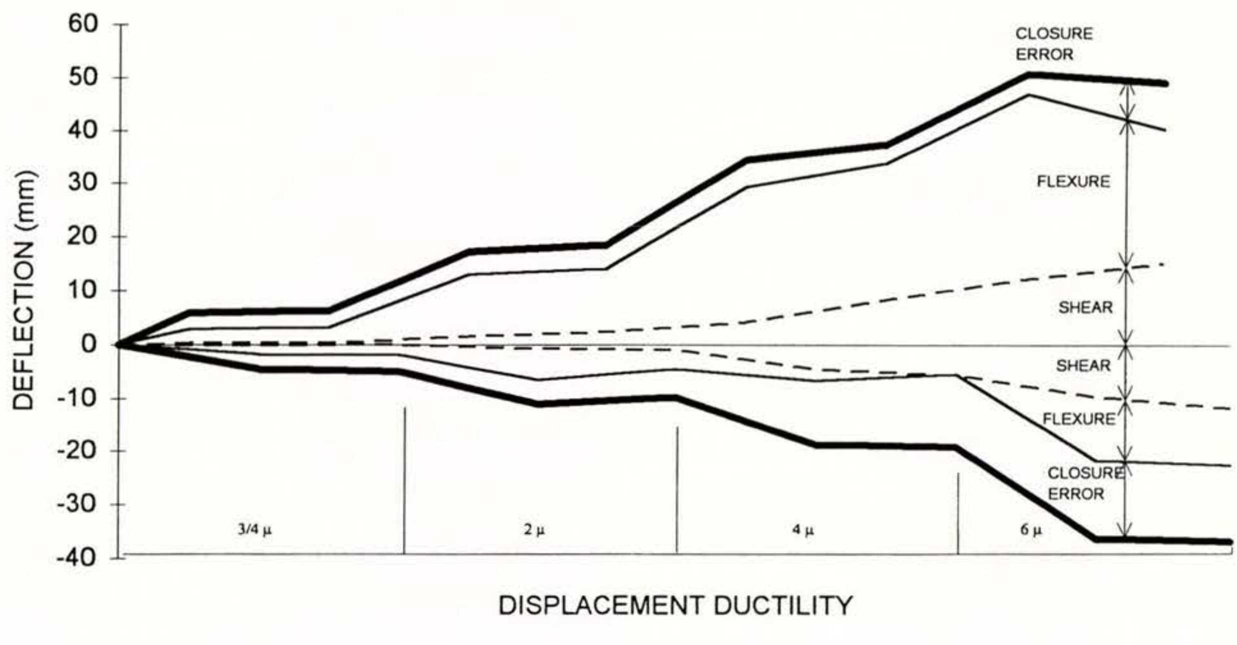

Fig. 5.15 c) Components of Bay 3 Mid-Span Displacement

5.5 SUMMARY

Unit 2 was tested under displacement controlled cyclic loading conditions to induce plastic hinging of the longitudinal beams adjacent to the columns. This test unit was designed and tested in the same way as the beam-column-slab unit. A maximum displacement ductility factor of 6μ was reached before significant strength degradation occurred.

Plastic hinging and significant shear deformation was observed at all plastic hinge zones along the main beam. Elongation of the plastic hinges was measured. The maximum measured elongation measured was 35mm at a displacement ductility factor of 4μ at an interstorey drift of 3.7%. Considerable buckling at a displacement ductility of 6μ occurred in the longitudinal beam steel at each plastic hinge reducing the amount of elongation recorded.

Permanent extensions of the compression zone longitudinal reinforcement were found to contribute to over half of the measured elongation. Good correlation between Equation 2.2 proposed for the elongation of reversing plastic hinge zones as discussed in Section 2.2.2 was found with the experimental results presented in this chapter.

Elongation was found to impose additional displacements on the columns. This additional displacement had a cumulative effect from one end of the unit to the other.

CHAPTER 6

COMPARISONS BETWEEN UNITS AND DISCUSSION

6.1 INTRODUCTION

In this chapter the general behaviour, deformation and force-displacement responses of both units are compared. Reference is also made to the comparative ductility capacity of the two units. The elongation of both units is compared with respect to interstorey drift. Discussion of the correlation of these results and the results of other researchers [Sakata and Wada] with the theory proposed for reversing plastic hinges is presented. A model for the effective width of slab contribution to the flexural capacity of a beam is discussed and used in reference to the results of extensions of the top the slab presented in Chapter 4.

6.2 GENERAL BEHAVIOUR AND FORCE-DISPLACEMENT RESPONSE

The crack patterns of both units shown in Fig.s 4.3 and 5.1 were indicated approximately the same level of deformation. From the results of the two units it can be seen that the presence of the slab in Unit 1 increased the stiffness of the of the beam-column system. The extrapolated displacement to cause the first yielding of the longitudinal flexural reinforcement in the plastic hinges (μ =1) was significantly greater in Unit 2 than Unit 1. Both units were forced to the same maximum ductility level of $\pm 6\mu$ and reached the same cumulative ductility.

Figure 6.1 shows the slab also increased the maximum lateral forces that the unit could sustain. This was attributed to all of the longitudinal slab reinforcement being effective in contributing to the flexural capacity of the beam. The inability of Unit 2 to reach higher applied lateral forces may have been a result of the significant buckling of the compression longitudinal flexural reinforcement in the plastic hinge zones of this unit. Spalling of the concrete from the plastic hinge zones would have reduced the lever arm between the concrete in compression and the tension longitudinal flexural reinforcement. This would have resulted in a reduction in the moment capacity of the plastic hinge zones and hence the lateral forces that the unit could have sustained would also have been reduced.

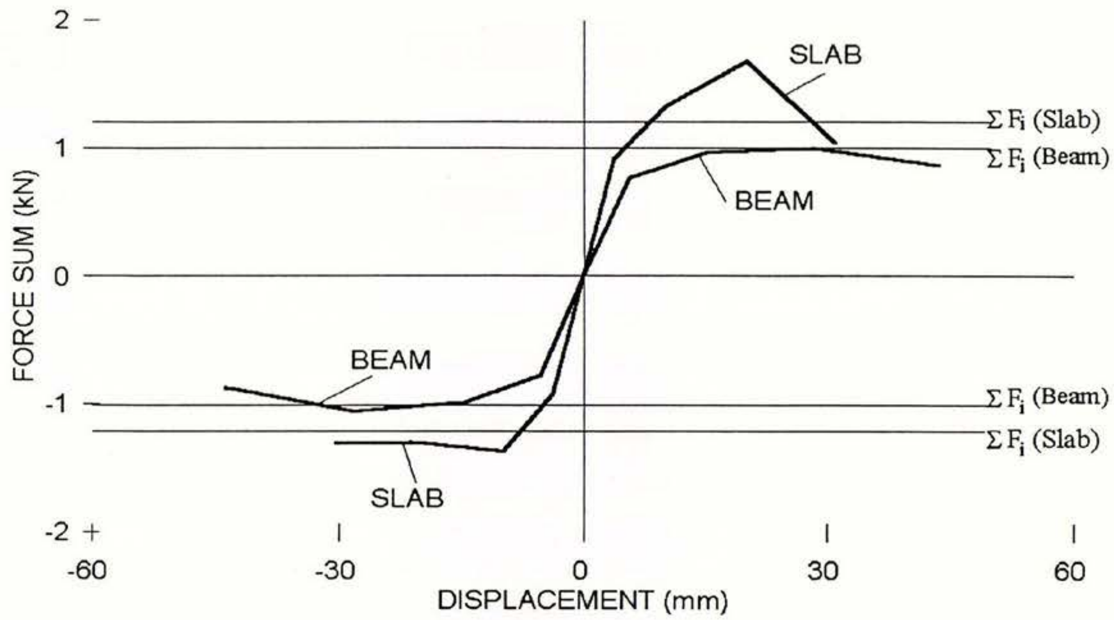

Fig. 6.1 Comparison of Peak Values of Force Displacement Response of Both Units (from the First Cycle of Each Ductility Level)

6.3 ELONGATION

The elongation results for both units are presented as a function of interstorey drift of the mid-span of the middle bay of each unit in Fig. 6.2 so that direct comparisons can be made. The interstorey drift of the mid-span gives an approximate relationship of the average plastic hinge rotation to elongation. This is consistent with the discussion presented for reversing plastic hinges in Section 2.2.2..

As expected Fig 6.2 shows that only a small amount of elongation during the elastic cycles of both tests. During the inelastic cycles the elongation increased significantly in both units to a maximum of approximately 33 mm over the whole length of the unit or 3% of the member depth per plastic hinge at an interstorey drift of 3.8%. At this stage of the test the compression longitudinal reinforcement in successive cycles started to buckle. This resulted in a reduction of the elongation of both units during subsequent cycles. The buckling may be seen in Fig.s 4.10 b) and 5 .10 b) where the elongation for both units is shown continuously. It is clear from Fig. 6.2, that the presence of the slab appeared to have no significant effect on the magnitude of elongation sustained by the beam.

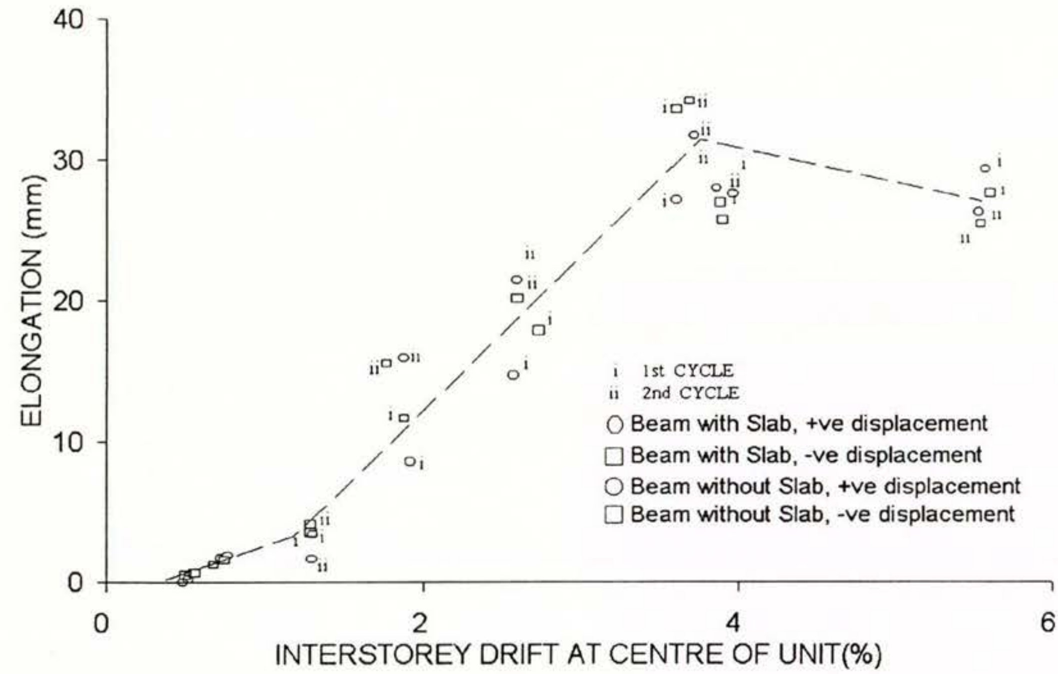

Fig. 6.2 Elongation Comparison of Both Units as a Function of Interstorey Drift

As presented in Section 5.4 the elongation of Unit 2 agreed with the relationship proposed for the elongation in reversing plastic hinges. This suggests that elongation of reversing plastic hinges can be predicted if an estimate of the plastic hinge rotations (θ) and the extension of the compression zone reinforcement "e" can be obtained. However it is realistically very difficult since there is no way of calculating "e" theoretically. The elongation measurements from a small scale model of a 7 bay 5 storey frame tested by Sakata and Wada are presented in Fig. 6.3. This specimen was tested under monotonic loading conditions and consequently the elongation can only be attributed to rotations of the plastic hinges as expressed in Eqn. 2.2. The compression zone reinforcement could not elongate since there were no load reversals. For this specimen the measured elongation reported can be compared with the values calculated from Eqn. 2.2 with e = 0 mm. The average rotation of the plastic hinges at levels' 2 and 5, were calculated from the deflections presented in Fig. 6.3 b). The plastic hinges were assumed to occur at a distance of one third of the beam overall depth away from the column faces. The beam was assumed rigid at all other points. This methodology is illustrated in Fig. 6.4. Table 6.1 presents a summary of these calculations compared to the measured results of Fig. 6.3 a).

Table 6.1 - Comparison of Predicted and Measured Elongation from Sakata and Wada

Level	Ave. Defl. (mm)	(d-d') (mm)	Hinge Rot. (θ) (rad)	δl per bay (mm)	**δl Total (mm)**	**δl Meas. (mm)**
2	5.65	34	0.0429	1.46	10.2	8.0
5	24.71	24	0.0715	1.72	12.0	14.7

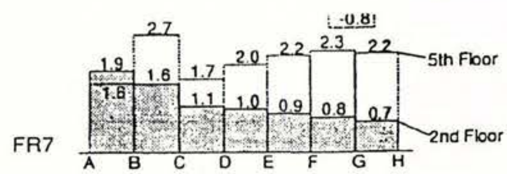

a)

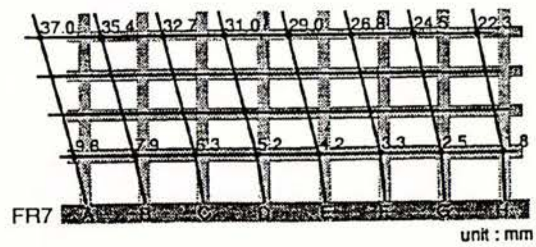

b)

Fig. 6.3 a) Elongation in each beam and b) Total Storey Deflections [after Sakata and Wada]

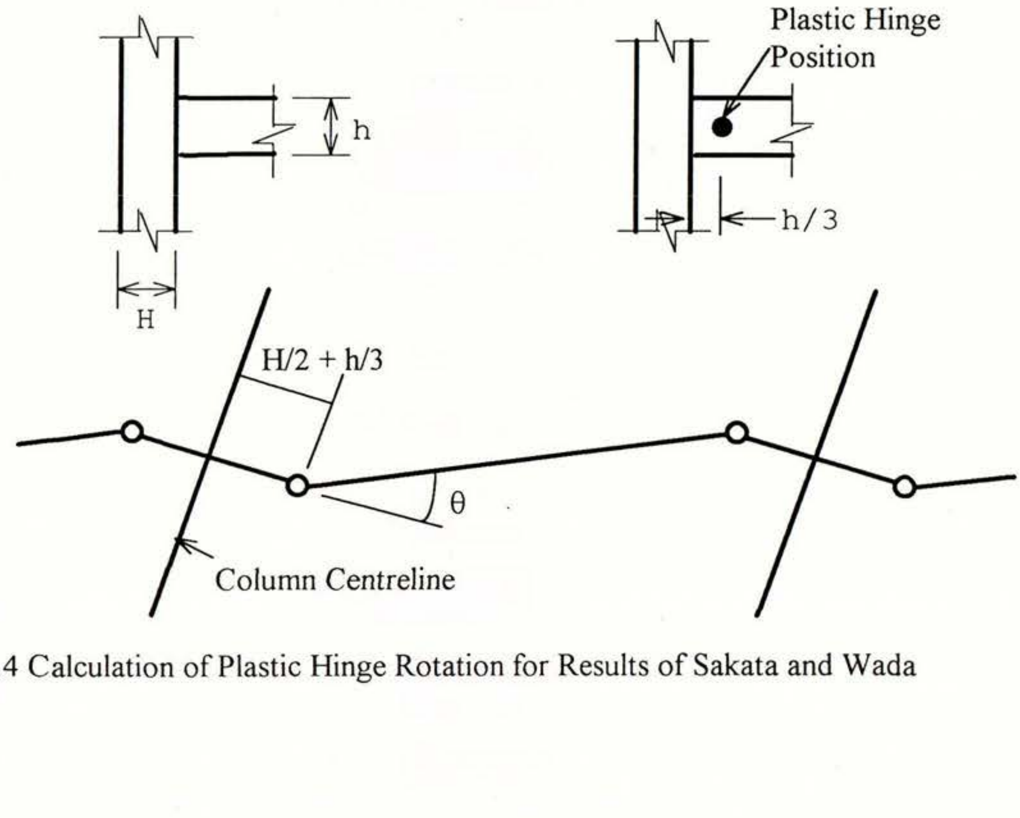

Fig. 6.4 Calculation of Plastic Hinge Rotation for Results of Sakata and Wada

The calculations in Table 6.1 are dependent on the position of the plastic hinges and the fact that the rotations are only taken at two specific points in each bay. However it can be seen that the results of Eqn. 2.2 still compare well with the experimental measurements of Sakata and Wada. This shows that hinge rotation component of the relationship expressed in Eqn. 2.2. can be used to predict elongation caused by rotation. A method of determining "e" is required if Eqn. 2.2 is to be used in predicting the elongation of reversing plastic hinges under inelastic cyclic actions.

6.4 EFFECTIVE WIDTH OF SLAB

In this discussion the effective width of a slab is taken as the width in which the longitudinal reinforcement has yielded. The yielding of this reinforcement can be considered to be a result of the dispersion of elongation at the slab level in a plastic hinge. If the elongation of the longitudinal reinforcement, at the level of the slab, in a plastic hinge is δl, then the effective width slab will extend to that line where the condition expressed in Eqn. 6.1 occurs.

$$l_e = \frac{\delta l}{\varepsilon_y} \tag{6.1}$$

where; l_e is the length over which an extension of δl of the longitudinal steel will just cause that steel to yield as shown in Fig. 6.5, and

ε_y is the strain at yield of the longitudinal steel .

Alternatively if the width where the longitudinal reinforcement has just yielded is known, then the angle of dispersion of the elongation in the slab at the plastic hinge may be determined. This can be given for a specific hinge rotation.

If the effective width of slab is w_{eff}, as shown in Fig. 6.5 and l_p is the plastic hinge length then ϕ can be expressed in terms of these parameters as in Eqn. 6.2.

$$\tan\phi = \frac{w_{eff} - \frac{b}{2}}{(l_e - l_p)} \tag{6.2}$$

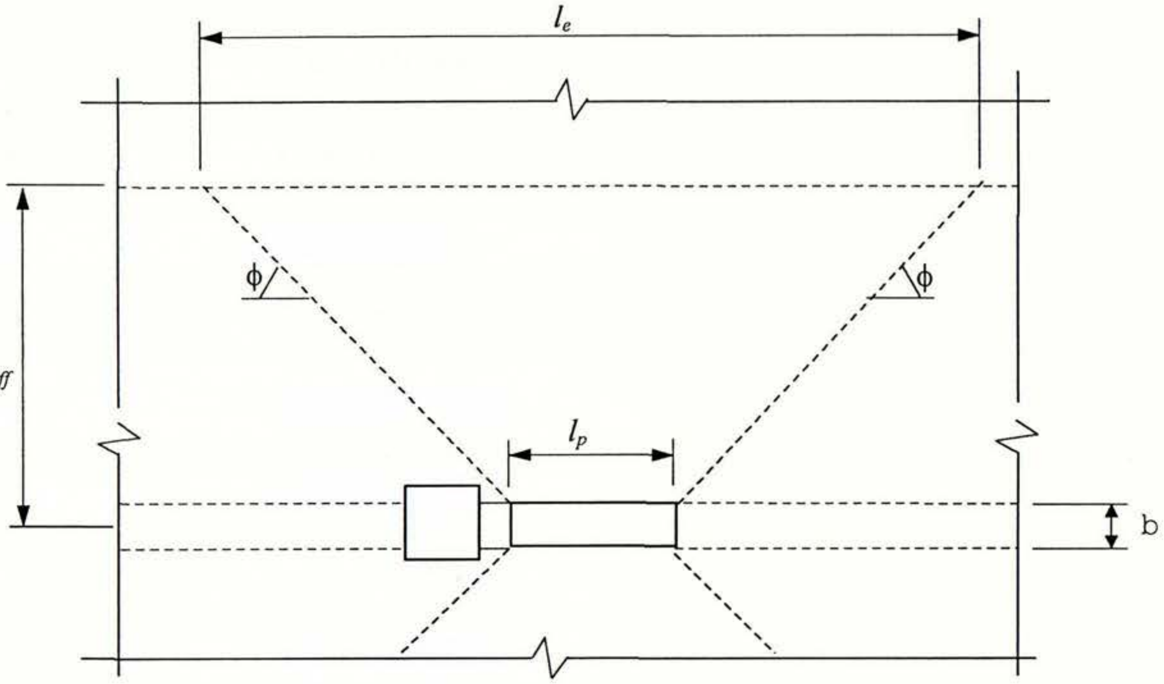

Fig. 6.5 Model of Effective Width Based on Elongation of Plastic Hinge Zone at Interior Connection

This model was applied to the results from the instrument lines' E,H,I and L so that yielding of the slab reinforcement could be traced across the slab. In addition the yield dispersion angle,ϕ, at the time of yielding could also be estimated. The hinge rotation was also noted.

These results showed that all of the slab reinforcement had yielded by the peak of the -4μi half cycle. This suggests that full width was effective in contributing to the flexural capacity of the beam. Once the reinforcement had begun to yield close to the longitudinal beam then the rest of the reinforcement in the slab yielded very soon after. All of the reinforcement had yielded before the plastic hinge rotations had reached 0.01. The calculations for ϕ adjacent to internal columns as summarised in Fig. 6.6 suggest that the angle for the dispersion of elongation across a slab was always greater than 45°. Note that the calculation of l_e is based on the assumption that yielding of the reinforcement occurs uniformly over l_e.. In reality the reinforcement is likely to be yielding only within the concrete cracks. However, ϕ, still gives a good indication of the yielding pattern of the slab reinforcement.

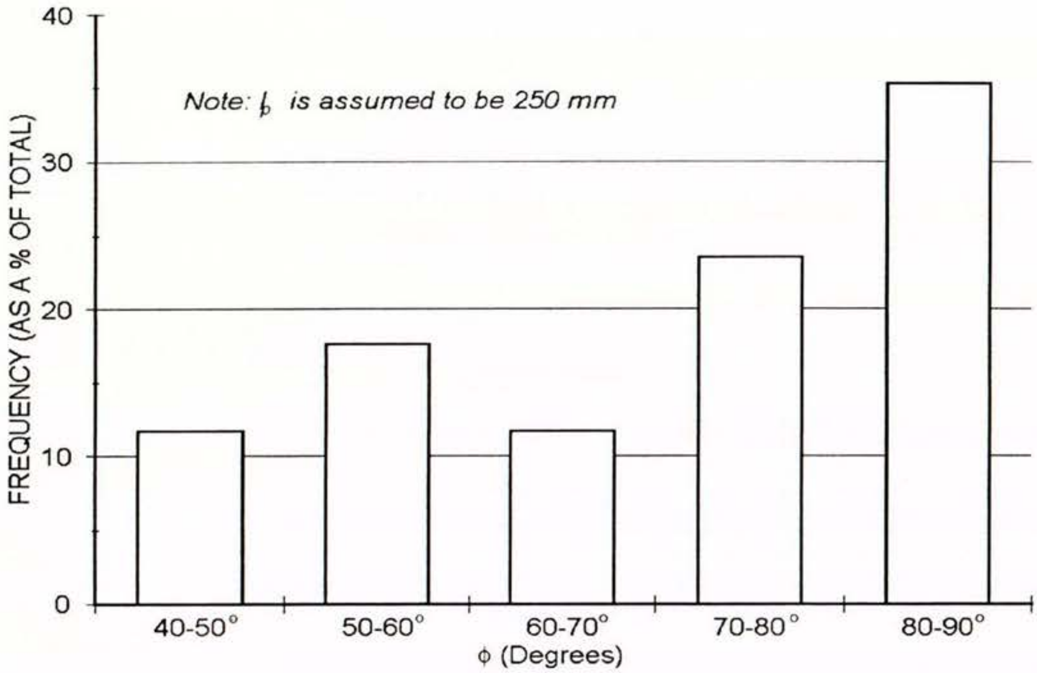

Fig. 6.6 Frequency as a Percentage of Total Number of Calculations of ϕ

6.5 SUMMARY

A comparison of the results of the two units shows:

(I) both units reached the same ductility level,

(ii) that the slab increased the strength and stiffness of unit 1, and

(ii) that the slab had no appreciable influence on the elongation recorded for unit 1.

A model for the effective width contribution of slab to the flexural capacity of a beam based on elongation was presented. By applying this model to the results obtained from unit 1, it was shown that all of the slab longitudinal reinforcement was effective in contributing to the flexural strength of the main beam. All of this reinforcement yielded before the plastic hinge rotations had reached 0.01. An estimate of the angle of dispersion of elongation is also given.

CHAPTER 7

CONCLUSIONS AND RECOMMENDATIONS FOR RESEARCH

7.1 CONCLUSIONS

Previous research in which elongation has been reported was reviewed. Elongation of reversing plastic hinges was shown to be a function of the rotations sustained by the plastic hinge and of the extension of the compression zone longitudinal flexural reinforcement. Elongation of 2% to 5% of the member depth per plastic hinge zone have been measured in tests on a variety of reinforced concrete systems including cantilever beams, a portal frame, shear wall coupling beams and statically determinate beam-column-slab units.

In the experimental section of this research two beam-column units, one with a cast insitu slab and one without, were tested under inelastic cyclic forces. The behaviour of the units was similar in that they both reached a maximum displacement ductility of $\pm 6\mu$ and sustained the same cumulative ductility at failure. In these tests elongation occurred in the beams. This caused differential displacements of the columns from one end of the unit to the other. Comparisons of the elongations measured in the two units showed that the cast-insitu slab had no significant effect on the elongation. A maximum elongation of 3% of the member depth per plastic hinge for both units was measured before the compression zone reinforcement began to buckle.

A model for determining when slab longitudinal reinforcement yields at a given width was presented. The test results indicated that the entire width of slab in unit 1 was effective in its contribution to the flexural capacity of the beam. Results of elongation measurements on the top surface of the slab supports this.

7.2 RECOMMENDATIONS FOR FURTHER RESEARCH

The tests showed that casts insitu slabs do not provide any significant source of restraint to elongation. Investigation into the effect of elongation through multi-storey frame structures should now be carried out. This should include the development of an analysis technique that implements the effects of elongation into design. Effects such as increased axial forces in the elongating members and corresponding increase in shear forces of adjacent columns need to be investigated in relation to multi-bay frame structures.

A method of predicting the extension of the compression zone reinforcement (e), to be used in the evaluation of elongation in reversing plastic hinge zones is needed. This could then be used so that tolerances for structural and non-structural elements in reinforced concrete structures could be adjusted to allow for elongation.

The model for the effective width contribution of slab presented needs further investigation to determine if it can be used reliably to predict the behaviour of slab reinforcement under cyclic actions. A check to determine whether the assumption of l_e is correct will also be necessary.

REFERENCES

Beekhuis, W.J., (1971), "An Experimental Study of Squat Shear Walls" M.E. Thesis, Department of Civil Engineering, University of Canterbury, Christchurch, 132 pp.

Binney, J.R., (1972), "Diagonally Reinforced Coupling Beams", M.E. Thesis, Department of Civil Engineering, University of Canterbury, Christchurch, 131 pp.

Cheung, P.C., (1991), "Seismic Design of Reinforced Concrete Beam-Column Joints with Floor Slab", PhD. Thesis, Department of Civil Engineering, University of Canterbury, Christchurch, 328 pp.

Cheung, P.C., Paulay, T., and Park, R., (1991), "Mechanisms of Slab Contributions in Beam-Column Subassemblages", SP123-10, Jirsa, J.O. (editor), "Design of Beam-Column Joints for Seismic Resistance ", A.C.I SP123, 518 pp.

Cheung, P.C., Paulay, T., and Park, R., (1992), "Some Possible Revisions to the Seismic Provisions of the New Zealand Concrete Design Code for Moment Resisting Frames", Bulletin of NZNSEE, Vol. 25, No. 1, pp. 37-43.

Davidson, B.J. and Fenwick, R.C., (1993), "The Seismic Response of Ductile Reinforced Concrete Frames with Uni-Directional Hinges", Report No. 527, School of Engineering, Department of Civil Engineering, University of Auckland, 59 pp.

Douglas, K.T., (1993), Davidson, B.J. and Fenwick, R.C., "Modelling Elongation in Seismic Resistant Concrete Frame Structures", The Thirteenth Australasian Conference on the Mechanics of Structures and Materials Proceedings, July 1993, Vol. 1,pp. 265-272

Durrani, A.J., and Wight, J.K., (1987), "Earthquake Resistance of Reinforced Concrete Interior Connections Including a Floor Slab", A.C.I Structural. Journal., Vol. 84, No5, pp.400-406.

Fenwick, R.C., (1991), "The Behaviour of Plastic Hinge Zones in Seismic Resistant Concrete Structures ",Earthquake Blast and Impact, SECED Conference Proceedings, pp. 221-230.

Fenwick, R.C. and Fong, A. (1979), "The Behaviour of Reinforced Concrete Beams Under Cyclic Loading", Bulletin of NZNSEE, Vol. 12, No. 2, pp. 158-167.

Fenwick, R.C. and Megget,L.M., (1993), "Elongation and Load Deflection Characteristics of Reinforced Concrete Members Containing Plastic Hinges", Bulletin of NZNSEE, Vol. 26, No. 1, pp.

Fenwick, R.C., and Nguyen, H.T., (1981), "Reinforced Concrete Beam-Column Joints for Seismic Loading", Report No. 220, School of Engineering, Department of Civil Engineering, University of Auckland, 62 pp.

Fenwick, R.C., Tankut, A.T., and Thom, C.W., (1981), "The Deformation of Reinforced Concrete Beams Subjected to Inelastic Cyclic Loading - Experimental Results", Report No. 268, School of Engineering, Department of Civil Engineering, University of Auckland, 72 pp.

Fenwick, R.C. and Thom, C.W., (1982), "Shear Deformation in Reinforced Concrete Beams Subjected to Inelastic Cyclic Loading", Report No. 279, School of Engineering, Department of Civil Engineering, University of Auckland, 51 pp.

Megget, L.M., and Fenwick, R.C., (1989), "Seismic Behaviour of a Reinforced Concrete Portal Frame Sustaining Gravity Loads", Bulletin of NZNSEE, Vol. 22, No. 1, pp. 39-49

Mejia-McMaster, J.C. and Park, R., (1994), "Precast Concrete Hollow-Core Floor Unit Support and Continuity", Research Report 94/4, Department of Civil Engineering, University of Canterbury, Christchurch, 104 pp.

NZS 3101, (1982), "Code of Practice for the Design of Concrete Structures", Parts 1 and 2, Standards Association of New Zealand, Wellington.

Pantazopoulou, S.J., and Moehle, J.P., (1987) " The Effects of Slabs on the Flexural Behaviour Beams" Report No. UCB/EERC-87/17, Earthquake Engineering Research Center, University of California, Berkeley, 122 pp.

Qi., X., and Pantazopoulou, S.J., (1991), "Response of RC Frame under Lateral Loads" Journal of Structural Engineering, A.S.C.E., Vol. 117, No. 4, pp. 1167-1188.

Restrepo-Posada, J.I., (1992), "The Seismic Behaviour of Connections Between Precast Concrete Elements", PhD Thesis, Department of Civil Engineering, University of Canterbury, Christchurch, 385 pp.

Tjokrodimuljo, K., (1985), "Dehaviour of Reinforced Concrete Under Cyclic Loading", M.E. Thesis, Department of Civil Engineering, University of Auckland, 151 pp.

Wight, J.K. (editor), (1984). "Earthquake Effects on Reinforced Concrete Structures", American Concrete Institute, SP-84, 428 pp.

Zerbe, H.E., and Durrani, A.J., (1989), "Seismic Response of Connections in Two-Bay R/C Frame Subassemblies", Journal of Structural Engineering, A.S.C.E., Vol. 115, No. 11, pp. 2829-2844.

Zerbe, H.E., and Durrani, A.J., (1990), "Seismic Response of Connections in Two-Bay Reinforced Concrete Frame Subassemblies with a Floor Slab", A.C.I. Structural Journal, Vol. 87, No. 4, pp. 406-415.

APPENDIX A

REINFORCEMENT TENSILE TEST RESULTS

KEY

SERIES S;	**ϕ3.125 mm WIRE** **(UNTREATED STIRRUP REINFORCEMENT WIRE)**
SERIES HS;	**ϕ3.125 mm WIRE** **(HEAT TREATED STIRRUP REINFORCEMENT)**
SERIES OB;	**D4 DEFORMED BAR** **(HEAT TREATED SLAB REINFORCEMENT, 1ST BATCH)**
SERIES OA;	**D4 DEFORMED BAR** **(HEAT TREATED SLAB REINFORCEMENT, 2ND BATCH)**
D10	**BEAM LONGITUDINAL FLEXURAL REINFORCEMENT** **TRANSVERSE BEAM LONGITUDINAL REINFORCEMENT**
D12	**COLUMN LONGITUDINAL FLEXURAL REINFORCEMENT**

TENSILE TEST STRESS - STRAIN CURVE

SPECIMEN S-1

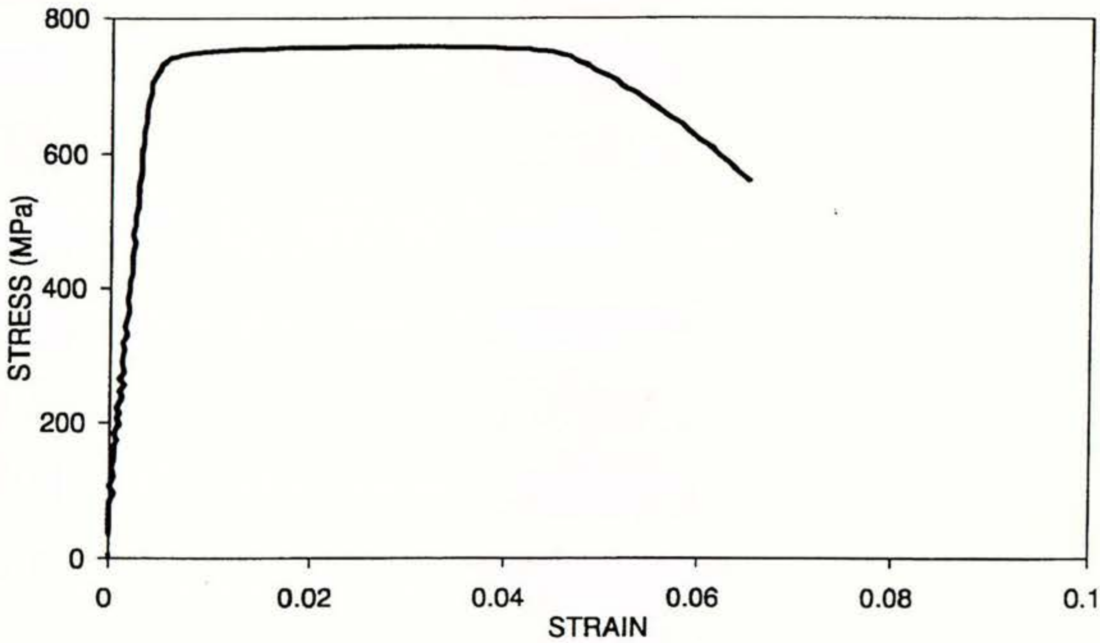

TENSILE TEST STRESS - STRAIN CURVE

SPECIMEN S-2

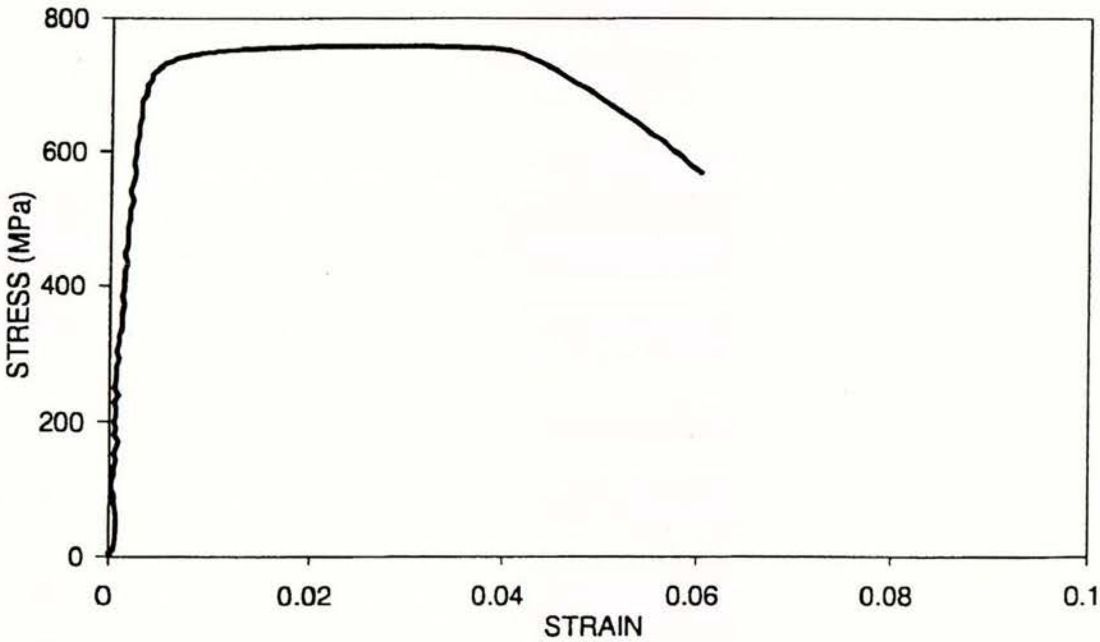

TENSILE TEST STRESS - STRAIN CURVE

SPECIMEN S-2

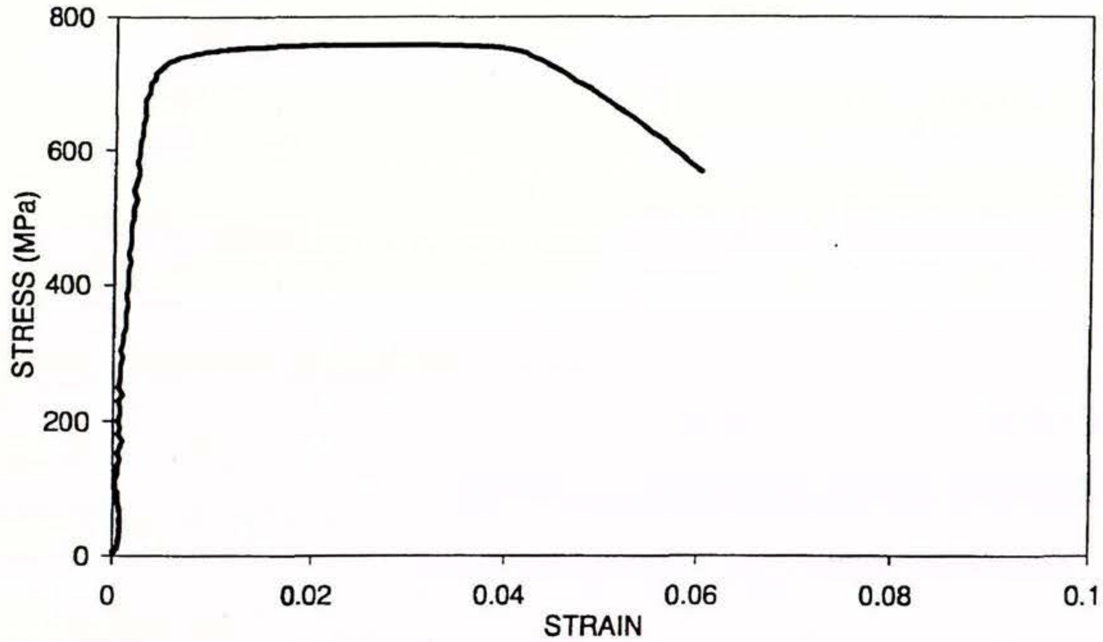

TENSILE TEST STRESS - STRAIN CURVE

SPECIMEN HS-1

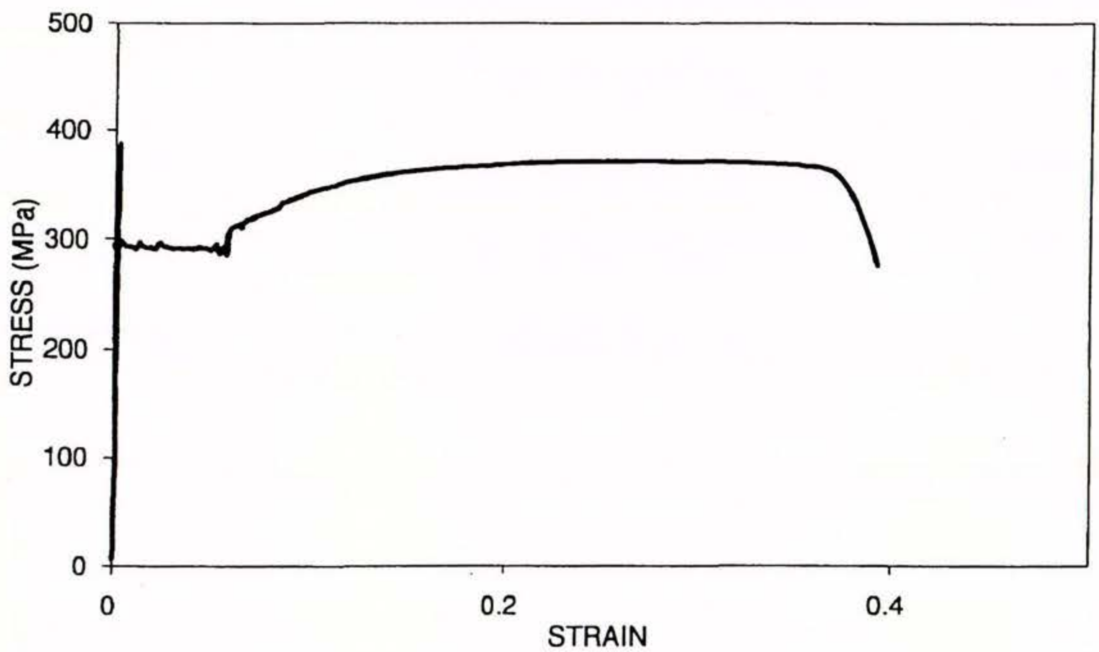

TENSILE TEST STRESS - STRAIN CURVE
SPECIMEN HS-2

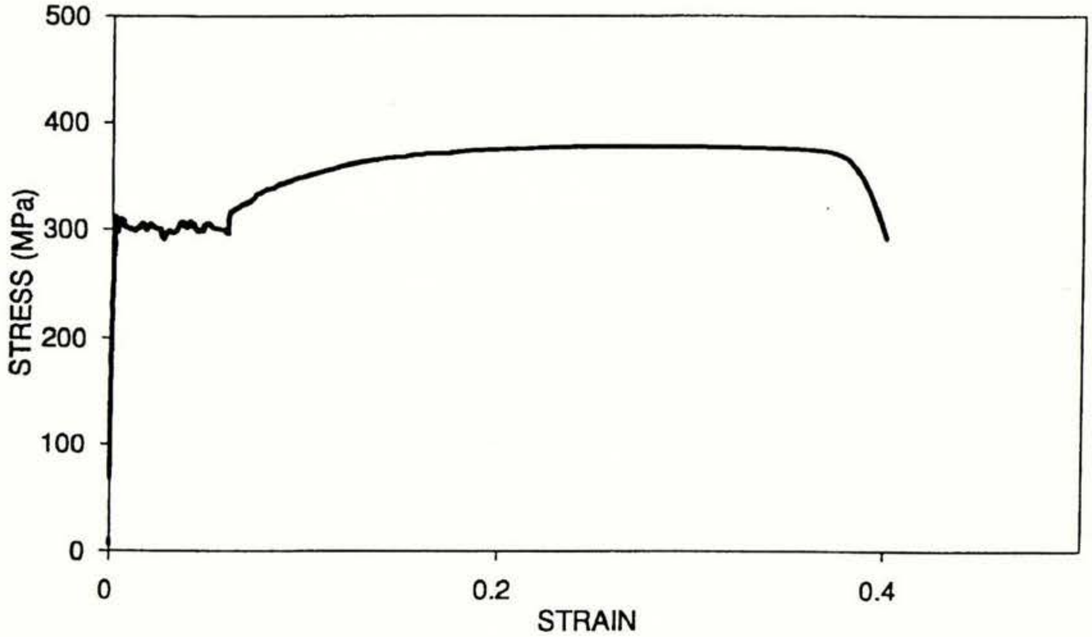

TENSILE TEST STRESS - STRAIN CURVE
SPECIMEN HS-4

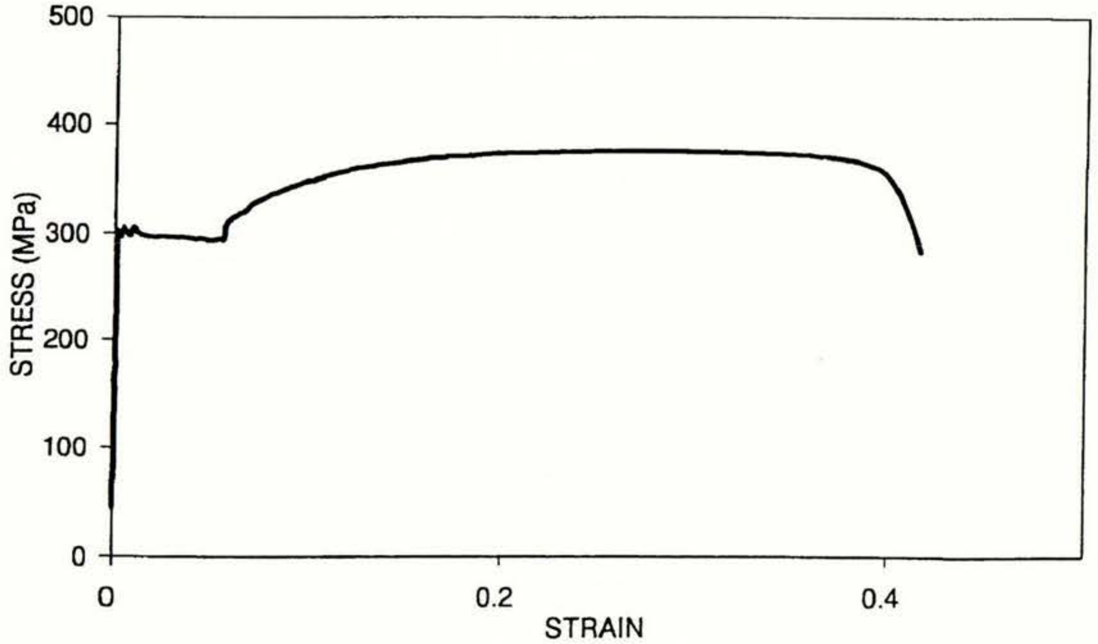

TENSILE TEST STRESS - STRAIN CURVE

SPECIMEN OB22

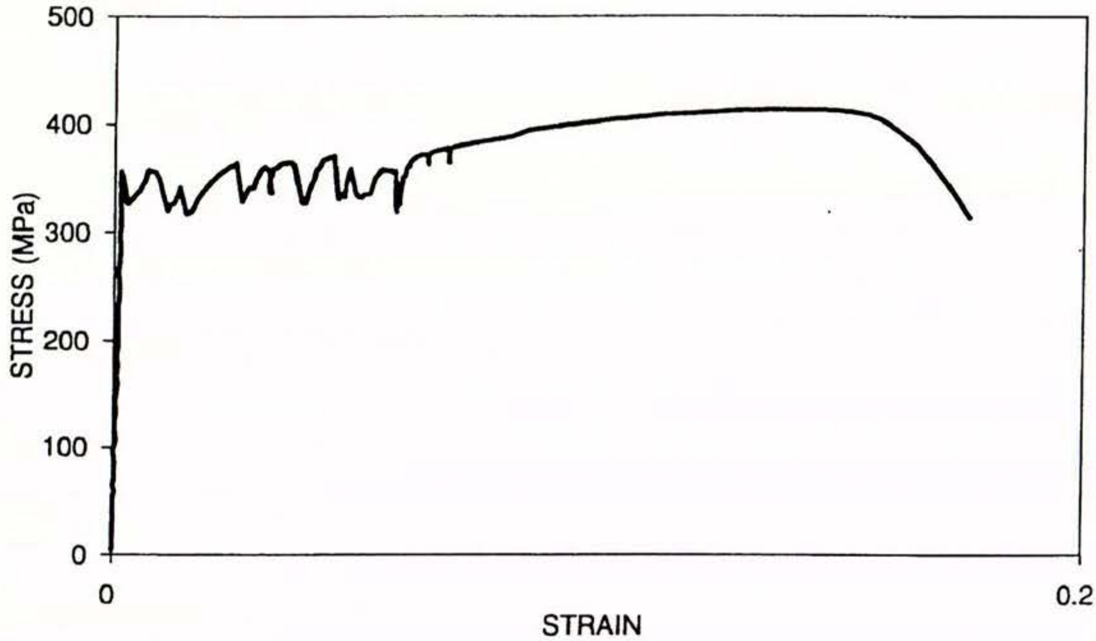

TENSILE TEST STRESS - STRAIN CURVE

SPECIMEN OB31

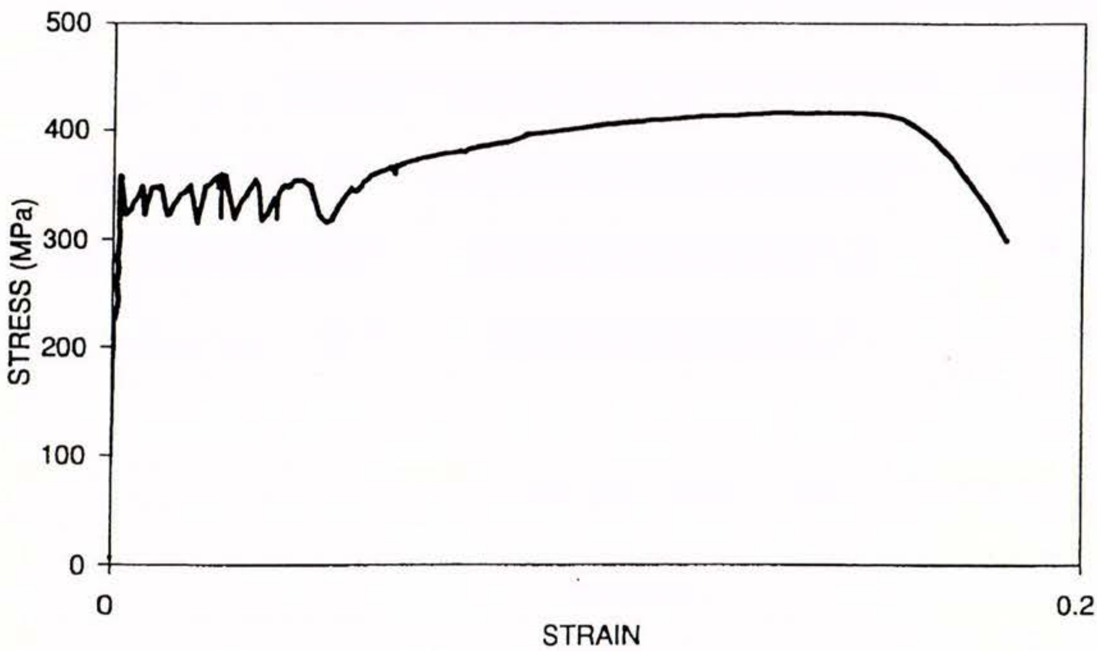

TENSILE TEST STRESS - STRAIN CURVE
SPECIMEN OA12

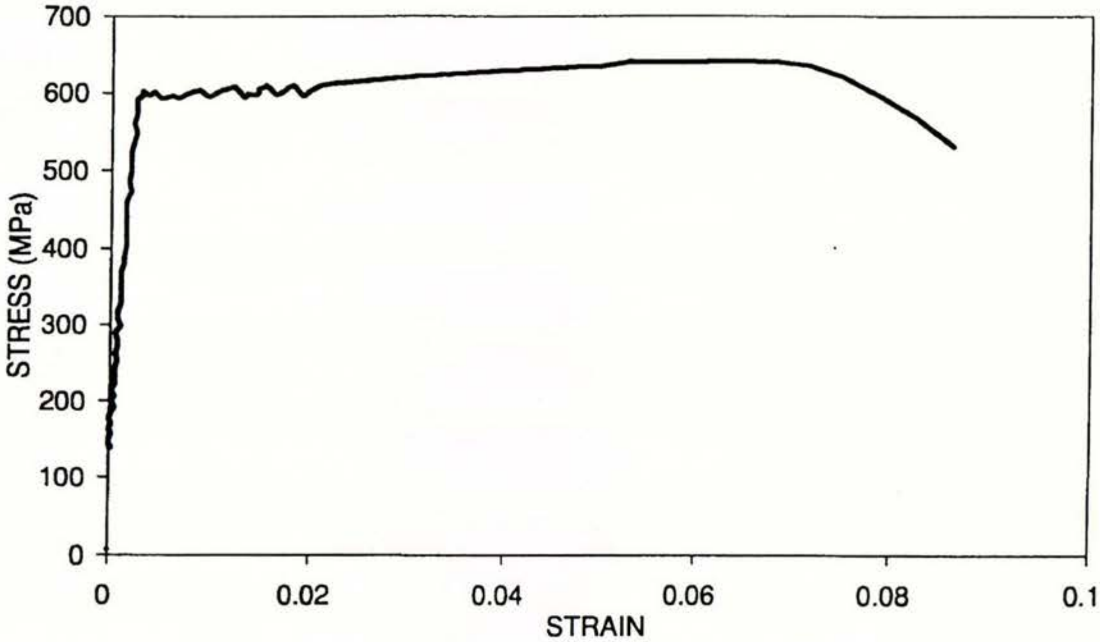

TENSILE TEST STRESS - STRAIN CURVE
SPECIMEN 0A21

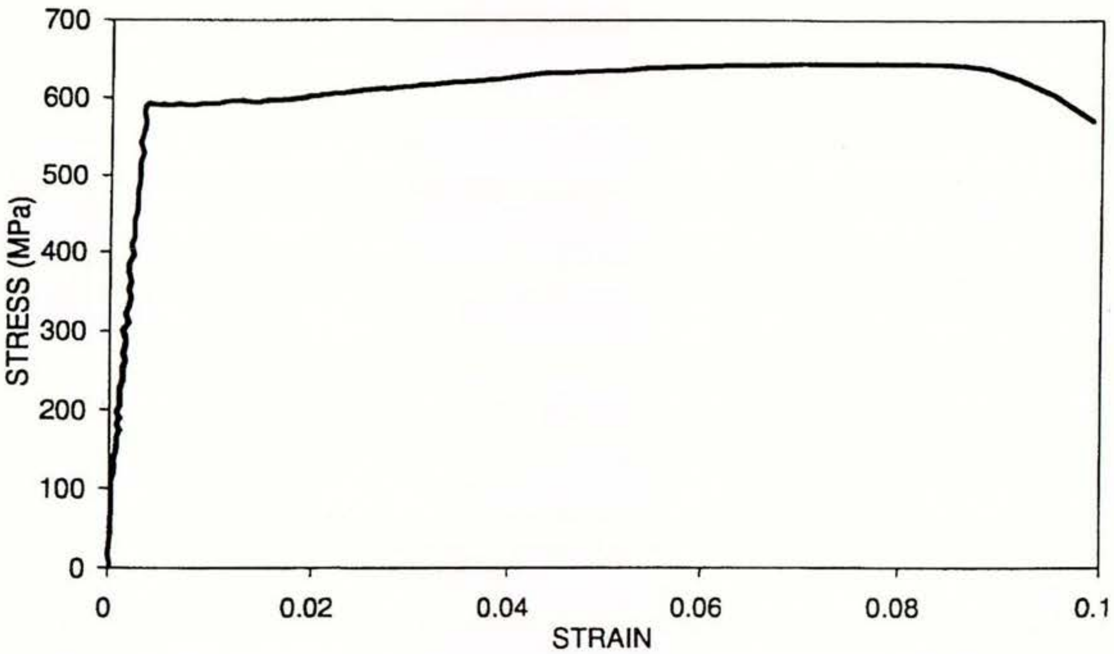

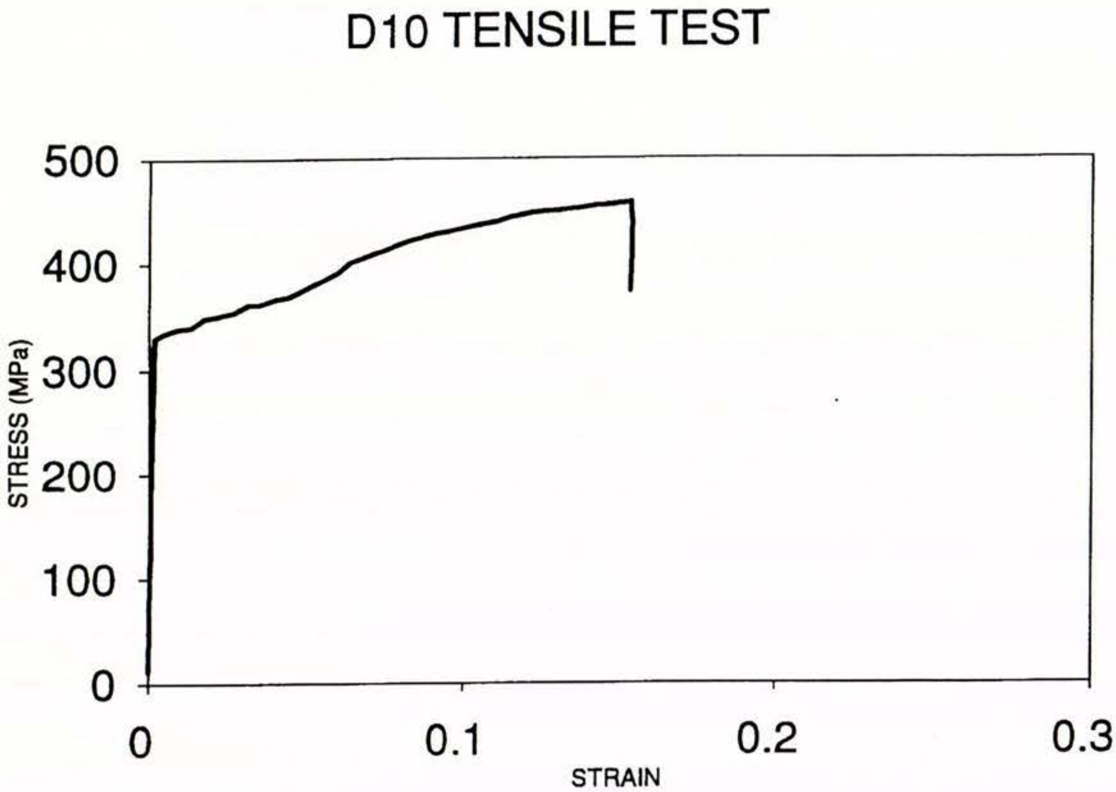
D10 TENSILE TEST
500
400
300
200
100
0
STRESS (MPa)
0
0.1
0.2
0.3
STRAIN

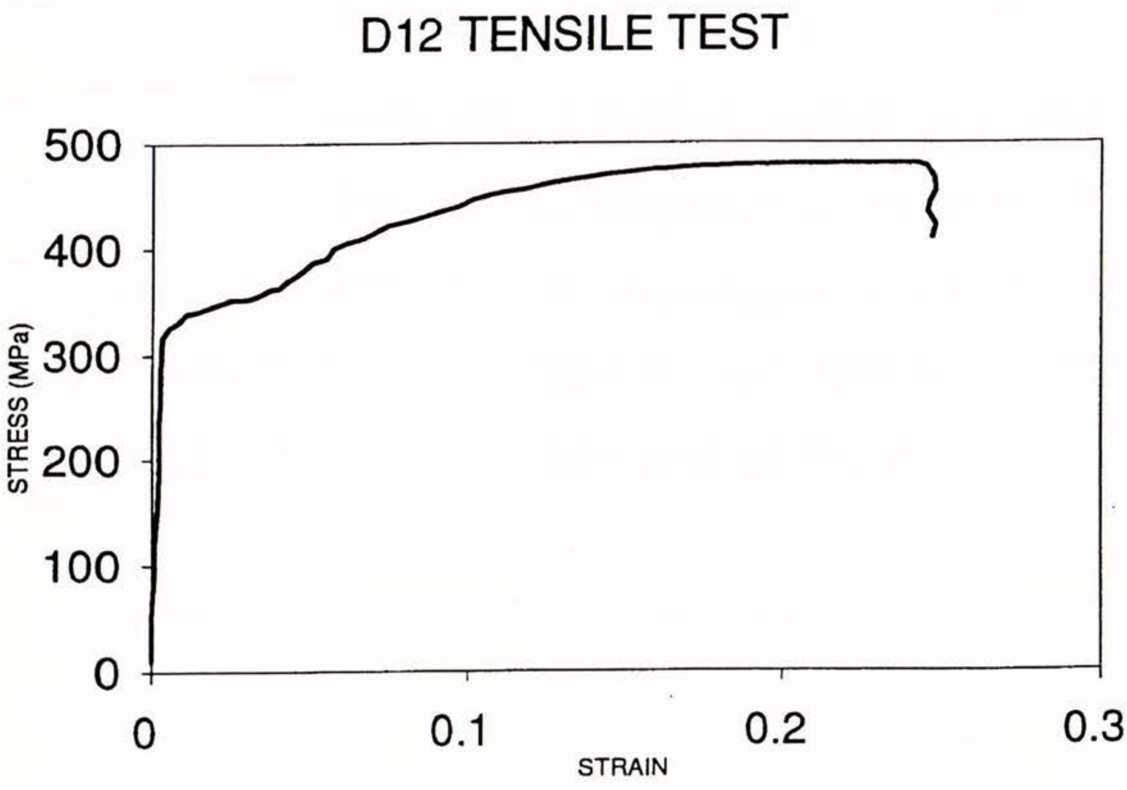
D12 TENSILE TEST
500
400
300
200
100
0
STRESS (MPa)
0
0.1
0.2
0.3
STRAIN

APPENDIX B

CRACK WIDTH DISTRIBUTION FOR SLAB IN UNIT 2

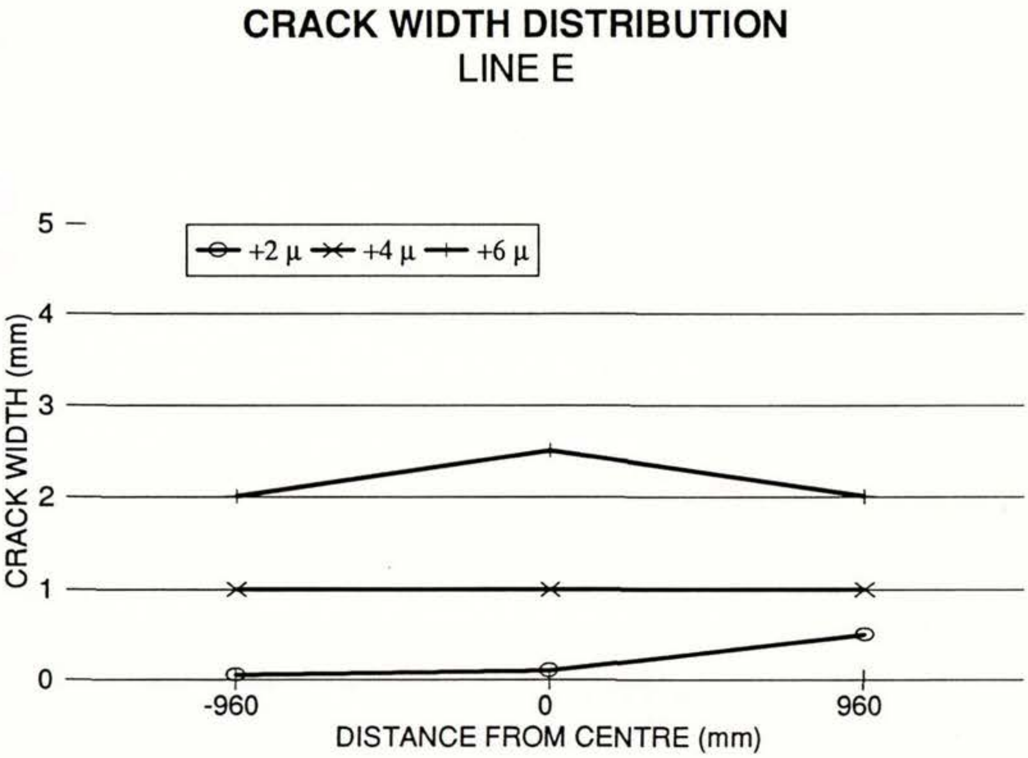
CRACK WIDTH DISTRIBUTION
LINE E
+2 μ
+4 μ
+6 μ
CRACK WIDTH (mm)
5
4
3
2
1
0
-960
0
960
DISTANCE FROM CENTRE (mm)

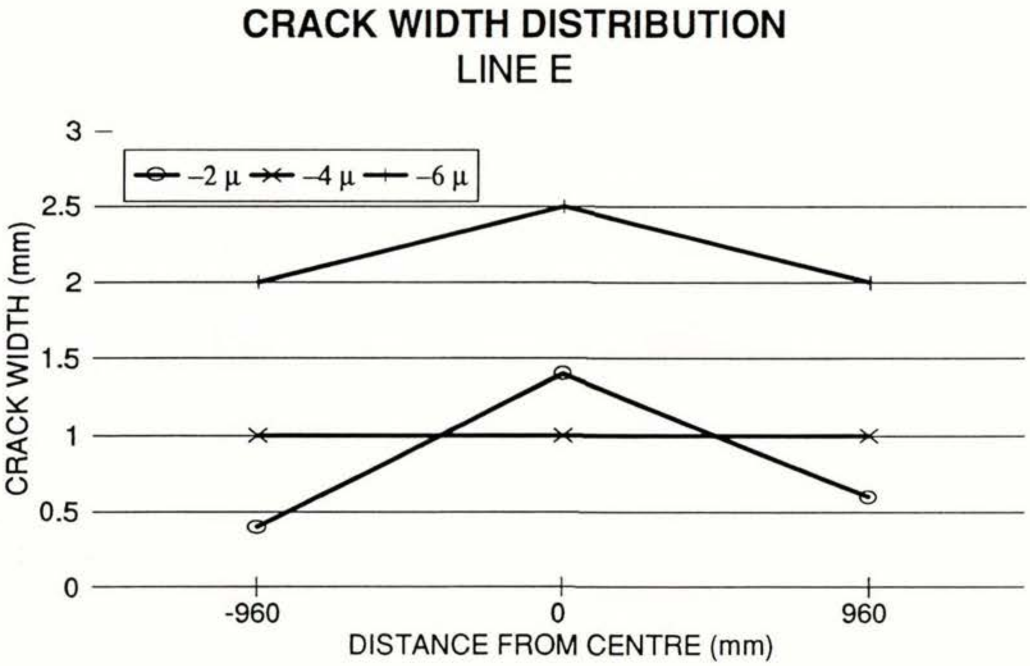
CRACK WIDTH DISTRIBUTION
LINE E
−2 μ
−4 μ
−6 μ
CRACK WIDTH (mm)
3
2.5
2
1.5
1
0.5
0
-960
0
960
DISTANCE FROM CENTRE (mm)

CRACK WIDTH DISTRIBUTION
LINE H

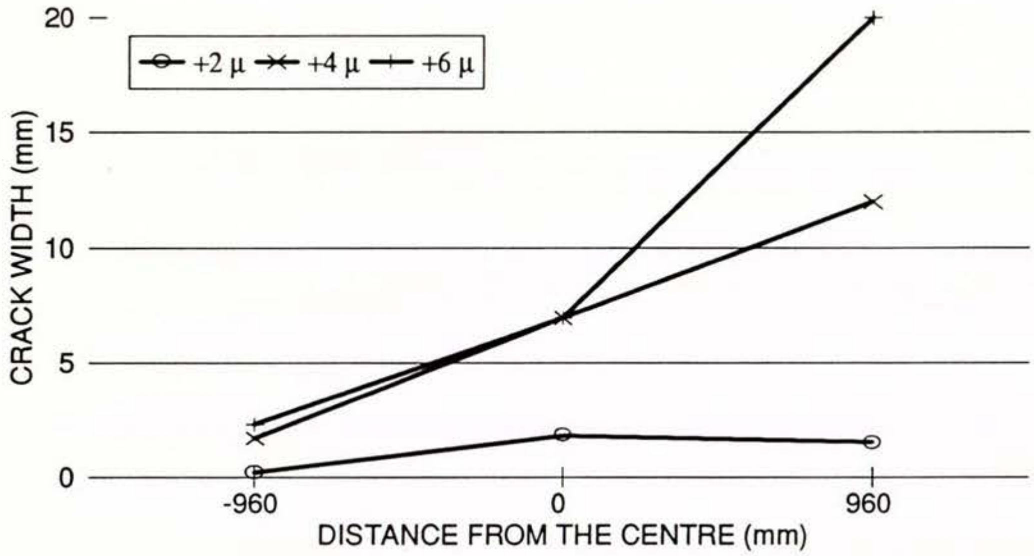

CRACK WIDTH DISTRIBUTION
LINE H

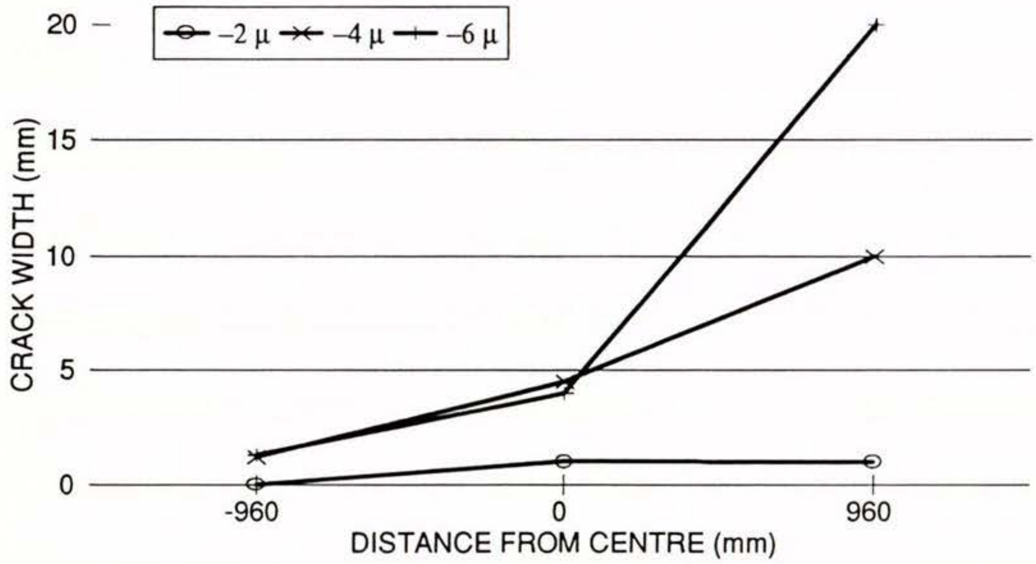

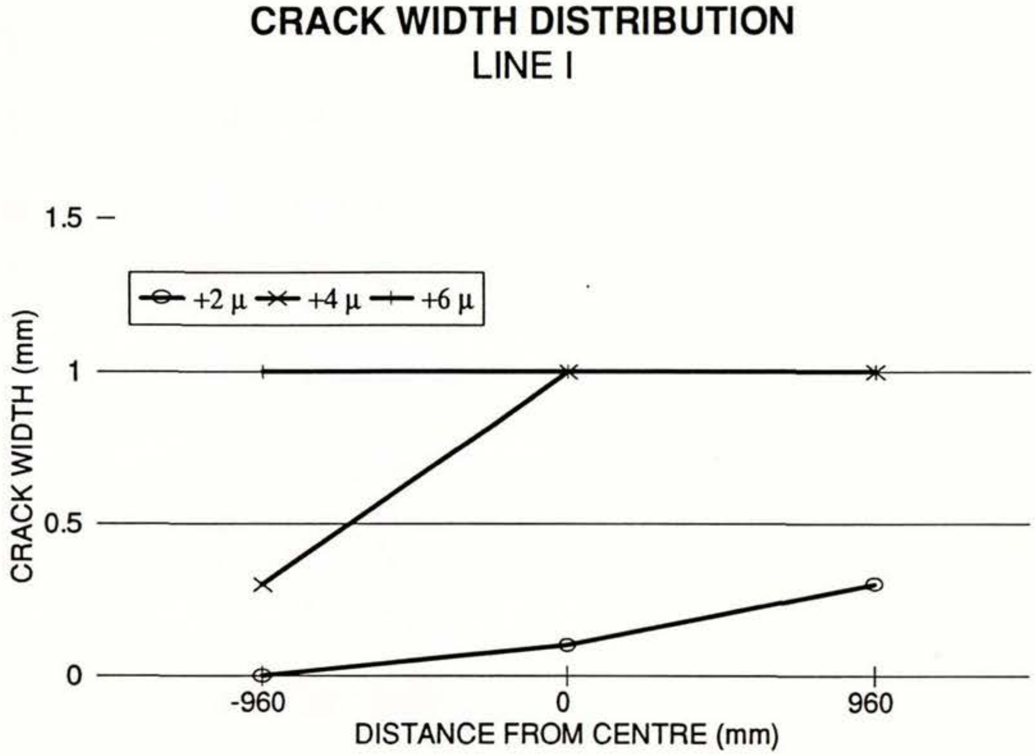
CRACK WIDTH DISTRIBUTION
LINE I
+2 μ
+4 μ
+6 μ
CRACK WIDTH (mm)
1.5
1
0.5
0
-960
0
960
DISTANCE FROM CENTRE (mm)

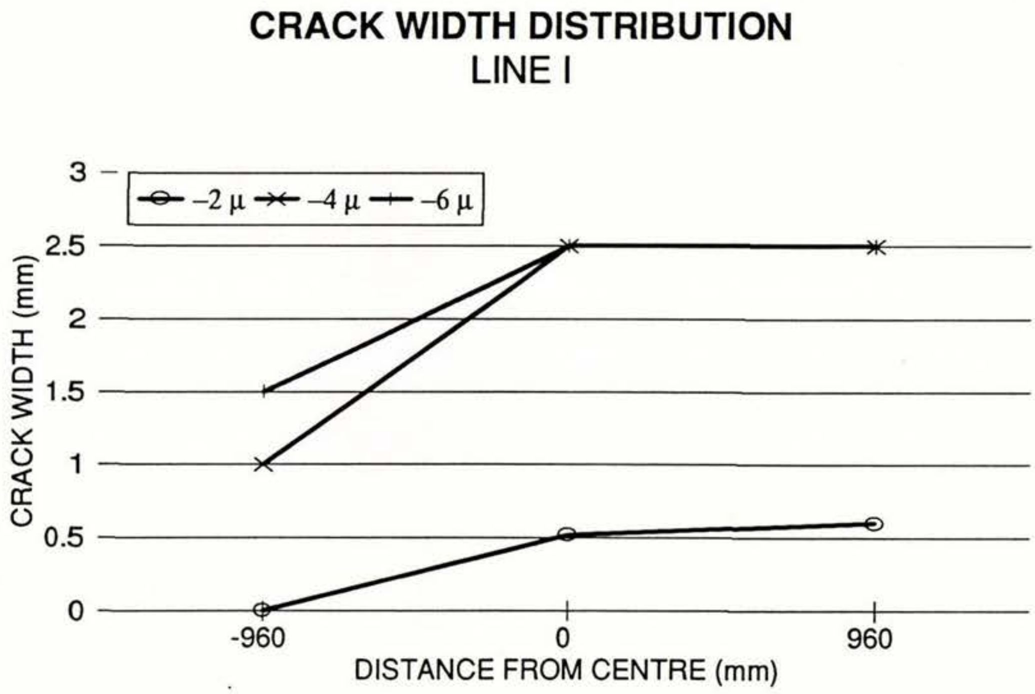
CRACK WIDTH DISTRIBUTION
LINE I
–2 μ
–4 μ
–6 μ
CRACK WIDTH (mm)
3
2.5
2
1.5
1
0.5
0
-960
0
960
DISTANCE FROM CENTRE (mm)

CRACK WIDTH DISTRIBUTION
LINE L

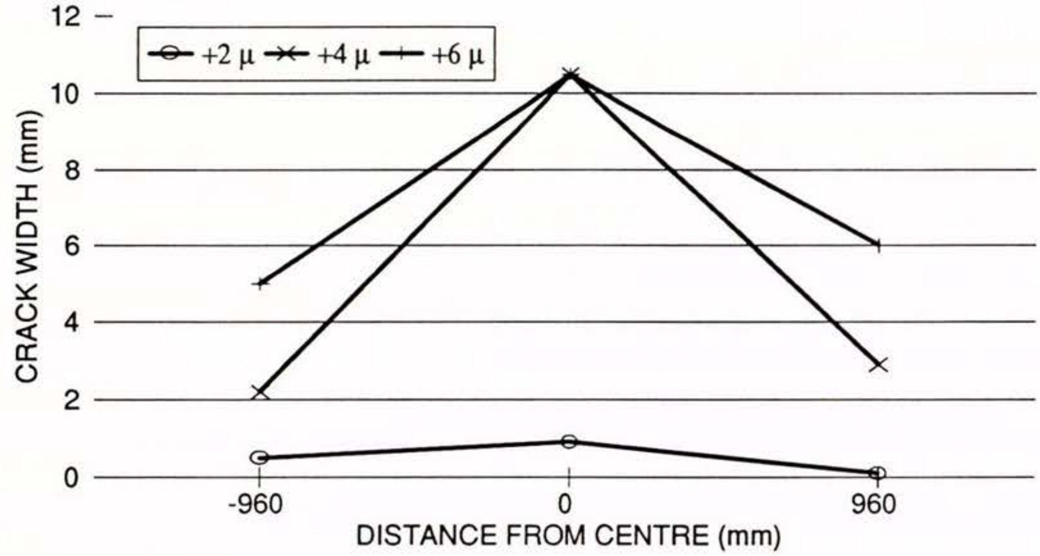

CRACK WIDTH DIXTRIBUTION
LINE L